University of Alberta

Ultrasensitive Viral Immunodiagnostics Using M13 as a Model Virus

by

Rajesh Vij ©

A thesis submitted to the Faculty of Graduate Studies and Research in partial fulfillment of the requirements for the degree of *Master of Science*

in

Pharmaceutical Sciences

Department of Pharmacy and Pharmaceutical Sciences

Edmonton, Alberta

Fall 2004

Canadä

ACKNOWLEDGEMENTS

No one can whistle a symphony. It takes an orchestra to play it. (H.E. Luccock)

To my supervisor, Dr. M.R. Suresh, for his never-ending support and patience.

I sincerely would like to express my gratitude for his constant guidance and for showing me how to use immunoassays in research. I remember the day I landed in Canada for my studies, since that day, he has been kind and helpful to me. I always looked for help from him and amazingly, I found that he was available. Again, I thank him very much.

Along the way, many other people have helped me in many ways. I would like to thank my lab colleagues, who made me feel at home during my entire journey. Dr. Pravin Bhatnagar, Mesfin Fanta, Dr. Jitra Kriangkum, Donald Husereau, Trivikram Chebrolu, and Dr. Biwen Xu, thank you for being my colleagues.

During this journey, I had a great chance to work with people from different departments. I thank them for welcoming me into their labs. Dr. Norm Dovichi, Dr. Hosseine Ahmed, Dr. Jed Harrison and Abebaw, thank you for your experimental help and guidance. My sincere thanks to Richard Sherbourne for his help in electron microscopy experiments.

During my research, some experiments were tried that did not lead to any conclusions. My sincere thanks to Chris and Ruan for helping me with atomic force microscopy experiments.

I also thank Dr. Steve McQuarrie for all his help and guidance. I learnt many things from him during my courses and while working with him.

I also thank my parents and my wife, Puja, for all their help and support. Finally, I thank all my friends who always stood by me and encouraged me, and without whom, this experience would have been incomplete.

Rajesh Vij

TABLE OF CONTENTS

LIST OF TABLES

LIST OF FIGURES

LIST OF SYMBOLS AND ABBREVIATIONS

μ	micro
μm	micrometer
[^{125}I]-MAb	Radiolabelled MAb
[^{125}I]-M13	Radiolabelled M13 phage
[^{125}I]-NaI	Radiolabelled sodium iodide
Ab	Antibody
ACE	Affinity Capillary Electrophoresis
ADH	Alcohol Dehydrogenase
AP	Alkaline Phosphatase
BSA	Bovine Serum Albumin
BS-ELISA	Biotin-Streptavidin ELISA
Ca^{2+}	Calcium ion
CARD	Catalyzed Reporter Deposition Assay
CE	Capillary Electrophoresis
cpm	counts per minute
$CsCl_2$	Cesium Chloride
CV%	Co-efficient of Variance
Da	Dalton
DMSO	Dimethyl Sulphoxide
DNA	Deoxyribose Nucleic Acid
E. coli	*Escherichia coli*
ELISA	Enzyme Linked Immunosorbent Assay
FAD	Flavin Adenine Dinucleotide
FADP	Flavin Adenine Dinucleotide phosphate

fg	femto gram, equal to 10^{-15} gram
fm	femto mole
g/L	Gram/liter
GMBS	N-γ-maleimidobutyryloxy succinimide ester
h	Hour
HRV	Human Rhinovirus
IEM	Immune Electron Microscopy
IgG	Immunoglobulin class G
IgM	Immunoglobulin class M
INT-violet	4-Iodonitrotetrazolium violet
LIF	Laser Induced Immunofluorescence
LLD	Lower Limit of Detection
mmol	millimole
MAb	Monoclonal Antibody
mg	milligram
$MgCl_2$	Magnesium Chloride
min	minute
MTS	3-Mercaptopropyl Trimethoxysilane
$NaBH_4$	Sodium Borohydride
NaCl	Sodium Chloride
NAD	Nicotinamide Adenine Dinucleotide
NADP	Nicotinamide Adenine Dinucleotide Phosphate
NaI	Sodium Iodide
NaN_3	Sodium Azide
NaOH	Sodium Hydroxide
NHS ester	N-hydroxy succinamide ester
nm	nanometer
NOS	N-oxysuccinamide
O.D.	Optical Density
OH	Hydroxyl group
PBS	Phosphate Buffered Saline

PBS-T	PBS containing 0.05% tween-20
PCR	Polymerase Chain Reaction
PEG	Polyethylene Glycol
pfu	plaque forming units
pI	Isoelectric Point
pNPP	p-Nitrophenyl Phosphate
RIA	Radioimmunoassay
rpm	Revolutions Per Minute
RSV	Rous Sarcoma Virus
RT	Room Temperature
SBMC	Streptavidin-Based Macromolecular Complexes
SD	Standard Deviation
TBS	Tris Buffered Saline
TCA	Trichloroacetic Acid
UV	Ultra Violet
v/v	volume/volume
w/v	weight/volume
Zn^{2+}	Zinc ion
$ZnCl_2$	Zinc Chloride

Chapter 1: INTRODUCTION

1.1   Importance of rapid viral diagnosis

The word 'virus', meaning poison, is used to denote the invisible agents causing diseases in humans. The hundreds of viruses belong to more than a dozen distinct families that still plague humans. Numerous antiviral drugs are available, or under development, that can or will be able to treat only a fraction of these viruses, and for some, no treatment is yet available. Unfortunately, different types of viruses may cause a single syndrome, such as viral respiratory tract infections, each of which may require treatment with a different drug. Unlike the treatment for bacterial infection, the choice of antiviral chemotherapy requires a specific laboratory diagnosis.

The need for appropriate viral chemotherapy demands a rapid viral diagnosis. As well, this type of diagnosis also has other advantages. A specific viral diagnosis could prevent the expense and toxic effects of the unnecessary use of antibiotics (which are ineffective) and anti-viral chemotherapy. A definitive viral diagnosis may also be important from an infection-control standpoint and also enables the initiation of epidemiological control measures. A specific diagnosis or a definitive diagnosis of a virus could also lead to an early intervention (Zaaijer et al., 1992) and development of antiviral drugs and vaccines (Crowther, 1995).

1.2   Virus architecture and M13 as a model for the filamentous viruses

In 1956, Crick and Watson pointed out that the nucleic acid in small virions was probably insufficient to code for more than a few proteins of limited size. The only reasonable way to build a protein shell, therefore, was to use the same type of molecules over and over again and hence their architecture with identical subunits. These subunits are packed to provide each with an identical environment. This is possible only if they are packed symmetrically. Crick and Watson pointed out that the only way to provide each subunit

1

with an identical environment was by packing them to fit some form of cubic symmetry. A body with cubic symmetry possesses a number of axes about which it may be rotated to give a number of identical appearances. Horne and Wildy (1961) showed that all the viruses then known (with the exception of a few bacteriophages) fell into two main morphological groups; those with cubic symmetry and the others with helical symmetry. The linear viral capsids have genomes that are encased in a helix of identical protein subunits and the length of the helical viral nucleocapsid is determined by the length of the nucleic acid.

The Fd, f1 and M13 phage are a group of related viruses, which are able to infect only those bacterial strains that express sex pili encoded by an F factor. All these virus particles are similar in size and shape. Their genomes are organized similarly, except for a small number of base changes. Their DNA sequences are all mostly identical. The M13 phage is about 900 nm long and 6-10 nm thick, with a molecular weight of 12×10^6 Da.

The M13 phage has circular, single-stranded DNA, and its genome consists of 6400 bases. The M13 genome codes for ten genes. Gene VIII codes for the major coat protein of the bacteriophage (Liu and Day, 1994) and gene III codes for the minor coat protein (Beck and Zink, 1981). Gene VIII protein forms a tubular array of approximately 2,700 identical subunits surrounding the viral genome (Figure 1). The viral coat also consists of four minor components such as the products of genes III, VI, VII and IX, presenting in about five copies each. The minor coat proteins are located exclusively at the ends of the filamentous phage.

The M13 phage is non-pathogenic for humans and is easily propagated and isolated from E.coli host. Therefore, the M13 phage was extensively used in our laboratory as a model virus to develop simple methods for virus detection and estimation. The concepts and methods developed could be extended to detect other medically important viruses.

2
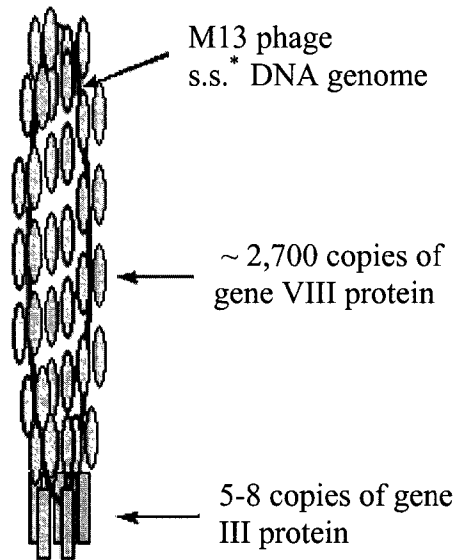
Figure 1: **M13 as model for the filamentous viruses**

The M13 phage has circular single-stranded DNA, and its genome consists of 6400 bases. The M13 genome codes for ten genes. Gene VIII codes for the major coat protein (Liu and Day, 1994) of the bacteriophage, and gene III codes for the minor coat protein (Beck and Zink, 1981). The gene VIII protein forms a tubular array of approximately 2,700 identical subunits surrounding the viral genome. It also consists of four minor components such as the products of genes III, VI, VII and IX, presenting in about five copies each. The minor coat proteins are located exclusively at the ends of the filamentous phage.

* Single stranded

3

1.3   Viral detection

1.3.1 Serologic diagnosis

This method involves the diagnosis of viral infection by detection of the immune response to virus exposure (Benne et al., 1994). Serological methods offer many advantages, but it fails to distinguish between the active state of infection and antibodies caused by a previous history of infection.

Alternatively, virus-specific IgM antibodies could be detected during the acute phase of viral illness, but this method presents some technical problems, e.g., the presence of competing virus-specific IgG or of rheumatoid factor (Meurman, 1983; Richman et al., 1984). Further, the IgM response may not always occur during primary infections, and this response is not limited to the primary infection (Meurman, 1983). For example, the reoccurrence of infection with viruses such as the cytomegalovirus and Epstein-Barr virus has been shown to induce the homologous IgM antibody response. As well, infection from these agents can induce the IgM antibody to different herpes viruses with which the patient has been previously infected.

The Roche Cobas Core automated enzyme immunoassay for the quantitation of antibodies against the hepatitis B virus surface antigen (anti-HBs) is commercially available and has been evaluated to have good precision (co-efficient of variance below 6% and 9% for intra- and inter-assay precision respectively) and accuracy: the detection limit of the test was 2 IU/l (Doche et al., 1996).

1.3.2 Viral isolation

Viral isolation and characterization are the preferred methods of diagnosis, especially for the definitive identification of the virus involved (Landry et al., 1982). The gold standard is the isolation of the virus, usually in organ tissue culture, eggs or animals. Although the viral particles cannot be seen as they replicate in cell cultures, their presence is signaled by changes in appearance of the virus-infected cells (Figure 2). These changes, called the cytopathogenic effect (CPE), can be detected when cells are viewed with an ordinary

4

Specimen selection, collection and transport

↓

Processing of specimen for inoculation into cell cultures

↓

Inoculation of cell cultures

↓

Incubation

↓

Examination of cell cultures for CPE

CPE present

↓

Identification of isolated virus by immunofluorescence or other methods ⬅ Result Positive ⬅ Perform hemadsorption or other detection method

↓

CPE Absent

↓

Negative result

↓

Culture result reported as "(Name of the virus) isolated"

Culture result reported as "no virus isolated"

Figure 2: Sequence of virus isolation procedures (CPE = Cytopathogenic Effect)

(Source: Diane, 1996)

5

light microscope. CPE may be detectable in 24 to 48 hours with viruses such as herpes simplex virus; however many viruses require 7-10 days or more for detection (Diane, 1996). The viral isolation method has been proven to be highly sensitive, perhaps because a single infectious virus particle can give a positive result. This method is also very specific in that only the virus is amplified, thus, sensitivity increases without any loss of specificity. Compared to other assays, which utilize specific probes such as antibodies or nucleic acids, virus isolation gives an unambiguous identification of the etiologic agent. Such assays cannot detect new agents or even old agents whose presence is not suspected. Despite all the advantages of virus isolation, it has some drawbacks, so we must look for alternative methods of viral detection. Viral isolation is often slow, requires sophisticated technical expertise, and expensive. It requires the use of an optimal culture system; for example, the optimal detection of respiratory viruses requires the use of four or five different cell lines.

1.3.3 Microscopic techniques

Electron microscopy (EM) and light microscopy provide alternative methods to detect the presence of a virus in a clinical specimen. These methods are of relatively less importance today for early diagnosis and are used more for confirming results obtained from other methods. Light microscopy was originally used to characterize the cytopathogenic features of rabies and herpes virus infection. However, light microscopy is not powerful enough to visualize viruses. Electron microscopy enables one to view the size (Sogo et al., 1974) and the shape of the virus. The viruses can be distinguished on the basis of capsid configuration, the size and the nucleic acid configuration. Clinical specimens or virus-infected culture fluid can be examined by using EM, thus providing a rapid diagnosis of virus infection (Hsiung et al., 1979), but this method has a limitation. A low virus-particle number in the sample makes viewing the virus very difficult. A number of techniques have been developed to enhance this viewing: the pseudoreplica technique (Smith and Melnick, 1962), agar gel diffusion (Anderson and Doane, 1972) and ultracentrifugation (Smith and Melnick, 1962).

6

In the pseudoreplica technique, a drop of the suspension of the virus is put on the agar surface and allowed to dry. A few drops of the formvar (polyvinyl formal resin, forms a superb support film for Transmission Electron Microscopy grids) (Wolff, 1988) are added to the agar and as a result, a thin film replica of the virus is formed. The film is transferred on a grid and treated with uranylacetate before being observed under electron microscope. A direct ultracentrifugation technique could result in more than 1000-fold increase in concentration of the virus particles compared to the conventional adsorptive techniques and consequently the rate of detection of virus increases (Jansons, 1985). Transmission electron microscopy was used to diagnose the nipah encephalitis virus during the 1998-1999 outbreaks in Malaysia (Chow et al., 2000).

With the use of immune electron microscopy (IEM), hepatitis A (Feinstone et al., 1973), rotavirus (Flewett et al., 1973) and the Norwalk agent (Kapikian et al., 1972) were first seen in stool contents. Serum-agar mixtures containing 1% agar in phosphate buffered saline and antisera are pipetted into disposable microtitre plates. A drop of the suspension of the virus is placed on the agar and a grid is floated for 80 min at 37° C. The grid is treated with uranylacetate and observed under electron microscope.

However, despite the many contributions of EM and IEM for virus diagnosis, this technique is still too expensive and cumbersome for routine application.

1.3.4 Molecular methods of diagnosis

Nucleic acid probes represent one of the most powerful and sensitive methods of viral diagnosis. In this technique, the virus is identified based on the unique regions in the nucleic acid sequences of most viruses. Enzyme-labeled, fluorescent and radioactive-labeled nucleic acid sequences for these unique regions are available commercially and, these labeled complementary sequences are called "nucleic acid probes" (Hyypia, 1989). These are capable of hybridizing complementary nucleic acid strands of RNA and DNA to form stable double strands. During the process of hybridization, any single-stranded

7

nucleic acid will attempt to pair up with a complementary strand. In this process, the labeled probe competes with the complementary strand for binding the target. The hybridized nucleic acid is harvested and subjected to a detection process that confirms the hybridization (Metcalf et al., 1988). The probing process could be carried out on samples collected from the patient or on material collected from virus-infected cells. The amount of viral nucleic acid collected from the patient's sample could be very small, thus the probing process is sometimes preceded by a technique called the polymerase chain reaction (Mullis, 1990; Bagasra and Pomerantz, 1994).

1.3.4.1 Polymerase chain reaction (PCR)

PCR is a nucleic acid amplification technique used for *in vitro* synthesis of specific DNA or RNA sequences. Initially, a target nucleic acid (RNA or DNA) is isolated from the tissues or fluids collected from patients or from infected cell cultures. If the target nucleic acid is RNA, it must be converted to DNA by using a reverse transcriptase before the process begins. The DNA is amplified enzymatically by PCR. PCR is a cyclic process, and its cycle involves three steps: (i) the target DNA is denatured by heating the reaction mixture: this process results in denaturation of the DNA strands; (ii) the reaction mixture is cooled; this cooling allows the primers to anneal to the template at complementary sites near the area of unique nucleotide sequences; and (iii) the temperature is increased to allow optimal polymerase activity. The DNA polymerase in the reaction mixture will add deoxyribonucleotide bases resulting in duplication of the target sequence. This cyclic process is repeated 20-40 times to amplify the original DNA in an, ideally, exponential fashion.

PCR enables faster diagnosis than the isolation of a virus in standard or modified cell culture systems (Kaneko et al., 1990). While the standard or modified cell culture system takes 24 h to 48 h to isolate certain viruses, PCR may yield results in 5 to 6 h after the sample is received in the laboratory. This facilitates an earlier disease diagnosis and intervention by the physician than would be possible otherwise. PCR can also be used in detecting viruses, which cannot be cultured in the standard cell-culture systems found in

8

most clinical diagnostic virology laboratories. For example, human papilloma virus, pavovirus B19, and hepatitis viruses (Garson, 1994) do not proliferate in standard cell cultures. In the detection of hepatitis B by serological approaches, the process cannot differentiate between past and present infection. However, the presence of hepatitis B viral nucleic acid in serum, detected by PCR, is definitive evidence of current infection. In hepatitis C infection, tell tale antibodies may not be produced in response to infection, especially in the early stages of the disease or in immuncompromised individuals. The PCR detection may be the only method available to reliably confirm an infection (Garson, 1994; Schlauder and Mushahwar, 1994).

PCR amplifies only a targeted portion of the nucleic acid sequence of interest. Typically, this target material is non-infectious and is not capable of independent biological activity, in contrast to cell culturing of infectious or dangerous viruses in laboratories. A typical example is the diagnosis of the HIV (De Rossi et al., 1991). It can be isolated in suspensions of phytohemagglutinin stimulated lymphocytes, but it poses a high risk of infection and needs a specialized facility. With PCR, HIV sequences can be detected in neonates, and the presence of these sequences correlates with the development of clinical HIV disease (Nesheim et al., 1997). PCR for HIV is also used to monitor the efficacy of antiviral drugs in terms of viral load, e.g., the anti-viral effect of interferon in hepatitis C virus infection (Garson, 1994). As well, PCR is also a very useful tool in analyzing clinical samples, which are typically small in size (e.g. a biopsy sample) or volume (e.g., cerebrospinal fluid samples in HSV patients).

Despite all these advantages, PCR also has some disadvantages. The technology is sophisticated, prone to amplification interference, needs sample extraction, and expensive, and the procedures require considerable expertise.

1.3.5 Viral antigen detection

The other option that could be considered for the detection of viruses is the detection of viral components. Viral components that can be easily detected include the structural

9

proteins (which are usually identified on the basis of their antigenicity), viral nucleic acids, and viral-induced enzymes. The virus-inducible enzyme system involves the use of molecular cloning technology, which has been used to prepare a cell line that will express an enzyme only after incubation with a specific virus (Stabell and Olivo, 1992). In this case the specific virus is HSV type 1 or type 2, and the cell line is a line of baby hamster kidney cells into which an *E.coli LacZ* gene has been inserted behind an inducible promoter from HSV-1 UL 39. The promoter encodes ICP6, an important part of ribonucleotide reductase. This promoter has no expression in uninfected cells, is activated specifically by HSV type 1 and 2, and expresses within hours after infection with HSV-1 or 2. When HSV-1 or –2 containing the protein VP16 enters the cell and triggers the HSV promoter, the *LacZ* gene is stimulated by ICP6 to express β-galactosidase. The β-galactosidase is detected by adding a solution of β-D-galactopyranoside, which turns blue in the presence of β-galactosidase. This method is called enzyme-linked virus inducible system (Diane, 1996). It has been used for diagnosis of hepatitis B (Krugman et al., 1974) and herpes virus (Gronowitz and Kallander, 1983).

The approach most extensively used for the detection of viral components is viral antigen detection. Immunofluorescence and immunoperoxidase-based microscopy are the examples of two techniques used for this purpose. In these techniques, antibodies specifically targeted to the virus, are added to a tissue or individualized cell population that has been fixed on a slide. In the simplest case, the antibody is bound to peroxidase or to a fluorescent element, as in the case of direct immunoperoxidase and direct immunofluorescence, respectively. The term "direct" refers to the fact that the antibody itself is labeled, though very often the primary antibody is not labeled and we use a secondary labeled antibody targeted to the primary antibody (i.e., indirect immunoperoxidase and indirect immunofluorescence). For example, immunofluorescence is used for a rapid diagnosis of respiratory syncytial virus and parainfluenza virus infections in young children with lower respiratory tract infections by the demonstration of viral antigens in nasopharyngeal aspirates. However, better methods are needed because these procedures are less sensitive and they require significant expertise in test performance and interpretation.

10

Enzyme immunoassays (Tijssen, 1985; Oellerich, 1984; Burgi et al., 1988) offer another alternative for the detection of virus particles and viral components (Laviada et al., 1992). It offers advantages like higher sensitivity, an objective end point, and ease of automation. Radioimmunoassays (RIA) also offers these advantages, but hazards and the cost of radioactive reagents limit their use in immunoassays.

Enzyme immunoassay for antigen detection has many formats, but the most common is the sandwich format (two-site immunometric assay), in which an anti-viral antibody of known specificity is immobilized on the solid phase (Diane, 1996). This immobilized antibody is incubated with the patient's clinical sample (a fecal sample, throat sample, lesion sample, or serum) or a suspension of virus-infected cells from a culture tube. The antibodies on the solid phase function in capturing any viral antigen that is present in the sample. This is followed by the addition of enzyme-conjugated antiviral antibodies.The enzyme-labeled antibodies bind to the viral antigen that was captured by the antibodies on the solid phase. After incubation and rinsing, a substrate solution is added, and the enzyme attached to the bound antibodies act on the substrate to produce a color change. The amount of bound antigen can also be detected and quantified by development of luminescence (Kricka, 1993) or fluorescence (Hemmila, 1985; Diamandis, 1988) when an appropriate substrate is added.

New ELISAs that permit the simultaneous detection of HIV antigen and antibody are available commercially. Examples include Enzymum-Test HIV Combi (Boehringer Mannheim) and VIDAS HIV DUO (Biomerieux). Enzymum-Test HIV Combi is an enzyme-linked immunosorbent assay for the simultaneous detection of HIV Ag and immunoglobulin G (IgG) and IgM antibodies in HIV (including subtype O) and HIV-2. VIDAS HIV DUO permits the simultaneous detection of p24 Ag and IgG antibodies against HIV-1 (including serotype O) and HIV-2. These ELISAs permit an earlier diagnosis of HIV infection through the detection of p24 Ag, which may be present in serum samples from individuals with recent HIV infection prior to seroconversion.

11

Enzyme-immunoassay methods for the detection of the rotavirus antigen are especially popular because this virus will not proliferate in standard cell cultures. Both the rotavirus and Hepatitis B virus do not proliferate in standard cell cultures and thus cannot be detected through immunofluorescence (Leland, 1996). The respiratory syncytial virus (RSV) is frequently detected through the antigen detection method, though RSV proliferates well in culture and can be detected by immunofluorescence. This is because enzyme immunoassays can accommodate a large volume of RSV tests performed during the RSV season and require less time to perform than immunofluorescence.

1.4   Immunoassay and strategies to increase analytical sensitivity

The enzyme immunoassay is a widely utilized technique and has been utilized to detect a variety of analytes including virus particles. Enzyme immunoassays compete with other well established techniques like RIA, luminescence and immunofluorescence. Most enzyme immunoassays have advantages over these methods. The major advantages are the stability of the reagents, ease of use, automation, and the ready availability of colorimeters. However, such immunoassays have moderate sensitivity with conventional substrates as they depend largely on the rate of detectable change catalyzed by the enzyme label. This dependence could be attributed to the difficulty in detecting, in a given time, the limited number of colored product molecules produced by only a small number of enzyme labels even though each enzyme molecule may be an effective catalyst of the chosen reaction. Thus, different strategies have been used to increase analytical sensitivity. The main strategies for ultrasensitive immunoassays have used amplifying labels, multiple labels, enzyme amplification cascade, immune complex purification, fluorescence and luminescence-detection methods.

1.4.1 Multiple labels

Multiple labels are employed to increase the number of enzyme molecules available to generate a signal. The increase in signal molecules could result in an increase in the sensitivity of the enzyme immunoassay. For example, biotin-avidin or biotin-streptavidin

12

interaction is widely used in multiple-labeling strategies (Wilchek and Bayer, 1988; Diamandis, 1988a). Biotin is a secondary component in the system and binds to avidin or streptavidin, which in turn is multiply labeled. Diamandis (1991) described a time-resolved fluorescence immunoassay system, involving the use of europium labels and streptavidin-based macromolecular complexes (SBMC). The SBMC reagent is streptavidin conjugated to thyroglobulin, labeled with a chelator, 4,7-bis(chlorosulfophenyl)-1,10-phenanthroline-2,9-dicarboxylic acid. When the SBMC reagent is incubated with europium ions, it forms a stable complex. The complex so formed contains up to 480 chelation sites for europium ions and has an intense long lived fluorescence. Catalyzed reporter deposition assay (CARD) is another technique. It uses a horseradish peroxidase label to generate multiple labels (Bobrow et al., 1989 and Bobrow et al., 1991). In the CARD assay a peroxidase label oxidizes a biotin or a fluorescein-labeled tyramine co-substrate to a free radical product, which reacts with the protein in the immediate vicinity of the label, leading to the deposition of multiple biotin or fluorescein molecules around the peroxidase label. The deposited biotin is detected with peroxidase-, beta galactosidase- or alkaline phosphatase-streptavidin. The deposited fluorescein is detected with peroxidase anti-fluorescein. The net result is that a single peroxidase label is amplified to a large number of enzyme labels, hence improving detection by a factor of up to 30 fold compared to the non-amplified procedure (Kricka, 1993).

1.4.2 Enzyme amplification cascade

The most common strategy to increase the sensitivity is to select an enzyme label that can initiate an enzyme amplification cascade. Enzyme cascades are produced by coupling enzyme reactions in such a way that the amplification properties of one enzyme are combined with the amplification properties of other enzymes in the cascade. As a catalyst a single enzyme can convert $> 10^7$ molecules per min, thus providing over a million-fold amplification compared to that of a label that produces only a single signal such as a radio-isotope.

13

Three types of cascade mechanisms are possible for alkaline phosphatase label: a cofactor recycling initiation reaction (Obzansky, 1991), an enzyme amplification cascade (Clark and Price, 1986) and an enzyme inhibition cascade (Mize et al., 1989). The technique of enzyme amplification depends on an enzyme label-giving rise to a primary product as a catalytic intermediate that further amplifies the detectable signal by a secondary step. For example, $NADP^+$, as the primary substrate, can be cleaved to NAD^+ (the primary product) by alkaline phosphatase (AP). The dephosphorylated cofactor then enters a highly specific redox cycle, where it is reduced to NADH by alcohol dehydrogenase. The oxidized form, NAD^+, is regenerated by diaphorase with the concomitant reduction of p-iodonitrotetrazolium violet (INT-violet) reagent to an intensely purple formazan dye. The oxidized form is continuously cycled with the formation of a detectable product with every turn of the cycle (Figure 3). It is estimated that each NAD^+ derived by the primary reaction enters the cyclical scheme about 600 times, thus amplifying the signal (Johannsson et al., 1986). Alternatively, the end products generated could be fluorescent or luminescent. The enzyme amplification cascade has a detection limit of 11 zeptomoles. The same cascade system has been employed in different immunoassays (Moss et al., 1985; Dhahir et al., 1992).

Enzyme-initiation cascade involves activation of the coupled enzyme (apo amino acid oxidase) while enzyme-inhibition cascade involves inhibition of the coupled enzyme (carboxyl esterase) (Table 1). Enzyme-initiation cascade has a sensitivity of 1 fm/L of alkaline phosphatase label wherein the cascade detects the alkaline phosphatase label *via* the dephosphorylation of the novel substrate FADP to produce the cofactor FAD, which binds stoichiometrically to inactive apo amino acid oxidase (AAO). The resulting active holo AAO oxidizes proline to produce hydrogen peroxide. It is quantified by the horseradish peroxidase-mediated conversion of 3,5-dichloro-2-hydroxybenzenesulfonic acid (DCHBS) and 4-aminoantipyrine to a colored product (Obzansky et al., 1991). In an enzyme-inhibition cascade, a masked inhibitor, 4-(3-oxo-4,4,4-trifluorobutyl) phenyl phosphate, is dephosphorylated by alkaline phosphatase. The resulting compound, 1,1,1-trifluoro-4-(4-hydroxyphenyl)-butan-2-one, acts as a potent inhibitor of the second enzyme, a liver carboxyl esterase. A determination of the residual esterase activity

14

(Substrate of AP)

$NADP^+$

Formazan* ← NAD⁺ — Ethanol

Diaphorase   Alcohol Dehydrogenase

INT-Violet — NADH ← Acetaldehyde
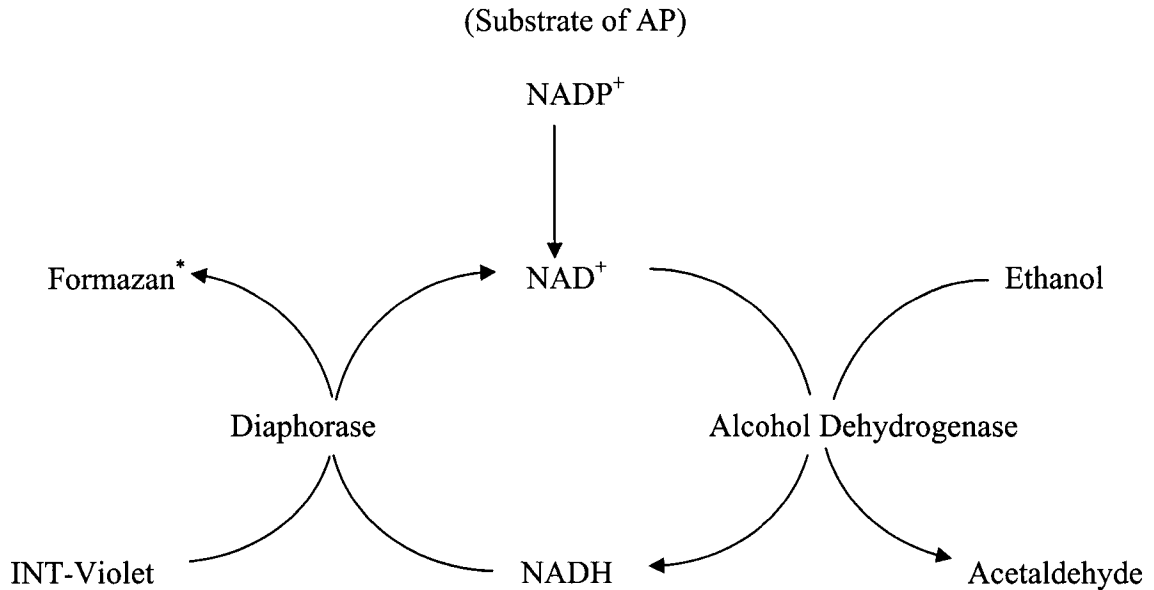
* Colored end product

Figure 3: Enzyme amplification cycle

The technique of enzyme amplification depends on an enzyme label giving rise to a primary product as catalytic intermediate that further amplifies the detectable signal by a secondary step. $NADP^+$, for example, as the primary substrate can be cleaved to NAD^+ by AP. The dephosphorylated cofactor then enters a highly specific redox cycle, where it is reduced by NAD+ specific alcohol dehydrogenase. The oxidized form is regenerated by diaphorase with the concomitant reduction of p-iodonitrotetrazolium violet (INT-violet) reagent to an intensely purple formazan dye. The oxidized form is continuously cycled with the formation of detectable product with every turn of the cycle (Lynch et al., 1988).

15

Table 1: Enzyme amplification cascade Schemes (adapted from Kricka , 1993)

Enzyme activation cascade (Obzansky et al., 1991), *Refer to Section 1.4.2*:

Initiation reaction:

	Alkaline Phosphatase label	
FADP	$\longrightarrow$	FAD

Amplification:

	FAD	
Apo amino acid oxidase	$\longrightarrow$	Holo amino acid oxidase

	Holo amino acid oxidase	
Proline + O_2	$\longrightarrow$	H_2O_2

	HRP	
H_2O_2 + DCHBS + 4AAP	$\longrightarrow$	Color (A_{520} nm)
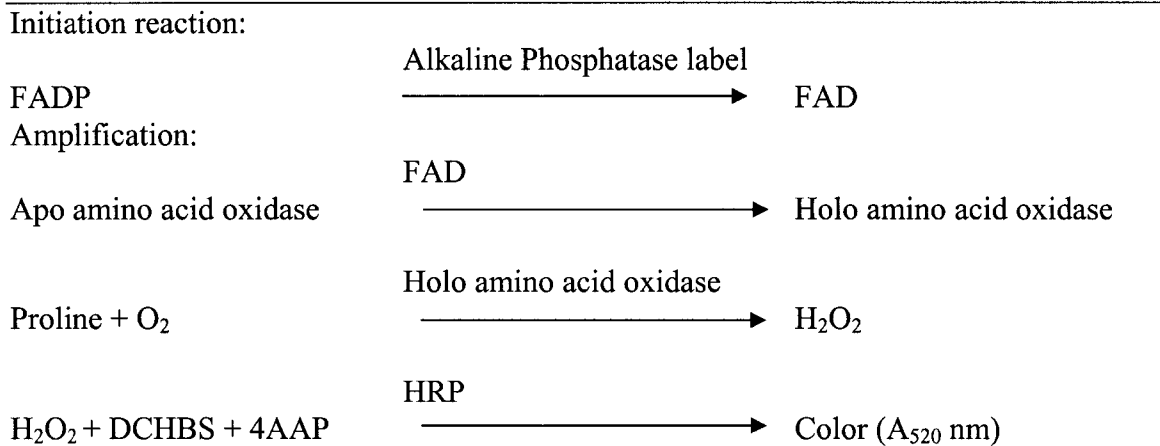
4AAP, 4-aminoantipyrine; DCHBS, 3,5-dichloro-2-hydroxy-benzenesulfonic acid; FAD, flavin adenine dinucleotide; HRP, horseradish peroxidase.

Enzyme inhibition cascade (Mize et al., 1989), *Refer to Section 1.4.2*:

Initiation reaction:

	Alkaline phosphatase label	
Inhibitor-PO_4	$\longrightarrow$	Inhibitor

Amplification:

	Inhibitor	
Esterase (active)	$\longrightarrow$	Esterase (inactive)

	Esterase (active form)	
DCIPB	$\longrightarrow$	Color (A_{620} nm)
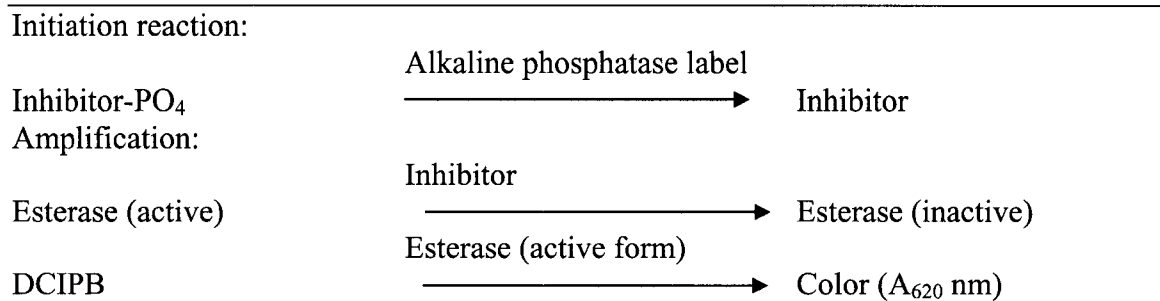
DCIPB, dichloroindophenol; inhibitor, 1,1,1-trifluoro-4-(4-hydroxyphenyl)-butan-2-one.

provides a highly sensitive indication of the original phosphatase concentration. An enzyme-inhibition cascade is 125-fold more sensitive than the conventional colorimetric assay of AP (Mize et al., 1989). The sensitivity of these methods in determining enzyme labels makes possible the construction of assays of high sensitivity.

1.4.3 Immune complex purification

This system has been shown to give more than 30-fold increase in the signal compared to the signal from a conventional immunoassay (Hashida and Ishikawa, 1990). The signal due to the non-specific binding of the labeled molecule to the solid phase is avoided by eluting the analyte: antibody-label complex, from the solid phase to a second solid phase (Hashida and Ishikawa, 1990). Two different antibodies are taken, one labeled with biotin and DNP and a second antibody labeled to an enzyme. An immune complex forms in solution (doubly-labeled-antibody: antigen: enzyme-labeled antibody). This immune complex is captured on a solid phase, polystyrene bead coated with anti-DNP IgG antibody. The complex is eluted from the anti-DNP IgG coated polystyrene bead by using dinitrophenyl-L-lysine and the displaced complex is then captured on a streptavidin coated polystyrene bead, and the bound enzyme is quantitated. This strategy is reported to have decreased the background, with a concomitant increase in sensitivity.

1.5 Covalent immobilization of proteins

Proteins have been immobilized on different solid macro surfaces for different purposes. The choice of a particular solid surface influences the sensitivity and the results of the experiment. Proteins have been immobilized on beads (latex particles, magnetic beads), membranes, glass (Polson , 1993; Obringer et al., 1995), gold (Karyakin, 2000), fused silica surface (Wu and Walters, 1988; Zhao et al., 1993), silicon wafers, multiple well plates (Plant et al., 1991) and optic fibers (Anderson et al., 1997). Proteins could be immobilized on solid surfaces through hydrophobic interactions or covalently by attachment to the pre-activated surfaces (Shenoy et al., 1992; Sigrist et al., 1992).

17

The adsorption of protein molecules is based on hydrophobic interactions and Van der Waals forces. The adsorption of proteins is successful in some cases, but in many cases, these forces may not be strong enough to resist the incubation and wash steps included in the assay, especially when it involves the use of ionic detergents such as Tween 20, Nonidet and Brij. Up to 70% of the adsorbed antibody can be removed from the surface in such steps (Engvall, 1980). As well, the precision and sensitivity of the assay are negatively influenced. In other cases, the antibody in question cannot be adsorbed to the surface to preserve its immunoreactivity. Alternatively, the proteins could be adsorbed to an ion exchanger, but such electrostatic binding is highly susceptible to pH and salt concentration changes, resulting in high non-specific binding in addition to the loss of sensitivity and precision (Ling and Overby, 1972). In some cases, the loss of activity upon immobilization has been noticed. One reason for this loss of activity is the random orientation of the antibody molecule on the solid support. This condition could be attributed to steric hindrance caused by the neighboring molecules and the distance between the antibody molecules (Turkova, 1999).

Thus, covalent immobilization is the method of choice for a molecule which does not adsorb at all, adsorbs weakly, or adsorbs with the wrong orientation. Covalent immobilization has also been shown to have resulted in a decrease in non-specific binding and an increase in the stability.

1.5.1 Surface modifications

Table 2 compares the different surface-modification techniques usually applied or available. A number of chemical and physical methods can be used to modify the supports for covalent immobilization of biomolecules:

1. Addition of amino groups by fuming nitrous acid (Rubin et al., 1980)

2. Bromoacetylation (Peterman et al., 1988)

3. Oxidation by the use of plasma, ultraviolet light or electron beams as sources in the presence of oxygen and air (Pearce et al., 1987; Munro, 1988)

4. Chemical grafting (Hoffman et al., 1991)

18

5.   Glutaraldehyde coating (Dubuco et al., 1981)

6.   Latex particle coating, non-covalent attachment of an affinity spacer aromatic group

7.   Photochemical coupling (Amos, 1995)

The methods 1- 4 produce covalent bonds and the methods 5-6 form non-covalent bonds to solid supports. Photochemical coupling results in a covalent bond.

Table 2: Comparison of surface modification techniques (adapted from Jill, 1996)

Different physical or chemical processes result in different types of preactivated surfaces

Characteristics	Photochemical coupling	Plasma treatment	Chemical etchants	Chemical grafting
Attainable properties	Many	Many	Single	Many
Substrate independence	Very broad	Broad	Limited	Limited
Change to surface morphology	No undesirable changes	Slight	Yes	No
Type of bond	Covalent	Some covalent	Non covalent	Some covalent
Ageing stability	Excellent	Some loss with time	Excellent	Excellent
Impact on environment	Not appreciable	Low	Moderate to severe	Moderate to severe
Process pressure	Atmosphere	Vacuum	Atmosphere	Atmosphere
Process control	Excellent	Moderate	Good	Moderate

1.5.1.1 Protein immobilization on silica

The attachment of antibodies on quartz and glass can be achieved by simple adsorption, but the immobilized proteins suffer partial denaturation and tend to leach or wash off the surface (Avrameas et al., 1984).

19

Non-functional proteins, can be adsorbed on the silica surface, on which the homobifunctional spacer arms can be attached covalently. The non functional protein could be a cross linked proteinaceous film enveloping the carrier body and essentially consists of a protein, partially hydrolyzed protein, peptide or a combination thereof (Van der Merwe, 1984). However, this immobilization is not completely covalent as the non-functional protein still adsorbs to the silica surface. Alternatively, Si-OH groups on the silica surface can be modified such that the non-functional protein or organic molecule attaches itself covalently. Coating the fused silica with a silane film provides a method to modify the OH reactive groups on the silica surface (Bhatia et al., 1989). Several methods for silanizing the organic substrate have been described and evaluated. The choice of the spacer arm determines the type of active surface produced. Once a silica film is covalently attached onto the reactive Si-OH groups, spacer arms can be attached covalently. The spacer arm can be homobifunctional or heterobifunctional. Based on the type of spacer arm, the covalent attachment of reactive groups produces different stable surfaces. The N-oxysuccinamide (NOS) surface covalently couples to amino groups, the maleimide surface couples to sulfhydryl groups and the hydrazide surface is reactive towards periodinate-activated carbohydrates (Bhatia et al., 1989).

1.6   Electrophoresis

Electrophoresis is a separation technique, which is used to study the migration of a charged molecule under the influence of an electric field. The rate of migration depends on the charge to mass ratio. The differences in this ratio result in different proteins migrating at different rates towards one of the electrodes. Electrophoresis can also be used as a method to study protein-protein interaction, whereby proteins are separated not only by the differences in their mobilities but also at the same time by interactions with other proteins.

Gel electrophoresis and capillary electrophoresis have been described as the most common methods used to protein-protein interactions. Gel electrophoresis is a well established method for protein analysis (Hames, 1998) but has not shown much promise

in measuring protein-protein interactions. On the contrary, the use of capillary electrophoresis and essentially affinity capillary electrophoresis (ACE) is gaining momentum in such applications.

1.6.1 Affinity capillary electrophoresis (ACE)

1.6.1.1 General principle

ACE (Shimura and Karger, 1994) works on the principle that the electrophoretic mobility of a protein changes on binding to a charged ligand present in the electrophoresis buffer, due to a change in its charge to mass ratio. When two molecules A and B having different electrophoretic mobility form a complex AB, it can have a different mobility from either of the component molecules due to the difference in the charge to mass ratio. The mobility of the complex is typically intermediate between that of the components. In the case of protein and small molecular weight ligand interaction, the charge on the ligand is the major source of the mobility change of the proteins, of which the change in molecular mass is negligible on binding the ligand. Molecular interactions can be observed in two formats of electrophoresis: equilibrium mixture analysis (Pritchett et al., 1995) and mobility change analysis (Chu et al., 1992).

1.6.1.2 Equilibrium mixture analysis

This format involves the zone electrophoresis of a preformed equilibrium mixture (Pritchett et al., 1995). The electric field induces the free component molecules to leave the zone of the complex toward both sides of the complex zone due to a difference in mobility between the complex and the individual components. The dissociation of the complex takes place during capillary electrophoresis without the complex reformation. If the dissociation rate is small relative to the separation time, a distinct peak or zone of complex formation can be detected.

21

1.6.1.3 Detection of complex formation

The evident change in the mobility of the complex upon protein-protein interaction can be the most direct evidence of molecular interactions between the components. Antigen-antibody complexes have been separated by using ACE with UV detection. (Nielsen et al., 1991; Arentoft et al., 1993). Complexes formed between a high molecular weight virus and their respective antibodies have been recently separated (Okun et al., 2000) wherein it was demonstrated that subtle differences on the viral surface are sufficient for electrophoretic resolution of the complex.

Titration of one interacting component with the other gives the binding stoichiometry. When one of the components is saturated, either the peak reaches its maximum size, or the excess of titrant appears as a separate peak. When the interacting components have a small difference in mobility, resolving both the complex and the free component in the same electropherogram can be difficult. If the complex formed is not resolved from the free components, the labeling of the selective ligand with a fluorophore enables the selective detection of the complex (Reif and Freitag, 1995). ACE can be coupled with LIF to amplify the fluorescence signal and detect the complexes (Chen and Evangelista, 1994).

1.6.1.4 Non competitive immunoassays

The combination of CE, fluorescence labeling and LIF allows for quantifying the unlabeled components in the form of a fluorescent complex. This forms the basis of CE-based immunoassays. For large macromolecular antigens, non-competitive immunoassays can be performed since antibody complex formation produces a large change in electrophoretic mobility. For macromolecular antigens, non-competitive immunoassays by using fluorescence labeled antibody can be perfomed. High sensitivities have been achieved in the separation of the antigen-ligand complexes. This high sensitivity could be attributed to the use of LIF and the focusing of the complex to its pI in a pH gradient in the influence of an electric field. A pH gradient is automatically

formed in the capillary upon application of the electric field, and proteins migrate and focus in the pH gradient at which the pH is equal to the isoelectric point of each protein. The shape of the pH gradient formed in a capillary is best defined by the use of an internal pH standard or pI marker, of which isoelectric points are known. This format enables it to discriminate among antigens differing in charge but sharing the same epitope (Shimura and Karger, 1994). The heterogeneity of the labeled antibodies is the major obstacle in this immunoassay application as it results in multiple peaks for the same antigen.

1.6.1.5 Competitive immunoassays

Competitive immunoassays are employed for low molecular weight compounds by using fluorescence-labeled haptenic antigens (Koutny et al., 1996). The fluorescent-labeled haptens are more readily available than the antibodies or their fragments. The method involves mixing the labeled antigen with antibodies and the unlabeled antigen. The mixture is equilibrated, and the amount of labeled antigen in free form is quantified by using CE and LIF. A positive correlation is observed in between the peak height or peak area of the free-labeled antigen and the amount of antigen to be determined in the sample. This method offers some advantages over the non-competitive immunoassay; for example, this method needs a very small amount of analyte, determines several analytes simultaneously (Chen and Evangelista, 1994) and allows for very accurate measurements.

1.6.1.6 Mobility change analysis

Low-affinity protein-protein interactions are commonly characterized by a relatively short lifetime of the complexes. These complexes can be analyzed by zone electrophoresis of one component in the presence of other component as the background. Multiple association and dissociation reactions during electrophoresis suggest the complex formation in the form of mobility change of the molecule applied as a zone.

23

This method has been used in determining the complex formation for metal binding proteins, for example, calmodulin with Ca^+ and carbonic anhydrase with Zn^+ (Kajiwara et al., 1991). The separation of complexes is possible due to the concomitant separation of the components in the mixture by using capillary electrophoresis. In addition, ACE has also been combined with mass spectrometry to separate peptides for binding to vancomycin from a combinatorial library, with on-line determination of structure (Chu et al., 1992).

1.7 Aims, objectives and hypothesis

1.7.1 Hypothesis

High-affinity monoclonal antibodies have been used to develop sensitive immunoassays for the detection of viruses. We hypothesize that since the architecture of most pathogens (e.g., viruses, bacteria, spores, etc.) incorporate multiple repeats of an identical surface or core antigens and epitopes, a poly-homosandwich design can be the basis of simple, inexpensive assays exhibiting ultrasensitive detection capabilities. We additionally hypothesize that such poly-homosandwich assays can exhibit ultrasensitivity due to the cumulative amplification theoretically expected at three levels: (a) solid-phase capture of pathogens by multiple epitope-paratope interactions, (b) amplified decoration of labeled antibodies distal to the solid phase, and (c) amplification of signal generation by cyclic enzymatic cascades. Lastly, we also hypothesize that the conventional 100 µl microtiter assays can be translated into capillary and microfluidic assay formats to further increase sensitivity.

1.7.2 Aims

The aims of this thesis is to initiate and develop different techniques for the development of a more sensitive immunoassay method to quantify the number of M13 virus particles, a model virus. The main objectives are:

1. To develop an enzyme amplification based immunoassay for the detection of the M13 phage by using traditional polystyrene surfaces and monospecific antibodies.

2. To study the use of a fused silica capillaries as an alternative surface for the demonstration of a sandwich assay by covalent immobilization of monoclonal antibodies by using heterobifunctional crosslinkers.

3. To assess the formation of virus-antibody complexes by using capillary electrophoresis.

25

1.7.3 Specific objectives

1. To purify the anti-M13 monoclonal antibody and investigate its multiple binding by electron microscopy.
2. To develop an enzyme-amplification based immunoassay by using monoclonal antibodies with AP as an enzyme label.
3. To covalently immobilize radiolabeled and unlabeled antibodies and other proteins on a fused silica capillary by using silanes and heterobifunctional crosslinkers as a first attempt to develop capillary sandwich assays.
4. To demonstrate virus-antibody complex formation by using capillary electrophoresis.

CHAPTER 2: Poly-homosandwich assay design for ultrasensitive immunoassay of M13 phage

2.1 Introduction

The major advances in immunoassays have focused on specificity (Winger et al., 1996), sensitivity, speed (Stanley et al., 1985) and convenience. New diagnostic markers have allowed for earlier therapeutic intervention than was possible previously. The ability to quantify the analyte concentration in the ultrasensitive range has the potential to identify very early disease at the asymptomatic stage or a residual and recurring disease several months and even years prior to its detection by conventional immunoassay procedures (Johannsson, 1985). Among the ultrasensitive methods available, the technique of enzyme amplification (Ishikawa et al., 1990; Hosogaya and Kume, 1995) is one of the most sensitive methods and is capable of detecting as little as 0.01 atto mole (am) of alkaline phosphatase (AP) (Johannsson et al., 1986).

The detection of viral or bacterial antigens and detection of the pathogen load present in body fluids is a desirable diagnostic or monitoring tool for many infectious diseases. In the case of HIV infection, for example, an HIV-antigen assay (Xu et al., 2002) or whole-virus assay (Fox, 1996) can be used for measuring the viral load to determine the prognosis of the infected individual and to monitor the effectiveness of the antiviral therapy (Pillay, 2002). Such a method would be better and more sensitive than the decrease in CD4+ blood cell counts (Aldhous et al., 1996.), which manifests much later in the time course of pathogenesis. Immunoassays are less expensive and are adaptable in almost all countries due to these assay's relative simplicity. Nucleic-acid-based qPCR/rtPCR methods (Ferre, 1994, Vandamme, 1994) are extremely sensitive and are plagued by the need for sample extraction, interference by a host of inhibitors, cost and complexity. These methods are more popular in the developed world and are a rarity in the developing or under-developed world.

27

In this study we describe the development of an enzyme-amplified ELISA for the detection of the M13 phage, a model virus, and also demonstrate that a sensitive immunoassay could be developed with monoclonal antibodies that could be extended for detection of medically important viruses such as HIV, hepatitis B and hepatitis C.

2.2   Materials and methods

2.2.1 Instrumentation

Optical density (absorbance) measurements were performed by using a Molecular Devices kinetic microplate reader (Molecular devices, USA).

2.2.2 Chemicals

The wild-type bacteriophage M13 and the *E. coli* strain JM109 were obtained from Dr. Bruce Malcolm, formerly at Department of Biochemistry, University of Alberta, Edmonton, Alberta. The p-Nitrophenyl phosphate (pNPP) microwell phosphatase substrate system was from Kirkegaard and Perry Laboratories Inc., Gaithersburg, MD, USA. NAD free NADP were purchased from Boehringer Mannheim GmbH, Germany. Alcohol dehydrogenase (ADH), p-iodonitrotetrazolium violet (INT-violet), diaphorase (EC 1.8.1.4), alkaline phosphatase (EC 3.1.3.1) from calf intestinal mucosa, bovine serum albumin fraction V, diethanolamine, streptavidin-alkaline phosphatase conjugate and Protein G-Sepharose 4B fast flow were purchased from the Sigma Chemical Co., St. Louis, MO, USA. The 96 well microtiter plates (Probind assay plates) were obtained from Becton Dickinson Labware, New Jersey, USA.

2.2.3 Antibodies and hybridomas

P93 is a murine hybridoma secreting anti-M13 phage monospecific MAb (IgG2a) previously developed in our laboratory (Liu, 1999). The antibody was purified by using Sephadex-protein G affinity chromatography (refer to section 2.2.5.2).

28

2.2.4 Purification and quantification of filamentous phage M13

Simple aqueous solutions of PEG and NaCl enable the bacteriophage either to be pelleted by brief low-speed centrifugation or to be settled out and be further concentrated by pressure filtration. With the appropriate procedure for a given bacteriophage, a further purification results in preparations free of PEG in yields of 65-95% based on the plaque-forming units (pfu) of crude lysates.

The wild-type M13 phage was purified by PEG precipitation by using the following procedure. 10 ml of *E. coli* (JM109 strain) were mixed with 200 μl of M13 bacteriophage stock (10^{13}/ml) and incubated for 20 min at RT. The infected *E. coli* was inoculated into four 1-liter flasks (5 ml. inoculate/flask) containing 250 ml of fresh media. The solution was incubated for 16 h at 37° C with constant vigorous shaking. It was centrifuged at 5000 rpm (g = 4420) for 20 min at RT in a Sorvall GS3 rotor, and the pellet discarded. *E. coli* supernatants were re-centrifuged at 8000 rpm (g=11300) for 10 min. PEG 8000 (39 ml of 20% PEG/2.5 M NaCl filtered stock solution per 310 ml phage suspension) was added to the *E. coli* supernatant to precipitate the phage, and these solutions were mixed and stored overnight at 4° C. The phage pellet was collected by centrifugation at 8000 rpm

(g =11300) for 40 min at RT. Supernatants were removed completely, and the pellet was re-suspended in 18 ml PBS. Excess PEG was removed by dialysis. The crude cultured and purified M13 phage was titered by a plaque-forming assay as described below.

2.2.4.1 Quantification of M13 phage

The phage solution was diluted in a logarithmic series in LB media (Bactotryptone 10 g/L, bacto-yeast extract 5 g/L and NaCl 10 g/L). A 100 μl volume from each dilution was mixed with 100 μl of fresh *E. coli* (JM109 strain) growing in a log phase (O.D.= 0.6-0.8) in a sterile tube and vortexed gently. After adding 3 ml LB top agar medium (LB medium plus bacto-agar 7 g/L) into the tube and gentle vortexing, the contents of this tube were immediately poured onto a plate containing 30-35 ml of hardened LB bottom agar

29

medium (LB medium plus bacto-agar at 15 g/L). The plates were incubated for 10 h at 37° C, and the plaques were counted.

2.2.5 Procedures

2.2.5.1 Ascites production

The best anti-M13 phage monoclonal antibody-producing hybridoma P93.1R1 was developed previously in our laboratory (Liu, 1999) and was used to produce ascites. Five Balb/c mice were primed with pristane (0.5 ml volume injected intraperitoneally). About 2.5×10^6 hybridoma cells were suspended in 250 µl of sterile PBS, and this suspension was intraperitoneally injected into the Balb/c mice after one week of pristane injection. The ascites was collected after 10 days by tapping the mice. An average of 1.5 ml of ascites were collected from each mouse. The pooled ascites were centrifuged at 2700 rpm for 10 min to pellet the cells. The ascites was collected and stored at -20° C.

2.2.5.2 Purification of MAb

The ascites or pooled culture supernatant was purified on a Sepharose protein G affinity column. The protein in the culture supernatant was precipitated by using 50% ammonium sulphate (w/v), and the solution was left overnight at 4° C with constant stirring. The precipitate was collected by centrifuging for 30 min at 3000 rpm. The precipitate was resuspended in 0.1 M sodium acetate pH 5 and dialyzed against 0.1 M sodium acetate (three times). The column was equilibrated with 0.1 M sodium acetate. The sample was loaded onto the column at a flow rate of 200 µl/min. The column was washed with 0.1M sodium acetate buffer until all unbound material was removed, as determined by UV monitoring at A_{280} with a UV monitor. The bound antibody was eluted with 0.1 M glycine buffer pH 2.7. The column was eluted at a flow rate of 400 µl/min, and 1 ml fractions were collected. 50 µl of 1 M tris pH 9 were added to each fraction (1 ml) to neutralize the acidity of the eluted fractions.

30

Alternatively, one volume of ascites was diluted in three volumes of PBS. The diluted ascites was filtered through a 0.8 μm filter and purified on a Sepharose protein G affinity column by following the same procedure described above.

Monoclonal antibody activity was determined by direct ELISA. The ELISA plate was coated overnight with the M13 phage at 10^6 phage/ml in PBS pH 7.2. The plate was washed three times with the PBS-T (PBS containing 0.05% tween-20) and blocked with 3% BSA in PBS. The plate was incubated for 1 h at RT. The plate was washed three times with PBS-T and tap-dried. A 100 μl volume of purified fractions was incubated with the antigen for 2 h at RT with constant shaking. The plate was washed three times with PBS-T. The plate was tap dried. Goat anti-mouse IgG-AP conjugate at 1:500 dilution in 1% BSA in PBS was dispensed in each well and incubated for 1 h at RT with constant shaking. The plate was washed three times with PBS-T and dried by tapping. A pNPP (100 μl) substrate was added to each well. The reaction was run for 20 min. The absorbance was read at 405 nm.

2.2.5.3 Preparation of anti-M13 antibody-biotin conjugate

Biotin was covalently coupled to IgG by using the N-hydroxysuccinamide ester of long chain biotin (LCB-NHS). The LCB-NHS was dissolved in DMSO to achieve a final concentration of 3 mg/ml. A 10 μl aliquot of the biotin solution was immediately added to 1 ml of 2 mg/ml MAb solution and mixed. The reaction mixture was left at RT for 50 min. The reaction was terminated by adding 1 mg of solid glycine. The excess of biotinylated glycine was removed by dialyzing the solution for 24 h to 48 h against 800 ml volume of PBS at 4° C. 0.1% (w/v) sodium azide was added as a preservative. The solution was aliquoted and stored at -20° C.

2.2.6 Enzyme amplification reaction

2.2.6.1 Dephosphorylation of NADP (preamplifier solution)

NADP (NAD-free) was dissolved in a 0.9 M diethanolamine buffer pH 9.5 to a final concentration of 0.2 mM. The buffer also contained 1 mM $MgCl_2$ and 0.1 mM $ZnCl_2$. A 100 µl aliquot of this solution was dispensed into a microtitre plate containing 10 µl of alkaline phosphatase. The reaction was allowed to run for 20 min at RT before addition of the amplifier.

2.2.6.2 Amplifier

For each 10 ml of the amplifier solution, 500 units of alcohol dehydrogenase and 25 units of diaphorase were dissolved in a 25 mM sodium phosphate buffer pH 7.2, which also contained 4 % (v/v) ethanol and 0.55 mM INT-violet.

A 100 µl aliquot of the 0.2 mM NADP in a 0.9 M diethanolamine buffer pH 9.5, containing 1mM $MgCl_2$ and 0.1mM $ZnCl_2$ were added to the wells, and dephosphorylation of NADP was allowed for 20 min. At the end of 20 min, 200 µl of the amplifier solution were added, and the absorbance was read at 490 nm after 5 min. The sensitivity of the amplifier solution to detect NAD molecules was tested.

2.2.6.3 Alkaline phosphatase

The calf intestine alkaline phosphatase was diluted in a 0.9 M diethanolamine buffer pH 9.5. Different molar dilutions of the alkaline phosphatase were made based on a molecular weight of 140 kDa. A 10 µl aliquot of AP with a varying number ranging from 10 molecules to 10^6 molecules was added to each well in triplicate. 100 µl of the preamplifier solution containing 0.2 mM NADP were added to each microtiter plate well. The samples were incubated at room temperature for 3 h with shaking. 200 µl of

32

amplifier solution were added to each well. The reaction was stopped after 5 min incubation by adding 50 µl of 0.4 M HCl. The absorbance was measured at 490 nm.

2.2.7 Development of ultrasensitive ELISA for detecting viral antigen

2.2.7.1 Homosandwich solid phase enzyme immunoassay

The homosandwich solid phase immunoassay format is used in most clinical virology laboratories. In homosandwich assays the antigen or the antibody is bound to a solid surface, which can be the surface of a test tube, a polypropylene microwell or a plastic bead. For antigen detection, a known viral antibody is coated onto the solid surface (100 µl of a 10-20 µg/ml for ~16 h, washed, and blocked with 200 µl of 1% BSA). The antibody-coated solid phase is exposed to 100 µl of the test material, a clinical sample from the patient or a suspension of virus-infected cells from a cell culture. The test material is allowed to react with the bound antibody. The unbound test material is washed away. The bound antigen is detected directly (by using the detector antibody conjugated to an enzyme label) or indirectly (by using a second enzyme-labeled anti-species antibody following the detector). The bound antibody-enzyme is detected by incubating with the enzyme-specific substrate solution. It reacts with the enzyme, and the amount of product so formed is determined spectrophotometrically. Sandwich assays have been developed for a number of viruses {e.g., rotavirus (Gerna et al, 1989, Kelkar et al., 2004), influenza and RSV (Gerentes et al., 1998)} and several are available as commercial kits.

2.2.7.2 Conventional ELISA

The M13 phage was also detected by using the conventional alkaline phosphatase substrate pNPP instead of the enzyme amplifier solution. The color was developed for 30 min, and the absorbance was read at 405 nm (Figure 4).

33

For each sample, the mean absorbance value of the test wells minus the mean absorbance value of the negative controls was calculated. The lower limit of detection was calculated by extrapolating the mean of 20 replicates of the blanks plus the two SDs.

2.2.7.3 Enzyme amplified ELISA

A microtiter plate was coated with protein G affinity purified anti-M13 monoclonal antibody (20 µg /ml) and stored overnight at 4° C. The plate was washed three times with PBS-T (PBS containing 0.05% tween-20) and tap-dried. The plate was blocked with 3% BSA in PBS pH 7.2 for 1 h at RT. A 100 µl aliquot of the phage with a varying concentration ranging from 10 pfu to 10^6 pfu was added to each well in triplicate, and the plate was incubated at RT for 3 h with constant shaking. The plate was washed three times with PBS-T (PBS containing 0.05% tween-20). A 100 µl aliquot of biotin conjugated-anti-M13 MAb in 1% BSA in PBS (5 µg/ml) was added and incubated for 2 h, followed by washing three times with PBS-T. The plate was tap-dried. Streptavidin-AP conjugate was added to the microtiter well at 1:500 dilution in 1% BSA in PBS (100 µl each well). The plate was incubated for 1 h at RT with shaking and washed with PBS-T three times and tap-dried. A 100 µl aliquot of NADP substrate buffer was dispensed, and the dephosphorylation was done for 20 min at RT. The amplification cycle was started by adding 200 µl of amplifier solution. The enzyme reaction was stopped after 5 min by adding 50 µl of 0.4 M HCl. The optical density was recorded at 492 nm by using a microtiter plate reader.

2.2.8 Electron microscopy (with the assistance of Mr. Richard Sherbourne of Medical Microbiology and Infectious Diseases)

The phage particles were purified by $CsCl_2$ gradient and subjected to reduction with $NaBH_4$ (Lopez and Webster, 1983). Phage samples were prepared in logarithmic dilution. Subsequently, the phage samples were incubated at 70° C for 10 min and adsorbed onto

34
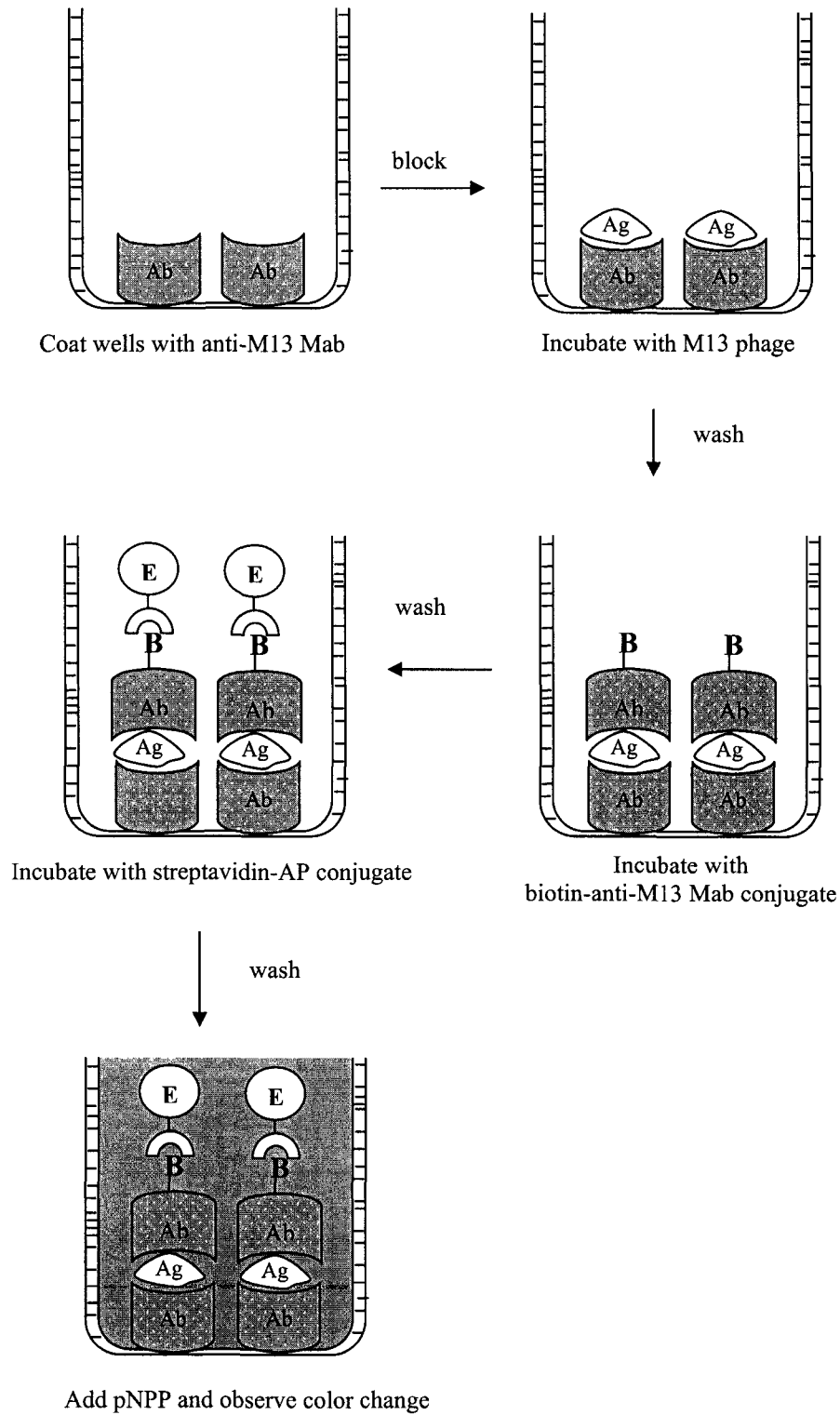
Figure 4: Solid phase sandwich immunoassay for the detection of M13 phage particles. Ag = antigen; Ab = antibody; B = biotin; E = enzyme

35

carbon-coated 400 mesh nickel grids for 10 min at RT. After a brief rinse in Tris buffer containing 0.1% BSA, the grids were floated for 30 min on 10 μl drops of anti-phage MAb. The anti-phage monoclonal antibody was incubated at different concentrations (diluted in TBS 0.1% BSA to 1.6 mg/ml, 1.25 mg/ml, 1 mg/ml and 0.8 mg/ml). The grids were washed for 10 min in TBS 0.1% BSA followed by washing three times with TBS for 5 min. The grids were floated for 30 min on 10 μl drops of the secondary antibody (anti-mouse IgG gold conjugate diluted 1:25 in TBS 0.1% BSA). The grids were washed with TBS-0.1% BSA for 5 min followed by a wash with TBS for 2 min and a final wash with distilled water for 2 min. The grids were negatively stained with 2% uranyl acetate 2.5% DMSO. The grids were examined under the electron microscope.

2.3   Results

2.3.1 Purification and biotinylation of anti-M13 monoclonal antibody

The monoclonal antibody was purified by using the Sepharose protein G affinity column. The purified antibody fractions were detected for immunoreactivity by using the direct ELISA. The concentration of antibody in each eluted fraction was measured spectrophotometrically at 280 nm (Figure 5). The molar extinction coefficient was taken as 1.44, i.e., a mouse IgG solution at 1 mg/ml = 1.44 absorbance units (Current Protocols in Immunology, supplement 21, Section 11.11.3). The yield for the purified MAb antibody was 1 mg of antibody per ml of the ascites fluid. The antibody was biotinylated and dialyzed against PBS. The concentration of the biotinylated antibody was determined by using the Bradford assay (Bradford, 1976).

2.3.2 Purification of M13 virus and titration

The M13 phage crude lysate was purified by using a PEG precipitation method in which PEG and aqueous solutions of NaCl enable the bacteriophage either to be pelleted by brief low-speed centrifugation or to be settled out. The preparation was dialyzed with

36
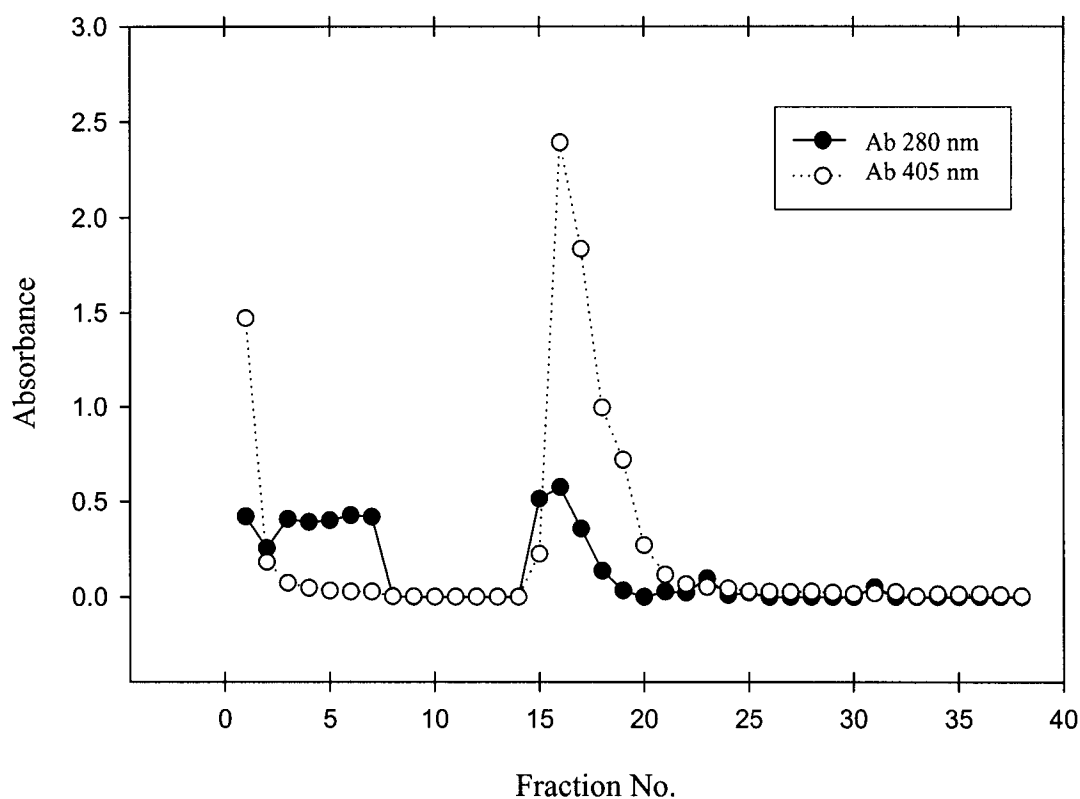
Figure 5: Purification profile of anti-M13 monoclonal antibody on Sephadex protein G affinity column

The monoclonal antibody was purified by using the Sepharose protein G affinity column. The purified antibody fractions were examined for immunoreactivity by using direct ELISA wherein the M13 phage was coated on the probind 96 well ELISA plate at 10^6 phage particles/ml. A 100 μl aliquot of each purified antibody fraction were tested in each well. The immunoreactivity was determined by using anti-mouse IgG-AP conjugate in 1% BSA in PBS. The colour was developed by using a pNPP substrate, and the absorbance was read at 405 nm.
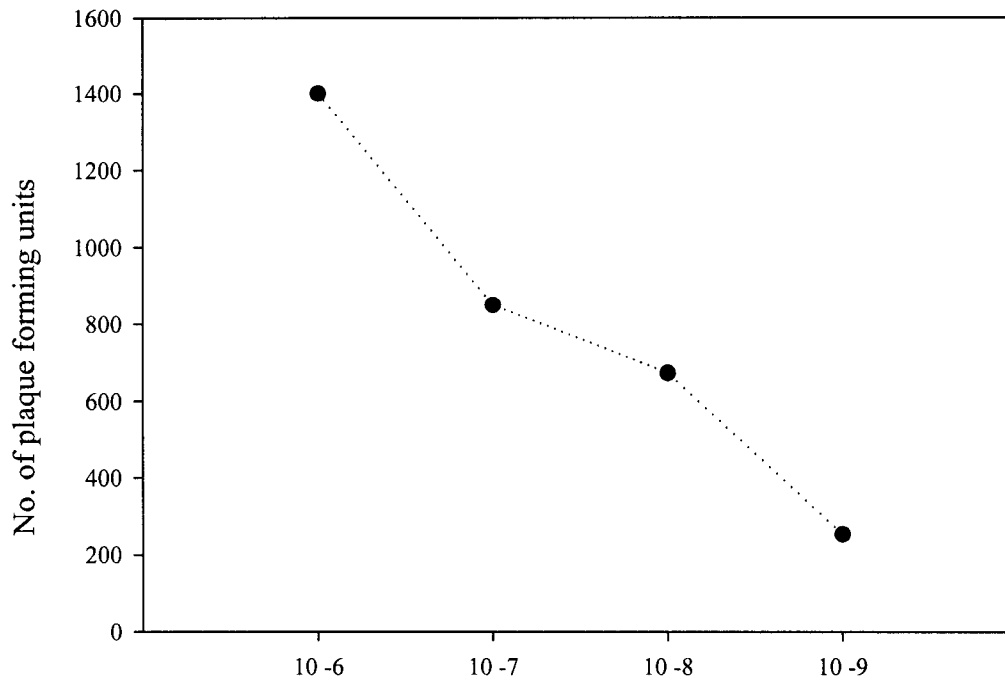
Dilutions of standard M13 phage solution

Figure 6: Plaque forming assay: titration curve for M13 phage particles

The phage solution was diluted in a logarithmic series in LB media (Bactotryptone 10 g/L, bacto-yeast extract 5 g/L and NaCl 10 g/L). A 100 µl volume from each dilution was mixed with 100 µl of fresh *E. coli* (JM109 strain) growing in a log phase (O.D. = 0.6-0.8) in a sterile tube and vortexed gently. After adding 3 ml LB top agar medium (LB medium plus bacto-agar 7 mg/L) into the tube and gentle vortexing, the contents of this tube were immediately poured onto a plate containing 30-35 ml of hardened LB bottom agar medium (LB medium plus bacto-agar at 15 g/L). The plates were incubated for 10 h at 37° C, and the plaques were counted.

PBS before quantitation of the M13 phage. Figure 6 shows the titration curve for the purified M13 phage at different logarithmic dilutions.

2.3.3 Electron microscopy

To visually demonstrate the multiple decoration of antibodies on the entire length of the M13 virus, electron microscopy was performed with M13 + P93, followed by gold-labeled anti-mouse antibodies. As Figure 7 reveals, the gold-conjugated secondary antibody decorates the phage particle completely. In other words, several hundred gold-conjugated antibodies bind to the hundreds of coat proteins on the phage particle. This decoration with immunoconjugate was observed at a concentration of 10^{13} phage/ml and at 1 mg/ml concentration of the detector antibody. This multiple decoration of the phage particles by the antibody represents one level of amplification. This decoration could also mean more avidity for the M13 phage when adsorbed onto a solid phase, providing the theoretical basis for an efficient, ultrasensitive homosandwich assay.

2.3.4 Assay development and optimization

The filamentous bacteriophage M13 has 2600-2700 copies of the coat protein (gene VIII) encapsulating its single-stranded DNA. Hence, we adopted a homosandwich format to detect the virus. This format employs the same P93 MAb as the solid phase capture and uses biotin-labeled P93 as the detecting agent. The assay was run in a solid-phase sandwich immunoassay format. The ELISA plate was coated with the capture antibody (anti-M13 monoclonal antibody) at 20 μg/ml. The plate was blocked with 1% BSA solution in PBS, followed by incubation with the M13 phage. The detector antibody (biotin-labeled anti-M13 Mab) was incubated to form the homosandwich. Biotin was detected by streptavidin-AP conjugate by reacting the conjugate with its substrate, p-nitrophenyl phosphate (pNPP). The absorbance was read at 405 nm.

The detector antibody (the anti-M13 monoclonal antibody) was conjugated to biotin by the process described in Section 2.2.5.3. To determine the optimum concentration of the

39

Figure 7: Electron microscopy of M13 phage: 30667X magnification

Phage particles were subject to reduction with $NaBH_4$. The phage samples were incubated at 70^0 C for 10 min and adsorbed onto carbon-coated 400-mesh nickel grids for 10 min at RT. After a brief rinse, the grids were floated for 30 min on 10 µl drops of anti-phage MAb

(1 mg/ml in TBS 0.1% BSA). The grids were washed with TBS for 5 min. To label the phage with solid particles the grids were floated for 30 min on 10 µl drops of the secondary antibody (anti-mouse IgG gold conjugate diluted 1:25 in TBS 0.1% BSA). The grids were washed and were negatively stained with 2% uranyl acetate 2.5% DMSO. The grids were examined under the electron microscope.

40

phage particles and the biotin-conjugated detector antibody, different dilutions of the detector antibody were tested at different log dilutions of the M13 phage, starting from 10 phage/ml to 10^{10} phage/ml. The detector antibody was tested at different dilutions starting from 10 μg/ml, or a 1:100 dilution of the stock (1 mg/ml), to a 1:400 dilution of the stock. Figure 8 show that the 1:100 dilution or 10 μg/ml gave a better absorbance for any given amount of phage particles in the range tested. In other words, a higher concentration provided a greater range and limit of detection. The same experiment was repeated again, but this time, the number of phage particles were kept constant at 10^6 phage/ml. In this study for the 10^6 phage/ml concentration, 10 μg/ml biotin-conjugated detector antibody in 1% BSA gave relatively higher absorbance for the same number of M13 phage particles (Figure 9). However, the data shows that at concentrations below 2 μg/ml of the detector antibody, the signal is pretty much flat and does not show a dose dependent response.

2.3.4.1 Conventional M13 homosandwich ELISA

A conventional homosandwich ELISA was run by using a commonly employed substrate pNPP. The ELISA plate was coated with the M13 monoclonal antibody followed by blocking with 1% BSA. Different dilutions of the M13 phage were incubated with the immobilized monoclonal antibody. The M13 phage was detected by using biotinylated anti-M13 MAb. Streptavidin-AP conjugate was used as the detector enzyme conjugate. The enzyme was detected by using pNPP. The absorbance was read at 405 nm. The lower limit of detection was found to be 10^6 M13 phage/ml.

2.3.4.2 Enzyme amplification reaction

2.3.4.2.1 Amplifier

The conventional pNPP substrate, although widely used in AP-labeled reactions has poor sensitivity. In order to increase the sensitivity of the assay system, we tested the cyclic

41
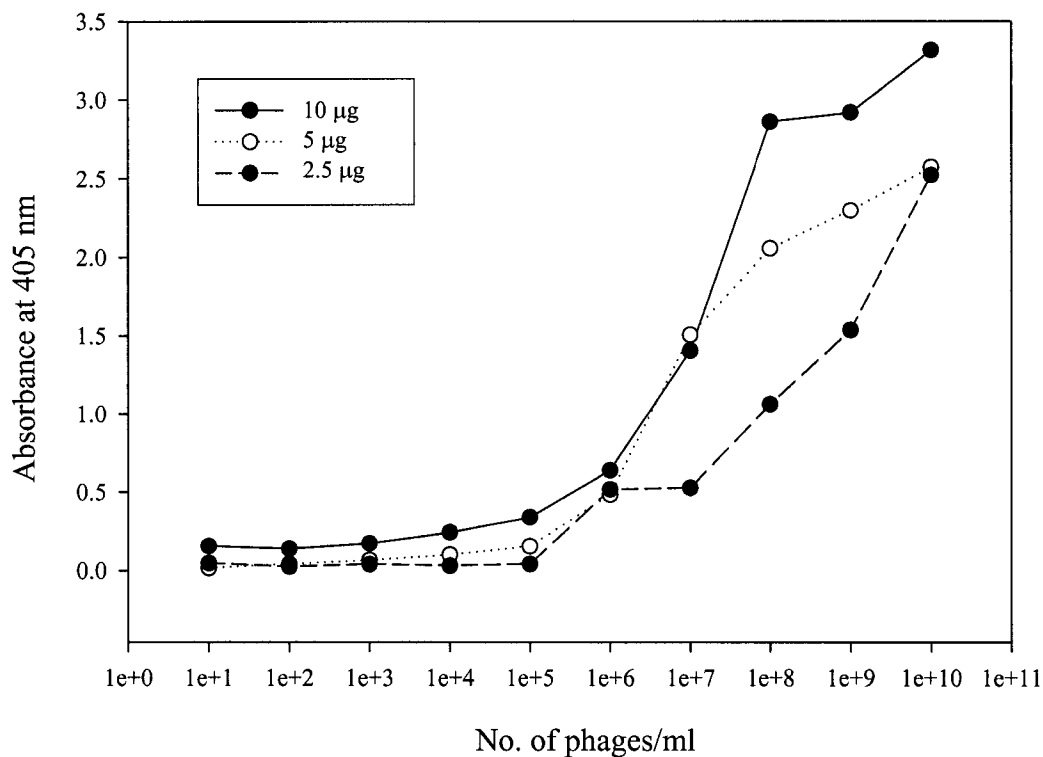
Figure 8: Effect of different concentrations of the analyte and the biotin labeled detector antibody on the detection of phage particles

The Probind assay plate was coated with capture antibody, anti-M13 monoclonal antibody at 20 µg/ml. The plate was blocked with 1% BSA solution in PBS followed by incubation with different dilutions of the M13 phage. The detector antibody, biotin-labeled anti-M13 MAb, was incubated at different dilutions. Bound biotin was detected by using a streptavidin-AP conjugate, and the absorbance was read by reacting the conjugate with the substrate, pNPP. The absorbance was read at 405 nm. For any given concentration of M13 phage particles, a 10 µg/ml detector antibody concentration gave higher absorbance compared to the absorbance given by 5 µg/ml and 2.5 µg/ml concentrations.
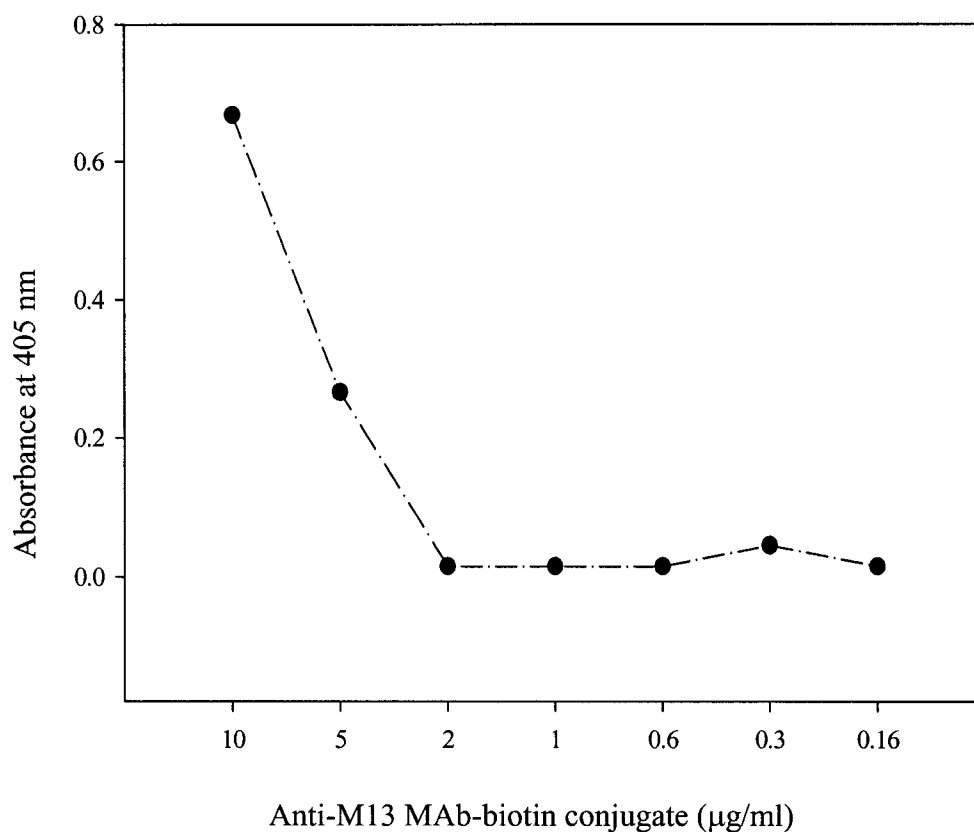
Figure 9: Effect of different concentrations of detector antibody for a fixed amount of phage particles (10⁶/ml)

The Probind assay plate was coated with capture antibody, anti-M13 monoclonal antibody at 20 μg/ml. The plate was blocked with 1% BSA solution in PBS followed by incubation with the M13 phage at 10^6 phage/ml. The detector antibody, biotin-labeled anti-M13 MAb, was incubated at different concentrations. Biotin was detected by using the streptavidin-AP conjugate, and the absorbance was read by reacting the conjugate with the substrate, pNPP. The absorbance was read at 405 nm. It was observed that a 10 μg/ml biotin-conjugated detector antibody in 1% BSA gave relatively higher absorbance for the same number of M13 phage particles while the other concentrations gave a much reduced response.

43
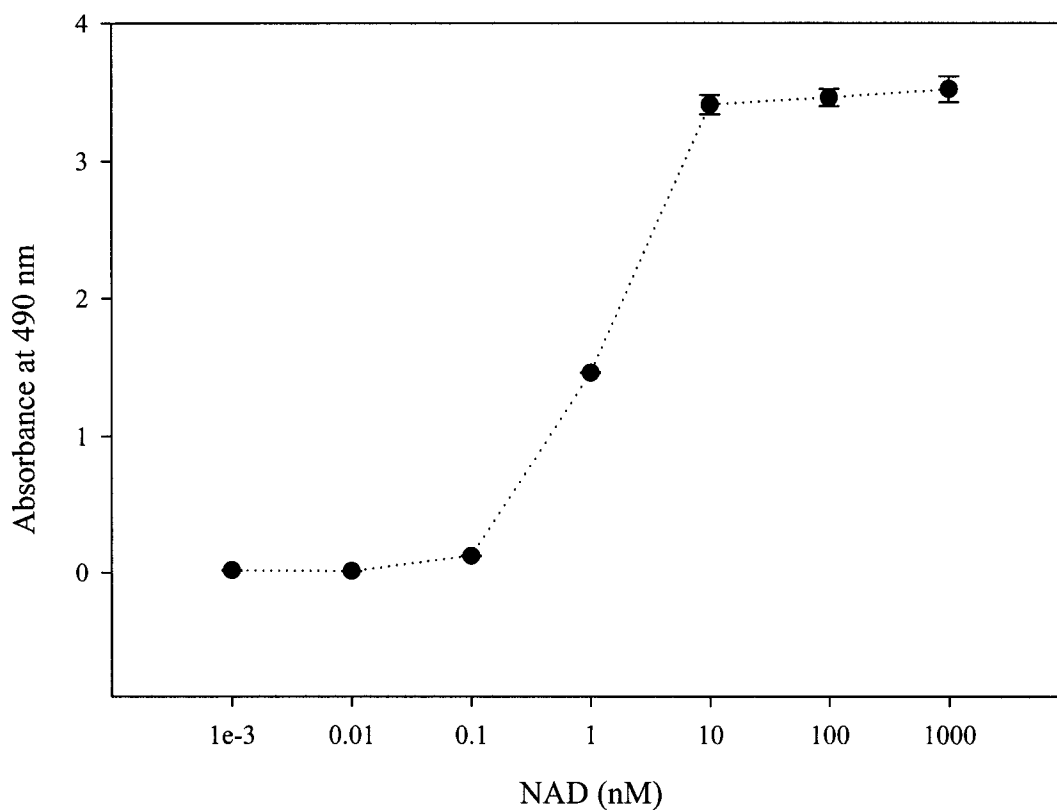
Figure 10: Detection of NAD molecules by using the enzyme amplification cycle

NAD was dissolved in a 0.9 M diethanolamine buffer at pH 9.5 at different concentrations starting from 0.001 nM to 1000 nM. 100 μl of this solution were dispensed onto a microtitre plate. 200 μl of the amplifier solution were added to each well. The absorbance was read at 490 nm . The cut-off value was calculated as the sum of the mean of the blanks plus 2 SDs. The cut-off was found to be 0.217, giving a LLD of 0.1 nM NAD.

44
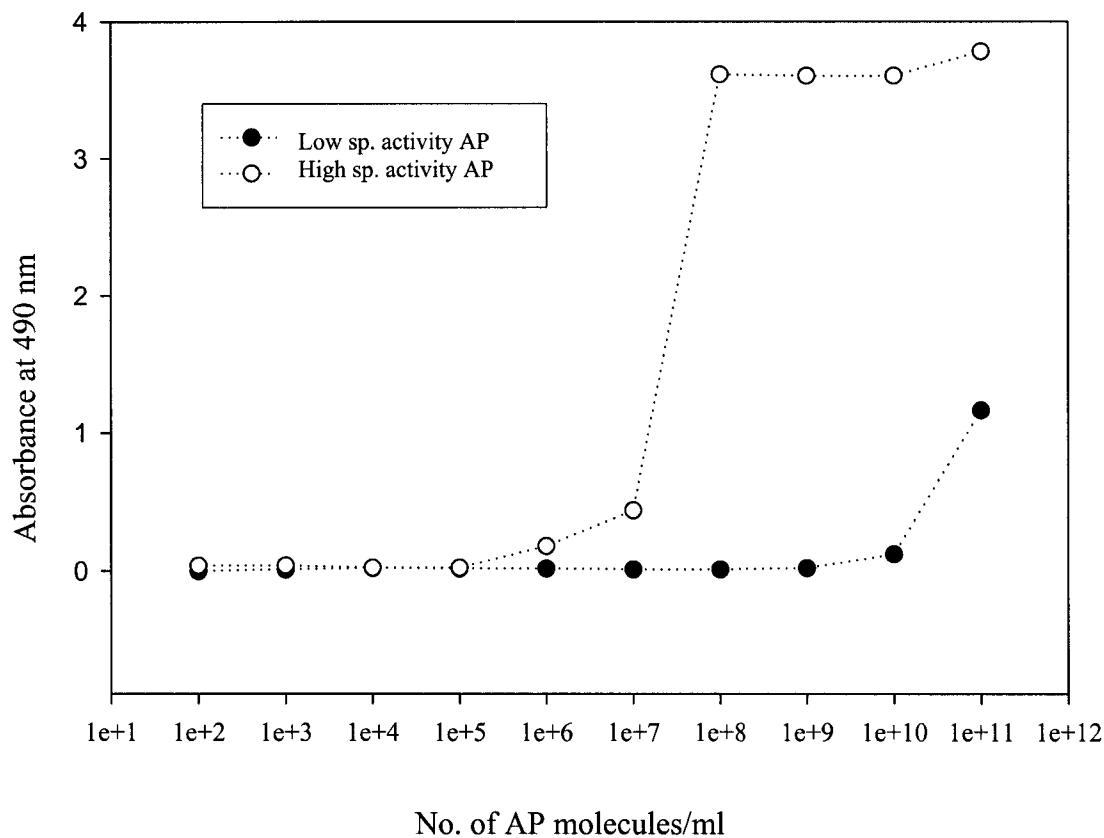
Figure 11: Detection of AP molecules by using the enzyme amplification cycle

10 μl of aliquots of different dilutions of AP were added to 100 μl of the substrate buffer containing 0.2mM NADP in microtiter plate wells. The samples (triplicate) were incubated at room temperature for 3 h. 200 μl of amplifier solution were added to each well, and the absorbance was measured after 5 min of incubation with the amplifier. The LLD was found to be 10^5 AP molecules or ~ 600 zeptomoles with the high specific activity AP.

45

amplification methodology (Johannsson et al., 1985) . The basic principle of this method is shown in Figure 3. We initially tested the various components of the amplification cascade. The sensitivity of the amplifier solution was tested by using NAD solution at different concentrations. Figure 10 shows the absorbance obtained at different concentrations. The lower limit of detection is calculated as the mean of the blanks plus 2 SDs, which gave a sensitivity of 0.1 nM NAD or 10 femto moles in 100 µl. Figure 10 shows that the rate of the reaction increased at an optimum concentration and that any excess of the substrate NAD tended to form a plateau. The absorbance was read after 5 min of incubation with the amplifier solution.

2.3.4.2.2 Detection of enzyme label

Two AP-specific activities were tested. To assess the sensitivity of the total system, AP was taken in different dilutions and allowed to react with NADP and subjected to the amplification cycles described in materials and methods Section. Figure 11 shows the dose response curve with the mean values (±SD). The sensitivity was assessed as the mean of the blanks+ 2SDs of the absorbance of the blank determinations. The lower limit of detection was found to be 10^5 molecules of AP in 10 µl of volume. The sensitivity for AP was higher with increased specific activity of the AP.

2.3.4.3 *Ultrasensitive ELISA for detecting viral antigens*

A solid-phase homosandwich ELISA was carried out for the detection of the M13 phage. The microtiter well was coated with the M13-specific monoclonal antibody. Aliquots of different dilutions of the M13 phage were incubated, and a sandwich was formed by incubation with anti-M13 MAb-biotin-streptavidin-phosphatase conjugate. The strength of signal observed was a function of the concentration of the phage particles. The enzyme label was developed by using two different methods. In conventional ELISA, p-nitrophenyl phosphate was used as a substrate wherein p-nitrophenyl phosphate was dephosphorylated to p-nitrophenol, and the absorbance was read at 405 nm for 30 min. In the enzyme amplified ELISA, the enzyme label, alkaline phosphatase, dephosphorylated

46
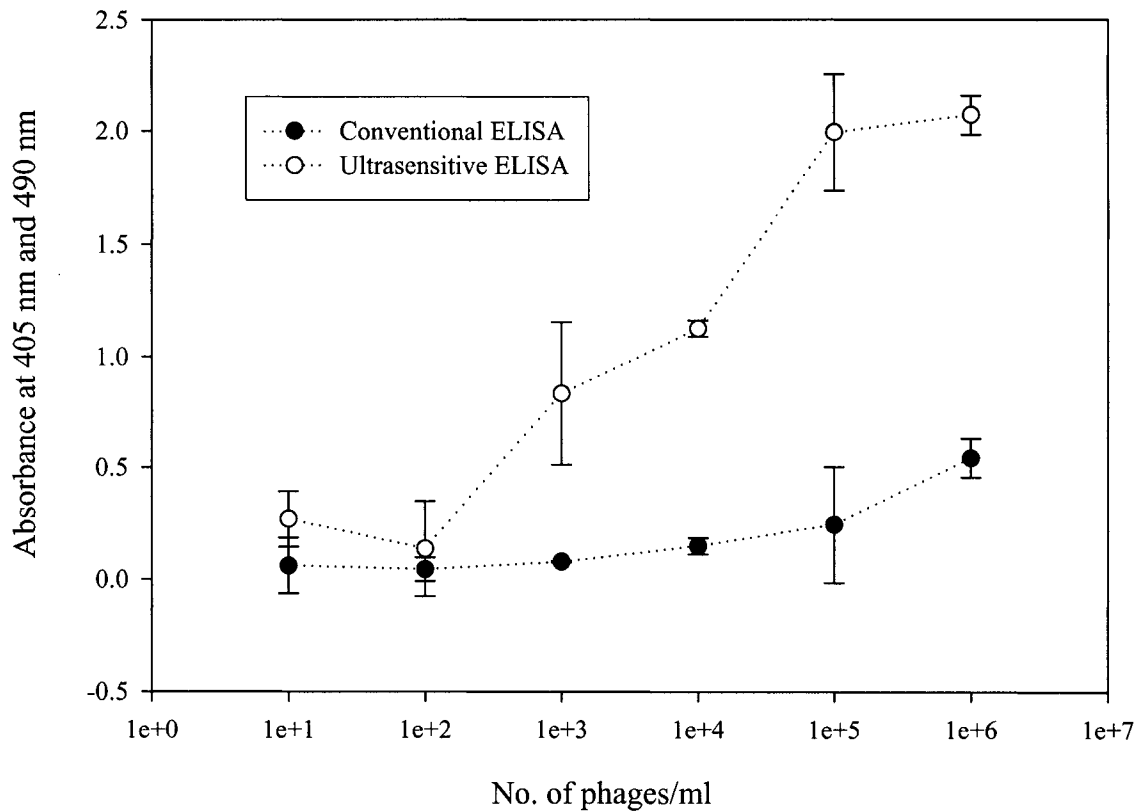
Figure 12: Comparison of ultrasensitive and conventional immunoassay

The microtiter well was coated with the M13-specific monoclonal antibody. Aliquots of different dilutions of the M13 phage were incubated, and a sandwich was formed by incubation with anti-M13 MAb-biotin-streptavidin-phosphatase conjugate. The enzyme-labeled AP was detected by using either the enzyme-amplification cycle (Absorbance read at 490 nm) or pNPP (absorbance read at 405 nm). The lower limit of detection (LLD) for the enzyme-amplified ELISA was determined to be 100 phage particles per 100 μl of volume. The LLD for the conventional ELISA was found to be 10^5 phage particles per 100 μl of volume (n=3). The LLD was calculated as mean of 20 blanks ± 2 SD.

47

$NADP^+$ to NAD^+, which entered a specific redox cycle wherein INT-violet was converted to a intensely red formazan dye (Figure 3). The absorbance could be read at 490 nm for the 1-10 min interval. The absorbance was directly related to the amount of NAD molecules formed, or indirectly, to the concentration of the viral particles in the sample.

The dose-response curve of the assay is shown in Figure 12. The reaction was stopped after 5 min incubation with the amplifier, and the absorbance was read at 405 nm. Measurements were taken as the mean of three replicates of the same standard. The lower limit of detection was taken as the mean of 20 replicates of the zero standard + 2 SDs. The LLD was determined to be 100 phage particles per 100 µl or 10^3/ml, which is equivalent to the 2.3 fg of the coat protein or 160 zepto moles.

Alternatively, conventional immunoassay was also run by using pNPP (alkaline phosphatase substrate). Figure 12 also shows the remarkable difference in the limit of detection when compared to that of the enzyme-amplified ELISA for the detection of the M13 phage. A 1000-fold increase in signal occurred when the enzyme-amplified ELISA procedure was used. The lower limit of detection for the conventional ELISA was found to be 10^5 phages per 100 µl or 10^6/ml compared to the enzyme amplified ELISA for the detection of the M13 phage. It is evident that there is a 1000 fold increase in signal when the enzyme amplified ELISA procedure is used. The lower limit of detection for the conventional ELISA was found to be 10^5 phage per 100 µl.

2.3.4.3.1 Precision

"Precision" is defined as the degree of mutual agreement among a series of individual measurements, values, or results; often, but not necessarily, expressed by the standard deviation. The precision of the assay was investigated for the M13 homosandwich immunoassay. Table 3 also shows the precision profile of the present immunoassay wherein the CV% range is 0.69 - 8.8%. Within the assay, precision was measured by assaying the 3 replicates of the same standard and 3 replicates of the control samples in a single assay. Inter-assay precision was obtained by measuring the absorbance in 2

48

different runs on different days and was higher than 10%, indicating the need to further improve the optimization of the assay system.

Table 3: Precision of present M13 phage assay *(Section 2.3.4.3.1)*

Within Run		
M13 phage/100 μl	Mean SD	CV%
10^2	.019	0.6
10^3	.038	5.7
10^4	.132	8.8
10^5	.110	2.4
10^6	.019	2.1
Between Runs		
10^2	.095	9.4
10^3	.154	9.25
10^4	.396	22.1
10^5	.701	28.7
10^6	.059	1.93

2.4 Discussion

The basic strategy of polyhomosandwich assays exploits the common surface repeat antigen or epitope architecture of viruses, bacteria and even spores (e.g., anthrax). This design incorporates multiple capture, multiplicity of distal decoration and enzyme amplified detection.

Electron microscopy was conducted to explore the immunoreactivity and the immunodetection of the phage particles. Figure 7 reveals the gold-conjugated secondary antibody decorated the phage particle completely. In other words, several hundred gold-conjugated antibodies bound to the hundreds of coat proteins on the phage particle was

49

observed confirming results from an earlier study (Lopez and Webster, 1983). This multiple decoration of the phage particles by the antibody could mean more avidity for the capture of phage when adsorbed onto a solid phase, providing the theoretical basis for an efficient homosandwich assay at low virus input. In the subsequent incubation step, the solution phase biotin-labeled MAb had the propensity to bind the distal (to the solid phase) unoccupied epitopes, again in a multiple fashion. Hence, the first and second steps provided two levels of amplification.

The enzyme-amplification-based ELISA was developed as the third level of amplification, and an increased sensitivity was demonstrated for the detection of the viral particles. The cyclic amplification ELISA was shown to have a much higher sensitivity compared to that of the conventional pNPP substrate-based color development (Self, 1985; Stanley et al., 1985).

The biotin-labeled monospecific monoclonal detector antibody was comparable in its sensitivity to the bispecific antibody (Liu et al., 2003). Liu (1999) followed a similar ELISA format to develop an ultrasensitive ELISA for the detection of the M13 phage, by using bispecific monoclonal antibodies as a detector instead of the monospecific monoclonal antibodies. This bispecific monoclonal antibody had one arm specific for the M13 phage and the other arm specific for the AP. The LLD was reported to be 100 phage particles per 100 μl of volume. This result was the same as reported here by using monoclonal antibodies. The monospecific monoclonal antibodies has the advantage of a potentially bivalent high-avidity binding to the surface of the M13, perhaps explaining the MAb's ability to be as good as the bispecific antibody (Liu et al, 2003). With further work on the design of a bivalent, bispecific Mab, the latter could have the additional advantage of being able to push the detection limit below 100 particles.

The enzyme amplification cycle was employed, as it has been proven a highly sensitive amplification technique for immunoassays (Self, 1985; Cook and Self, 1993). The major crux of the whole amplification process is the tremendous amplification of signal for each molecule of AP that is bound to the detector antibody. For each molecule of NADH generated, ~ 600 molecules of formazan dye may be produced by a redox amplification

50

system in ~ 10 min (Johannsson et al., 1986). The formazan dye color is conveniently read colorimeterically. The dynamic range could also be increased by means of kinetic ELISA techniques (Vander et al., 1994).

Electron microscopy failed to detect any virus particle at lower phage concentrations. This failure could have been because electron microscopy needs a higher count of phage particles to be visible under the microscope. This decoration with immunoconjugate was observed at a concentration of 10^{13} phage/ml and at 1 mg/ml concentration of the detector antibody. This multiple decoration of the phage particles by the antibody represents one level of amplification. The decoration of the gold particles all along the surface of M13 indicates visually the expected multiplicity of epitope-paratope interactions. The amplification technique has the advantage of amplifying the signal many fold, and a small trace of AP molecules conjugated on the probe can easily be detected (Self, 1982). This system or the model described here could potentially be extended to design body fluid assays for the detection of the various medically important virus particles such as HCV, hepatitis and HIV or related viruses. However, M13 is an ideal model, and pathogenic viruses have additional features that may present unique challenges. Firstly, not all viruses are filamentous, for many are roughly spherical, and hence, geometry may decrease the magnitude of avidity-based capture by the solid phase.

Filamentous viruses such as Ebola (Casillas et al., 2003), Marburg (Roberts and Kemp, 2001) and tobacco mosaic viruses (Turpen, 1999) can be potentially better detected than non-filamentous viruses (on the basis that the filamentous viruses have a larger surface). Secondly, shed viral antigen monomers may be present, potentially interfering and reducing sensitivity. Lastly, natural IgM and IgG antibodies in serum (Meurman, 1983; Richman et al., 1984) against viral proteins could also interfere in the assay design (Plebani et al., 1986; Ho et al., 1989). The dissociation and inactivation of the antibody may hence be required. Nevertheless, the increase in sensitivity by using the enzyme-amplification system could allow for the detection of the lower concentrations of the viral antigen, compared to the detection of anti-viral antibodies. The latter provides

51

information about only the exposure to the virus and not the current status of infection or the viral load.

The current assay was designed for use with the biotin-streptavidin-phosphatase conjugate system (BS-ELISA) (Mortensson and Kjeldsberg, 1986). In the BS-ELISA, the biotin-labeled antibody was used in combination with the streptavidin-alkaline phosphatase complex. This BS-ELISA inherits many advantages from this complex, for biotin is a small molecule and can easily be covalently coupled to an antibody without affecting the antigen-antibody binding capacity. As well, one molecule of streptavidin can bind four molecules of biotin, giving streptavidin the added advantage of increasing the sensitivity of detection (Nerurkar et al., 1984; Gould et al., 1985).

The results of our investigation clearly revealed the superiority of the enzyme-amplified poly-homosandwich ELISA over the conventional assays. The amplified ELISA showed higher sensitivity and was as easy to perform as the conventional ELISA. The use of the amplified ELISA could be extended as a routine ELISA for ultrasensitive detection of medically important viruses, bacteria and spores.

CHAPTER 3: Capillary sandwich assay

3.1 Introduction

Different immunosensor techniques have been available for immobilizing the antibodies and other proteins on the silica surface for monitoring antigen-antibody interactions and immunoassays. The different immunosensors are based on optical, electrochemical or piezoelectrical methods. The protein can be adsorbed on the silica surface or covalently immobilized as an alternative approach (Wood and Gadow, 1983). The protein can be covalently immobilized to increase its stability and to minimize the loss of the immobilized protein upon exposure to harsh conditions as in the case of the regeneration of the sensor surface or a capillary column (Jonsson et al., 1985). The chemistry of the immobilization of the proteins, the amount of protein immobilized, and its stability are influenced by the pH and ionic strength. Other factors influencing the experimental results are the uniformity, stability and reproducibility of the immobilization of the proteins on the solid surface. (Jonsson et al., 1985). These factors could be of importance in experiments where immobilized protein is signalled by a change in the refractive index or any surface physical factor, e.g., immunosensors based on optical (Parry et al., 1990), electrochemical (Chetcuti et al., 1999) or piezoelectrical methods (Halamek et al., 2002). These methods measure directly the change in surface concentration on a solid surface when an antigen interacts with an immobilized antibody.

Capillary electrophoresis has been used in conjunction with laser-induced immunofluorescence (LIF) to develop immunoassays (Chen and Dovichi, 1994). Dr. Norm Dovichi, Department of Chemistry, University of Alberta, has been successful in detecting a single molecule of alkaline phosphatase by using capillary electrophoresis and LIF. This very fact led us to collaborate with Dr. Dovichi's lab. It was hypothesized that the homosandwich ELISA, described in Chapter 2, could be run on a fused silica capillary surface where the signal molecule, alkaline phosphatase, could be detected by using capillary electrophoresis and the signal could be amplified by using LIF.

53

Although high surface densities have been obtained for antibodies immobilized on silica, the major obstacle to the detection of antigens or haptens is the non-specific binding of foreign molecules to the sensing surface (Ahluwalia et al., 1992). As a prerequisite, we had to study the silica surface and various conditions that could influence the immobilization of antibodies and proteins on the silica surface.

The present chapter describes the immobilization of the proteins on the silica surface by using heterobifunctonal crosslinkers to explore capillary sandwich assays. The clean silica surface is initially coated with silane film. A heterobifunctional crosslinker with different reactive groups on each end is coupled to silane at one end. The free end of the cross linker forms an amide bond with the terminal amino group on the protein (Bhatia et al., 1989; Shriver-Lake et al., 1997).

3.2   Materials and methods

3.2.1 Apparatus

Capillary filling apparatus: The set-up was used to push liquid into the uncoated fused silica capillary (from Composite Metal Services Ltd., 50 μm internal diameter and 150 μm outer diameter). A 120-cm-long capillary was connected to the nitrogen tank (Figure 13). A molecular sieve trap was in place before delivering gas into the solutions used in the capillary. The trap ensured the anhydrous condition of the nitrogen gas. The reagents were held in a disposable vial held by 'reactivial'. The nitrogen gas that went into the 'reactivial' increased the pressure and consequently displaced the reagents into the capillary tube.

54
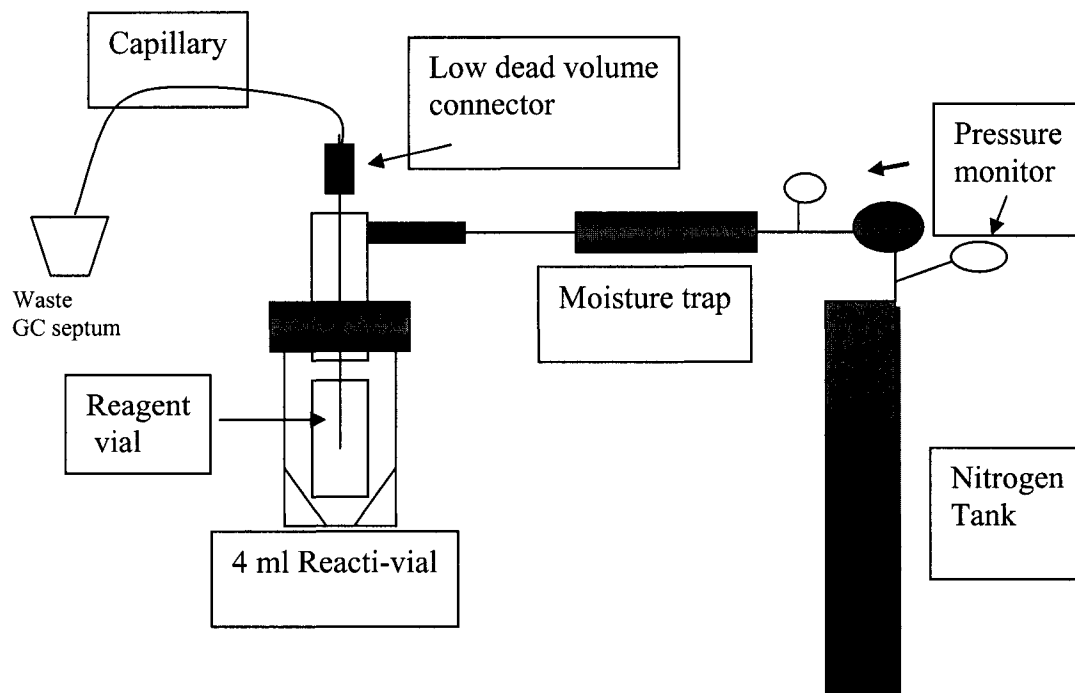
Figure 13: Apparatus for filling capillaries

A 120-cm-long capillary was cut (50 μm internal diameter and 150 μm outer diameter) and was connected to the nitrogen tank. A molecular sieve trap was in place before delivering the gas into the solutions used in the capillary. The trap ensured the anhydrous condition of the N_2 gas. The reagents were held in a disposable vial held by reactivial. The nitrogen gas that went into the reactivial increased the pressure and consequently displaced the reagents into the capillary tube. The capillary containing the reagent was incubated by sealing one of the ends with a GC septum.

55

3.2.2 Reagents

P93 is a murine hybridoma secreting anti-M13 phage monospecific MAb (IgG2a). The antibody was purified by using Sephadex-protein G affinity chromatography, as described in Chapters 1 and 2. The wild-type bacteriophage M13 was obtained from Dr. Bruce Malcolm, formerly at Department of Biochemistry, University of Alberta, Edmonton, Alberta. 3-Mercaptopropyl trimethoxysilane (MTS) and NN-γ-maleimidobutyryloxy succinimide ester (GMBS) were obtained from Fluka, Switzerland. non-radioactive-sodium iodide, trichloroacetic acid, sodium hydroxide and toluene were purchased from BDH Chemicals, Toronto, Canada. [^{125}I]-sodium iodide was procured from Amersham Pharmacia Biotech. Iodogen and protein G were purchased from Sigma Chemicals Co. St. Louis, USA. Plastic scintillation vials were purchased from Fisher, Canada. Methanol was obtained from Mallinckrodt Baker Inc. Paris, Kentucky. Anachemia Canada Inc., Montreal, Canada and Commercial alcohols Inc., Ontario, Canada, supplied methanol and ethanol, respectively. All the chemicals were of analytical grade.

Milli Q water was used in the preparation of all reagents. The reagent solutions were filtered through a 2 μm membrane filter before passing them through the capillary.

3.2.3 Procedures

3.2.3.1 Iodination of anti-M13 MAb, M13 phage and protein G (Iodogen method)

Anti-M13 MAb, M13 phage and protein G were iodinated by using iodogen as the oxidizing agent (Saha et al., 1989). Iodogen provides mild labeling conditions, and thus, the activity of the protein is generally not compromised. The percentage of protein-bound iodine was determined by trichloroacetic acid precipitation.

56

The iodogen-based iodination procedure allowed the protein to be labeled by first oxidizing the [^{125}I] to an electropositive species. This process took place by an interaction between the iodogen coated on the reaction vessels and the radioiodide in solution. The oxidized iodine then underwent electrophilic aromatic substitution to give [^{125}I]-labeled protein.

Iodogen was dissolved in chloroform to give a concentration of 2 mg/10 ml. 50 µl of stock solution of iodogen were added to the test tube and allowed to evaporate with a stream of air, resulting in 10 µg of the reagent on the test tube wall. Protein G, the antibody or the phage solution in PBS (pH 7.2) was added to the reaction vessel (100 µl containing 50-100 µg). This process was followed by adding [^{125}I]-NaI in a 0.05 M-phosphate buffer to give a final activity of 200 µCi. The reaction was allowed to run for 30 min with intermittent mixing. The reaction mixture was transferred into a clear test tube. This procedure ended the reaction since the iodogen remained behind on the walls of the test tube. A 60 µl aliquot of freshly prepared unlabeled 1 M NaI solution were added to the reaction mixture, which was left to stand for 10 min. This excess of NaI solution eventually saturated the iodine-binding sites on the protein and stopped the reaction. The total activity was measured by using the Beckman gamma counter (Beckman, USA). The labeled antibody was tested for immunoreactivity by using direct ELISA. The procedure followed was the same as that described in Section 2.2.5.2.

3.2.3.2 Gel filtration

The total activity measured in the radioiodination reaction mixture contained the radioiodinated protein with the radioiodine covalently bound to the protein molecule. In addition, the solution also contained some unreacted radioiodine or unbound iodine. The free radioiodine present in the reaction mixture was present mainly in the form of [^{125}I]-NaI. This was effectively removed from the protein by passing the solution through a Sephadex G-25 column (medium) in PBS. The Sephadex G-25 column separated the molecules based on their molecular weight. The high molecular weight of the labeled antibody/M13 phage/protein G allowed it to pass freely through the column while the

57

lower molecular weight materials were retarded. This process of removing inorganic salts from the protein solution is referred to as "desalting by gel filtration".

A long Sephadex G25 column (~30 cm) was prepared and equilibrated with 0.05 M PBS pH 7.2. Once equilibrated, the column was washed with 1% BSA solution in 0.05 M PBS to saturate the non-specific sites on the Sephadex. The column was washed and equilibrated with PBS. The PBS level above the gel was brought down for the loading sample, and the radioactive reaction mixture was added on top. Care was taken to add a small amount of the elution buffer, 0.05 M PBS (pH 7.2), on the top, starting from 100 µl volume and gradually increasing the volume as the reaction mixture passed down the column (determined by the yellow coloration of the reaction mixture) in order not to disturb the gel bed. Fractions were collected in 30 test tubes. Each fraction had 16 drops, or approximately 0.8 ml of the volume. A 10 µl aliquot of each fraction were taken, and the radioactivity was determined by using the sodium-iodide detector. A histogram was plotted, and the labeling efficiency was calculated. The radiochemical purity of the collected fractions, with high activity, was determined by using trichloroacetic acid (TCA) precipitation.

3.2.3.3 Trichloroacetic acid (TCA) precipitation

TCA precipitation was chosen to determine the radiochemical purity or percentage of bound radioiodine in the reaction mixture. The dissolved protein was precipitated from the solution by adding trichloroacetic acid. The precipitate was then isolated by centrifugation, and the activity of both the precipitate and the supernatant was determined by using a gamma counter (Beckman, USA). The percentage of the radioactivity present in the precipitate was the percentage of bound radioactivity.

500 µl of 1% BSA (non-radioactive BSA) in PBS were added to a 1.5 ml eppendorf tube as a carrier protein to add bulk to the precipitate. Approximately 1 µl of the labeled protein fraction (purified) was added to the non-radioactive BSA, followed by 5 µl of the 1 M NaI (non-radioactive). Approximately 500 µl of the trichloroacetic acid, 20%

58

solution in PBS, were added to the solution in the eppendorf tube and mixed thoroughly by using a vortex. The sample tubes were kept in an ice bath for 5 min and were then centrifuged at 8000 rpm for 2 min. The eppendorf tubes were removed from the centrifuge. The supernatant was transferred from one eppendorf tube to a second eppendorf tube. The two tubes, one containing the precipitate and the other containing the supernatant, were placed into scintillation vials, and the radioactivity was measured in the gamma counter.

3.2.4 Capillary immunoassays

The anti-M13 MAb, M13 phage and protein G were immobilized on the treated capillary wall by adsorption and by using covalent approaches. All experiments were done in triplicate.

Both adsorption and covalent coating were carried out in 0.05 M PBS pH 7.2. As described in Chapter 2, anti-M13 MAb was chosen as the capture and detector antibody. The M13 phage was the antigen, and 1% BSA in PBS was the blocking protein. As well, protein G was also used as the capture protein in some experiments as it binds the Fc portion on an antibody molecule in order to properly orient the molecule. The washing buffer contained 0.05% tween-20 in PBS (PBS-T). These substances were quantified by using physicochemical methods. The M13 phage was quantified by the plaque-forming assay, as described in Section 2.2.4.

In both cases, the protein solution was pushed into the capillary by using the capillary-filling apparatus (Figure 13). Nitrogen gas that went into reactivial displaced the air and consequently displaced the reagents into the capillary tube. The capillary containing the reagent was incubated by sealing one of the ends with a GC septum.

3.2.4.1 Capillary surface pretreatment

Before the proteins were adsorbed or covalently linked onto the capillary wall, a 10 mM NaOH solution was passed through the capillary for 30 min. This procedure facilitated

59

the cleaning of the capillary and resulted in the formation of Si-O⁻ reactive groups on the capillary wall. The capillary was finally washed with an excess of Milli Q water for 1 h (Bhatia et al., 1989)

3.2.4.2 Immobilization of the proteins by adsorption

3.2.4.2.1 Non covalent immobilization of the antibody

Purified [^{125}I]-anti-M13 MAb was passed through the capillary (120-cm-long). The solution was run through the capillary for 10 min and later was incubated for 1 h at RT by sealing one end of the capillary with a GC septum. The capillary was subsequently washed with the wash buffer (PBS-T) for 30 min. The capillary was cut 10 cm on both ends to avoid possible contamination at the ends. The whole capillary was wound and transferred to a scintillation vial and assessed by using the gamma counter to measure the total amount of radioactivity bound. The 100-cm-long capillary was subsequently cut into 10 segments each 10 cm long. The cut pieces were transferred into the scintillation vials, and the amount and uniformity of surface-bound protein was determined by using the gamma counter. This procedure allowed us to observe the consistency of the capillary surface in various segments throughout the length of the capillary.

Antibodies have been observed to lose or reduce their immunoreactivity on passive adsorption, partly because of the random orientation of the antibody molecule on the solid support. Thus, an ordered or oriented immobilization of the antibody was attempted by using protein G. Protein G solution in PBS at a concentration of 1 mg/ml was passed through the capillary and incubated for 1 h at RT. The capillary was washed with the wash buffer for 30 min. The capillary surface was blocked with 1% BSA solution in PBS for 1 h. The capillary was again washed with wash buffer for 30 min and incubated with a solution of [^{125}I]-anti-M13 MAb for 1 h. The capillary was washed with wash buffer for 30 min. The amount of protein non-covalently immobilized on the silica surface was determined by using a gamma counter.

60

3.2.4.2.2 Binding of the radiolabeled antigen by immobilized antibody

The unlabeled antibody was adsorbed on the silica surface as described in the previous section. The capillary surface was blocked with 1% BSA in PBS for 1 h. The [^{125}I]-M13 phage solution was passed through the capillary for 10 min and incubated with the immobilized antibody for three hours by sealing the loose end with a GC septum. The capillary was washed with washing buffer for 30 min. and was read as described in Section 3.2.4.1

3.2.4.3 Immobilization of the proteins by covalent linking

Proteins were covalently immobilized on the fused silica surface by using silanes, mercaptopropyl trimethoxysilane (MTS) and heterobifunctional crosslinkers, N-γ-maleimidobutyryloxy succinimide ester (GMBS). This preactivation of the silica surface for the covalent immobilization of the proteins produced the N-oxysuccinamide (NOS)-stable surface that covalently coupled to the protein amine groups. NOS reacts almost exclusively with primary amine groups, with the exception of mercaptans. This nucleophilic substitution reaction covalently immobilizes biomolecules *via* the available amine moieties by forming a stable amide bond (Figure 14 and 15).

3.2.4.3.1 Silanization of the silica surface and treatment of silanized surface with a heterobifunctional crosslinker

The capillary was cleaned as described in the previous section. A 4% solution of mercaptopropyl trimethoxysilane (MTS) in toluene was drawn into the capillary by applying 20 psi pressure. Both ends of the capillary were sealed with a GC septum, and then the capillary with the MTS solution in it was incubated for one hour at RT. The capillary was flushed with toluene for 30 min. A 2 mM N-γ-maleimidobutyryloxy succinimide ester (GMBS) solution was introduced into the capillary and incubated at room temperature for another hour. The capillary was rinsed with an excess of milli Q water for 30 min.

61
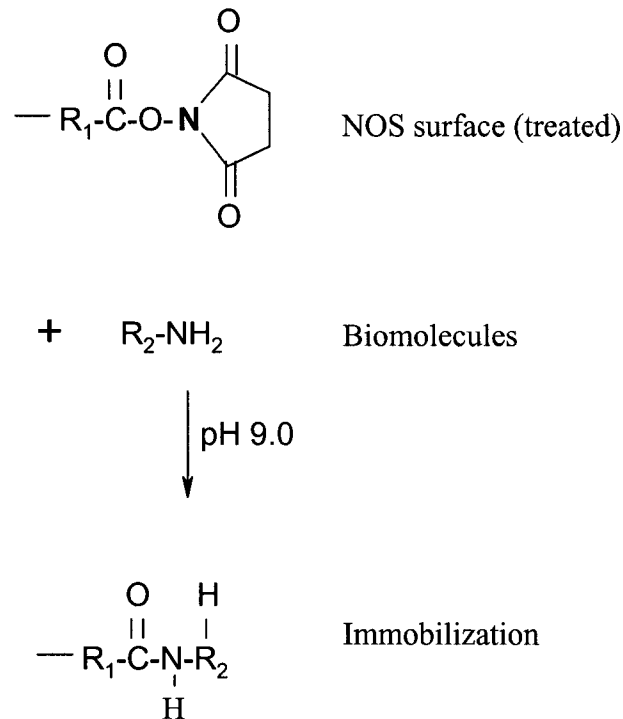
Figure 14: The N-oxysuccinamide surface coupling to amine groups

R₁= spacer arm; R₂ = protein, DNA etc.

(Source: Jill, 1996)

The NOS surface couples almost exclusively with the primary amine groups, with the exception of mercaptans. The nucleophillic substitution reaction covalently immobilizes biomolecules *via* the available amine moieties by forming stable amide bonds.
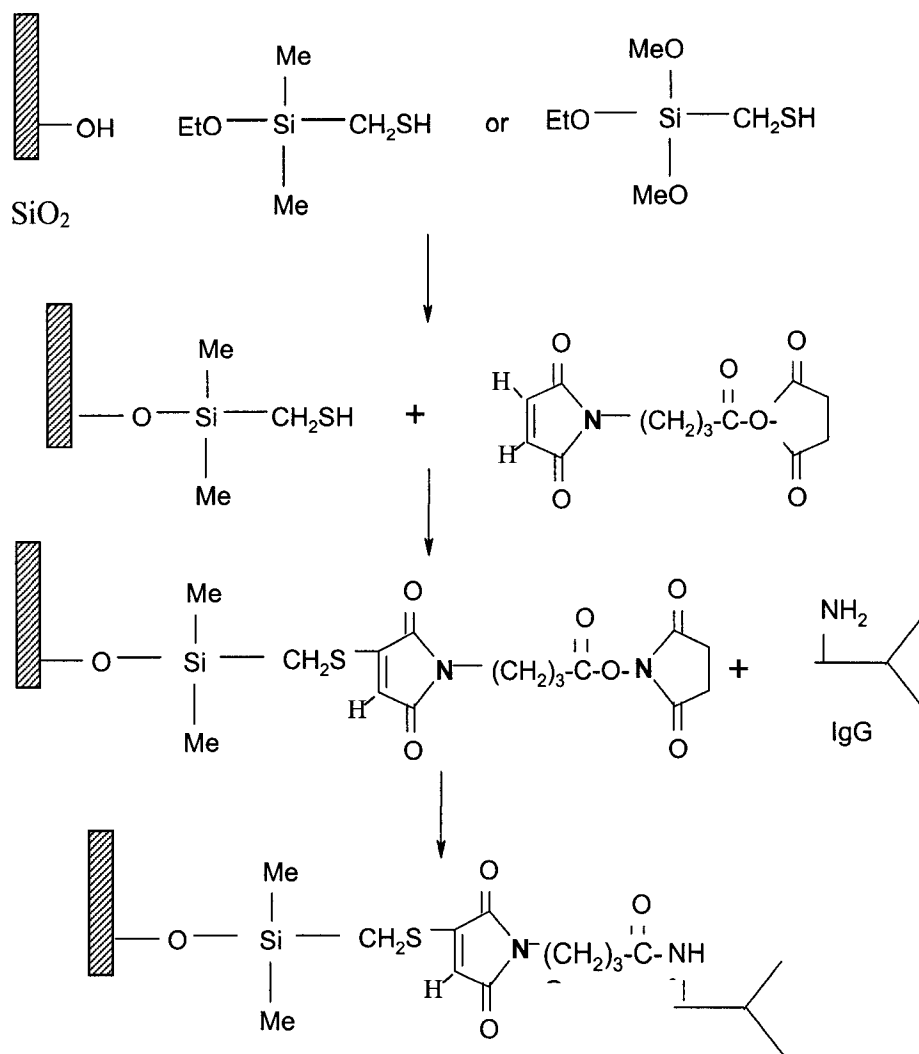
Figure 15: Silanisation of the silica surface and treatment of silinized surface with a heterobifunctional crosslinker

(Source: Bhatia et al., 1989)

The capillary was cleaned as described in Section 3.2.4.1. A 4% solution of mercaptopropyltrimethoxysilane (MTS) in toluene was drawn into the capillary by applying 20 psi pressure. Both ends of the capillary were sealed with a GC septum, and the capillary with MTS solution in it was incubated for 1 h at room temperature. The capillary was flushed with toluene for 30 min, and a N-γ-maleimidobutyryloxy succinimide ester (GMBS) solution was introduced into the capillary and incubated at room temperature for another hour. The capillary was rinsed with an excess of milli Q water for 30 min. Finally, the substrate was dried with inert Nitrogen gas. The protein solution (IgG, protein G or even M13) was subsequently incubated to covalently immobilize the sample.

63

3.2.4.3.2 Immobilization of antibody

$[^{125}I]$-anti-M13 MAb in PBS was passed through the surface coated with silane and crosslinker and allowed to incubate for 1 h. Then the capillary was washed with wash buffer for 30 min. The amount of the immobilized antibody was determined by using a gamma counter. The antibody was also immobilized alternatively by using protein G as the capture protein for the potential ordered orientation of the antibody. The capillary wall was coated with MTS and the crosslinker, GMBS. 1 mg/ml of protein G in PBS was passed through the capillary for 1 h. The capillary was washed with wash buffer for 30 min. The radiolabeled anti-M13 antibody solution was passed through the capillary for 1 h. The capillary was washed with the wash buffer for 30 min and estimates were made of the immobilized antibody on the capillary wall. The immobilization was done at room temperature.

3.2.4.3.3 Binding of radiolabeled antigen by immobilized antibody and sandwich formation

The unlabeled antibody was covalently immobilized on the capillary by following the same method described in Section 3.2.4.3.2. The capillary wall was blocked with 1% BSA in PBS for 1 h, followed by incubation with $[^{125}I]$-M13 phage for three hours at RT. The capillary was washed with the wash buffer for 30 min. The amount of immobilized antigen was determined by using a gamma counter. A sandwich was also formed on the capillary wherein the activated surface was incubated with 1 mg/ml Mab. The covalently linked antibody was incubated with unlabeled M13 phage, 10^7 phage/ml for 3 h at RT. The capillary was washed with wash buffer for 30 min. The antibody was allowed to capture the antigen. In the last step, specific $[^{125}I]$-anti-M13 Mab was passed through the capillary and incubated for one hour to form the sandwich complex. The capillary was washed with wash buffer for 30 min, and the amount of bound labeled antibody was by determined by using a gamma counter.

64

The capillary was cut 10 cm on both ends to avoid possible contamination at the ends. The whole capillary (after cutting the ends) was wound and transferred to a scintillation vial and counted by using a gamma counter. The 100-cm-long capillary was subsequently cut into 10 segments each 10 cm long. The cut pieces were transferred into the scintillation vials, and the amount of bound protein was determined by using a gamma counter.

3.3 Results and discussion

The results presented and discussion in this chapter explored the possibility of developing a capillary sandwich assay as an additional method for developing ultrasensitive immunoassays. Chapter 2 outlines the results of sandwich immunoassays on the traditional polystyrene (plastic) microtiter plates.

In the very first runs on the capillaries using $[^{125}I]$-Mab, we found excessive variability in the bound radioactivity, depicting no uniformity in the coating process. The problem was found to be in the handling of the capillary while cutting. The residual radioactivity on the work benchcoat or gloves contributed to the outliers. The second and third run were conducted, and in these experiments, each time the capillary was handled, it was cleaned with detergent, and gloves were changed very frequently. As well, a generous 10 cm end of the capillary dipping into the vial was discarded.

3.3.1 Iodination of the anti M13 Mab, M13 phage and protein G (Iodogen method)

The M13 phage, protein G, and anti-M13 Mab were iodinated by using the iodogen method. Iodogen acts as an oxidizing agent and provides milder conditions, and thus, the activity of the protein is not compromised.

The iodination of the antibody provided a challenge because of the very low iodination efficiency. Iodination of the antibody was attempted many times, but each time with the

65

same iodination efficiency ranging from 20-30%. Iodogen was coated on to the bottom of the test tube so as not to leave any residue in the end product. The iodogen concentration was varied from 10 µg to 40 µg, with a proportionate increase in non-radioactive NaI. The iodine-conjugated antibody was separated from the free iodine by using gel column radio chromatography (Figure 16). The iodinated fractions were collected in 0.8 ml volume. The concentration of each fraction was determined by using Biorad total protein assay kit using BSA as standard. The fraction with the highest activity was estimated for the total protein. The purity of the fraction was determined by using trichloroacetic acid precipitation and was found to be 90.8%. Each µg of the antibody immobilized on the capillary was equivalent to 644 cpm of activity. The iodination efficiency for the antibody was found to be 20%. The activity was corrected for decay from the time of the iodination.

Protein G and M13 phage were also iodinated at a higher iodogen concentration (40 µg). The iodination efficiency and purity for Protein G were found to be 30% and 75%, respectively (Figure 17). 16817 cpm units were equivalent to the immobilization of 1 µg of the protein G.

The M13 phage gave the best iodination efficiency and purity at 64% and 99.3%, respectively. Figure 18 implies that the free iodine was relatively well separated while using the same column used to obtain the results shown in Figure 16 and 17.

3.3.2 Immobilization of proteins

A major obstacle observed in the detection of antigens and haptens has been the non-specific binding of foreign molecules on the silica surface (Ahluwalia et al., 1992). Thus the capillary was exposed to many experimental conditions to account for any non-specific binding or background noise. Table 4 shows the different conditions to which the capillary was exposed prior to [^{125}I]-NaI adsorption. The pieces of untreated capillary, 100 cm in length, were counted in a gamma counter to establish the background radioactivity and non-specific binding of the free [^{125}I]. An untreated capillary was

66

flushed with $[^{125}I]$-NaI solution, and the activity was read to determine the non-specific adsorption, if any. Lastly, the capillary surface was pretreated with 10 mM NaOH before a $[^{125}I]$-NaI solution was passed through the capillary. This set of experiments could imply that $[^{125}I]$-NaI does not bind to the capillary surface non-specifically, whether the capillary is pretreated or not.

In another set of experiments, the effect of covalent immobilization on the amount of protein deposited when compared to the protein being adsorbed to the capillary wall was investigated. Table 5 and Figure 19 shows the activity observed for each capillary, which was 100 cm long. A significant increase of antibody immobilized on the capillary wall was absorbed by using heterobifunctional crosslinkers as compared to passive adsorption. The amount of antibody coupled to surfaces was measured by immobilizing the radiolabelled antibody on the silica surface coated with MTS and GMBS. The maximum amount of antibody specifically bound to the silica wall was found to be 15.8 ± 0.4 µg/cm^2, and that due to passive adsorption was found to be 5.4 ± 0.3 µg/cm^2. The mean ± SD values for antibody immobilization were calculated from three different capillaries treated at the same time. The amount of antibody covalently bound appeared to be significantly higher than the amount of protein G, which was in ng range/cm^2.

The amount of protein G specifically bound to the silica wall was found to be 47.8 ± 3 ng/cm^2. The results presented in Table 6 clearly show an increase in protein-binding capacity upon covalently immobilizing the protein. This increase in density could relate to the greater sensitivity in the detection of the antigen or hapten, and also suggests that the covalently immobilized protein molecules are less prone to leaching than the protein adsorbed onto the capillary wall.

67
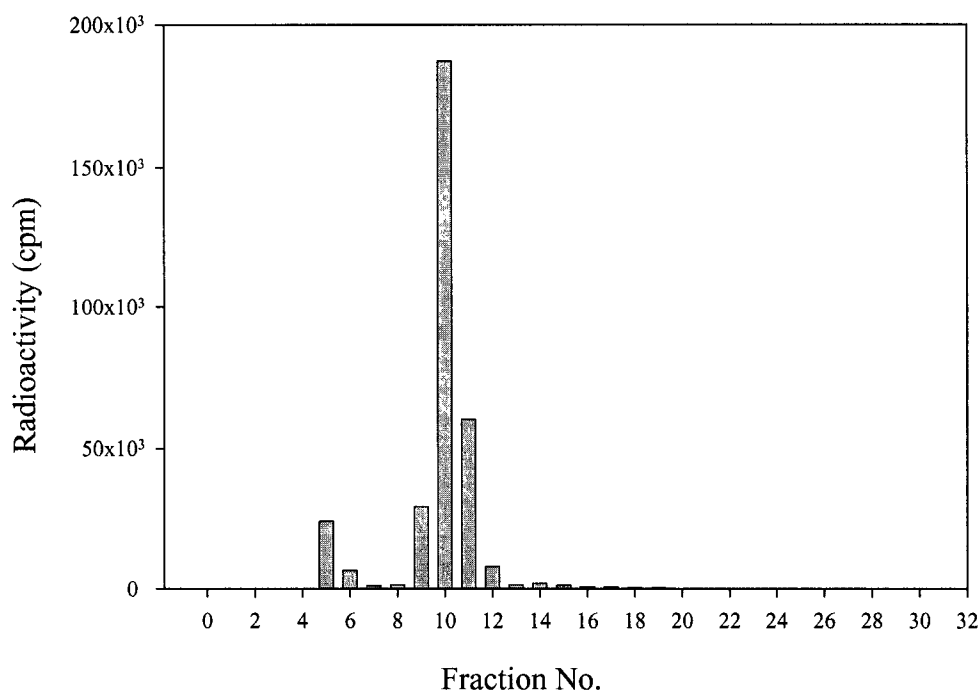
Figure 16: Gel Column radio chromatography profile: Anti-M13 Mab Iodination

Fraction No.5

Purity of the fraction * (Trichloroacetic acid precipitation)	90.8 %
Radioactivity in cpm units	24147 cpm units
Concentration of the anti-M13 Mab in the fraction	340 µg/ml
Activity/concentration (cpm/µg)	644 cpm/µg

* Purity of the fraction was determined as the activity of the precipitate divided by the total activity in both supernatant and precipitate (23885/26301 X 100)

68
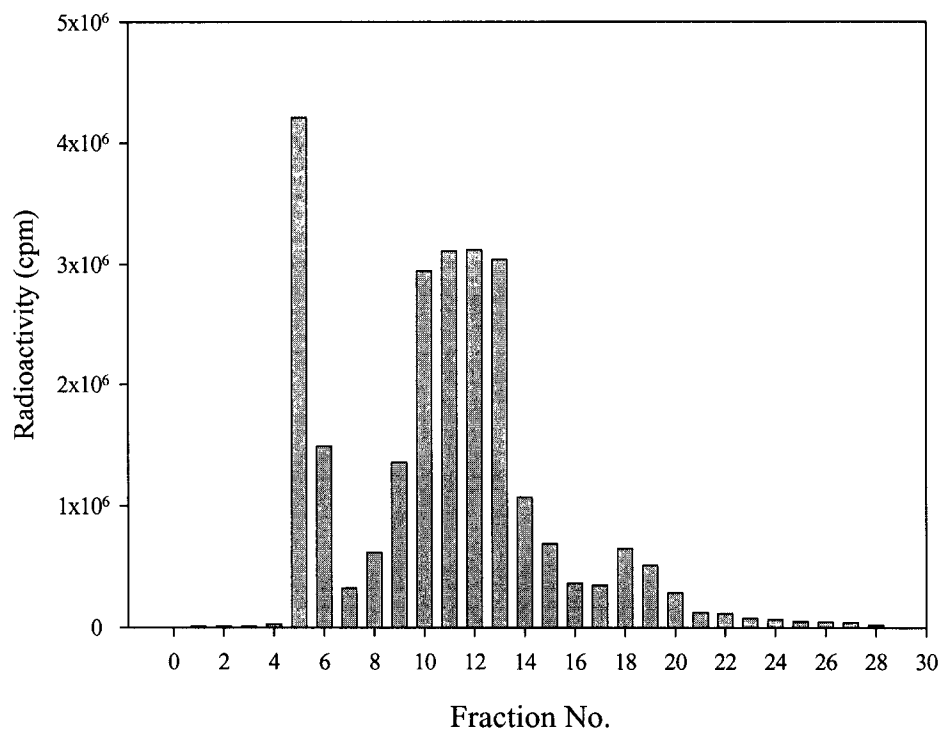
Figure 17: Gel Column Chromatography profile: protein G Iodination

---

Fraction No.5

Purity of the fraction * (Trichloroacetic acid precipitation)	74.8%
Radioactivity in cpm units	4204345
Concentration of the protein G in the fraction	250 μg/ml
Activity/concentration (cpm/μg)	16817 cpm/μg of protein

---

* Purity of the fraction was determined as the activity of the precipitate divided by the total activity in both supernatant and precipitate (18023/24082 X 100)

69
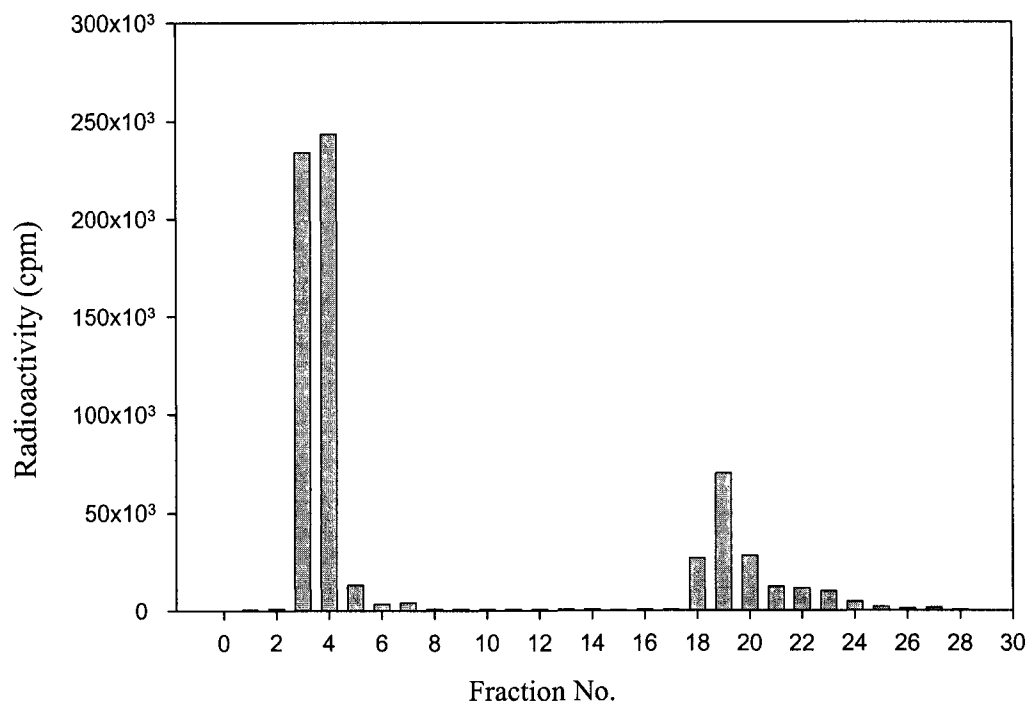
Figure 18: Gel Column Radio chromatography profile: M13 Phage Iodination

Fraction No.4

Purity of the fraction * (Trichloroacetic acid precipitation)	99.3%
Radioactivity in cpm units	243264 cpm

* Purity of the fraction was determined as the activity of the precipitate divided by the total activity in both supernatant and precipitate (260832/262661 X 100)

70
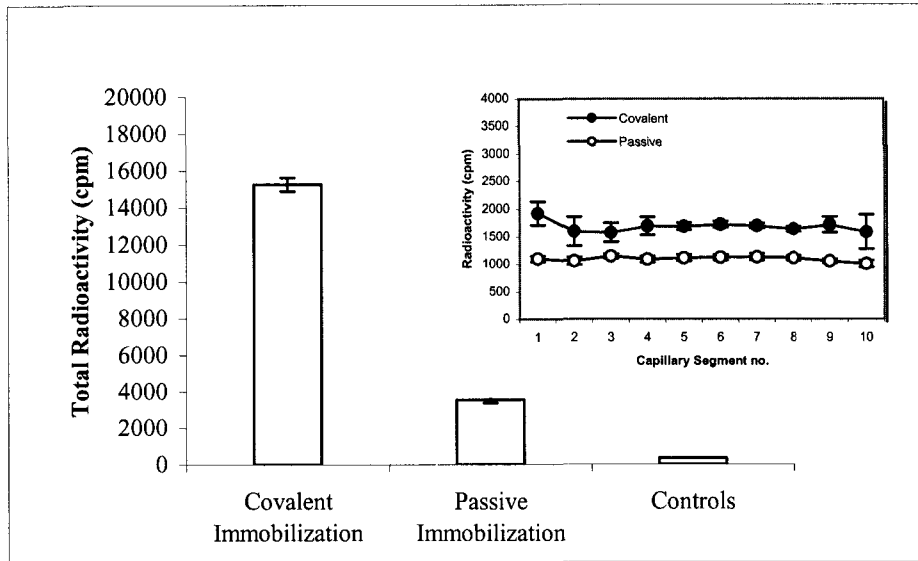
Figure 19: Immobilization of [^{125}I]-anti-M13 monoclonal antibody: comparison of covalent and passive immobilization.

Note: Inset shows the uniformity of the coating on the silica surface for the each 10 cm segment.
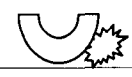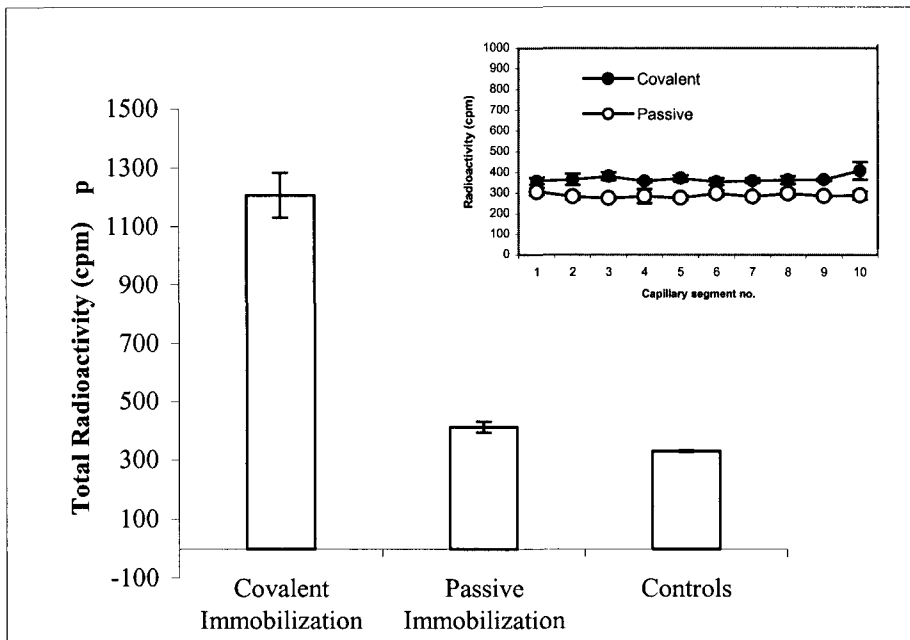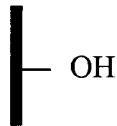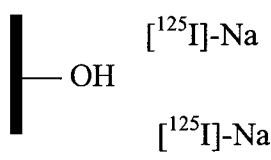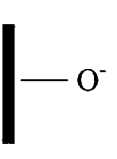
Figure 20: Immobilization of [^{125}I]-protein G: comparison of covalent and passive immobilization.

Note: Inset shows the uniformity of the coating on the silica surface for the each 10 cm segment.

71

Table 4: Adsorption of $[^{125}I]$-NaI on the silica surface

Condition	Surface of fused Silica Wall	Counts for individual capillary (10 pieces, 10 cm each) (cpm)										Mean
		1	2	3	4	5	6	7	8	9	10	
Capillary Untreated	▐— OH	57	52	73	64	68	66	56	69	61	61	62.7 ± 6.5
Capillary untreated and $[^{125}I]$-NaI solution is passed through	$[^{125}I]$-Na ▐— OH $[^{125}I]$-Na	80	67	70	65	61	88	77	76	74	75	73.3 ± 7.8
Capillary washed with 10 mM NaOH and $[^{125}I]$-NaI solution is passed through	$[^{125}I]$-Na ▐— O⁻ $[^{125}I]$-Na	67	59	69	77	70	78	80	52	57	96	70.5 ± 12.9

NOTE :The capillary was cut to 10 pieces 10 cm each after the respective treatment of the capillary. Each piece of the capillary was transferred to the liquid scintillation vial and read. Capillary was washed with 10 mM NaOH solution to activate the OH groups available on the fused silica into Si-O⁻. Such a capillary was referred to as a "treated capillary", and the capillary not washed with 10 mM NaOH, or, in other words the capillary with intact OH groups was referred to as an "untreated capillary". As can be seen, the $[^{125}I]$-NaI did not adsorb on the untreated capillary as well as it did on the treated capillary wall.

Table 5 : Immobilization of [^{125}I]-anti-M13 MAb on silica surface: comparison between adsorption and covalent immobilization

	Covalent Immobilization			Passive Immobilization		
	^{125}I labelled anti-M13 MAb was immobilized covalently (cpm)	Area of capillary 50 μm internal diameter and 100m length (cm^2)	Antibody /cm^2 (μg /cm^2)	^{125}I labelled anti-M13 MAb was immobilized passively (cpm)	Amount of Ab adsorbed passively (μg /cm^2)	%age antibody immobilized due to passive adsorption
Capillary 1	15184.0	1.5 cm^2	15.7 μg /cm^2	3562.0	5.5 μg /cm^2	
Capillary 2	14926.0	1.5 cm^2	15.5 μg/cm^2	3358.0	5.2 μg/cm^2	34%
Capillary 3	15644.0	1.5 cm^2	16.2 μg /cm^2	3741.0	5.8 μg/cm^2	
Mean (cpm)	15251.3± 363		15.8 ± 0.4	3553.7± 191	5.4± 0.3 μg/cm^2	
Within Run CV%	2.3%			5.5%		

Table: Average of the anti-M13 monoclonal antibody bound to capillary wall (100 cm length)

	Capillary of 100 cm length
Area	1.5 cm^2
Antibody Immobilized	15.8 ± 0.4 μg/cm^2

Note: Mean ± SD values for the antibody immobilized (anti-M13 MAb) were calculated from three different capillaries by using MTS film and GMBS crosslinker performed at the same time. The activity for the control samples was 376± 7 (for the capillary received from the manufacturer), 390 ± 12 (for the capillary with NaOH wash), and 327± 7(for the vials themselves). The activity for the control samples was the average of the 3 capillaries measured at the same time.

Table 6: Immobilization of [125I]-protein G on to the capillary: comparison between passive and covalent Immobilization

	Covalent Immobilization			Passive Immobilization		
	^{125}I labelled protein G was immobilized covalently (cpm)	Area of capillary 50 μm internal diameter and 100m length (cm^2)	protein/area (ng/cm^2)	^{125}I labelled protein G was immobilized passively (cpm)	protein/area (ng/cm^2)	%age protein immobilized due to passive absorption
Capillary 1	1145	1.5 cm^2	45.0ng/cm^2	417	16.5ng/cm^2	
Capillary 2	1183	1.5 cm^2	46.8 ng/cm^2	430	17.0ng/cm^2	34%
Capillary 3	1293	1.5 cm^2	51.2 ng/cm^2	391	15.5ng/cm^2	
Mean (cpm)	1207 ± 76		47.8 ± 3 ng/cm^2	412 ± 19	16.4 ng ± 0.8 ng/cm^2	
Within Run CV%	6.3%			4.8%		

Table: Average of the protein G bound to capillary wall (100 cm length)

Capillary of 100 cm length	
Area	1.5 cm^2
Antibody Immobilized	47.8 ng ± 31 ng/cm^2

Note: Mean ± SD values for protein G immobilized (anti-M13 MAb) were calculated from three different capillaries by using MTS film and GMBS crosslinker performed at the same time. The activity for the control samples was 376± 7 (for the capillary received from the manufacturer), 390 ± 12 (for the capillary with NaOH wash) and 327± 7 (for the scintillation vials themselves). The activity for the control samples was the average of the 3 capillaries measured at the same time.

3.3.3 Binding of radiolabelled antigen to the immobilized antibody and sandwich formation

To establish that the antibody function was maintained during the process, the immobilization procedure was repeated with an unlabelled antibody, anti-M13 Mab. The capillary was blocked with 1% BSA in PBS. The immobilized antibody was incubated with excess iodinated antigen, [^{125}I]-M13 phage. In a control experiment, BSA was adsorbed onto the fused silica wall, and the labeled M13 phage was passed through the capillary. Table 7 and Figure 21 show that non-specific binding contributed $\approx$ 30% of the total activity being observed. In a separate experiment, the antibody was immobilized by using protein G as the capture protein, which itself was covalently immobilized. Table 7 shows an evident increase of the M13 phage immobilized when compared to the random immobilization of the capture antibody (p = 0.009). This increase accounted for 30% of the total activity and could be attributed to some degree of the ordered orientation of the antibody. The ordered orientation of the antibodies could have resulted in a greater affinity and avidity for the phage particles, or, in other words, more antibody molecules bound each phage particle being immobilized (Schramm et al., 1987). The greater avidity allowed the phage particles a greater association with the antibody molecules. Thus, a lesser amount of phage particles would have leached out during the washing with the wash buffer. This result also suggests that more phage particles could have been captured and detected.

In another experiment, a sandwich immunoassay was attempted. Anti-M13 MAb was immobilized on silica coated with MTS and GMBS. An excess of the antigen solution, 10^7 phage/ml, was passed through the capillary. The antigen immobilized by the antibody was detected by passing [^{125}I]-anti-M13 MAb.

In an alternative strategy, the antibody was captured by protein G, which itself was covalently immobilized onto the capillary and bound the antibody at its Fc portion. The

75

results in Figure 22 indicate that the activity observed in the sandwich formation showed no significant difference when the antibody was immobilized either directly or indirectly through its Fc portion by using protein G as the capture protein (random vs. ordered p=0.09). A control experiment was run wherein no antigen was passed through the capillary, and the same procedure was followed for the sandwich formation. The activity so obtained could be attributed to the non-specific binding of $[^{125}I]$-Mab on the capillary wall. Table 8 clearly indicates that the activity observed in the various columns showed a trend in the right direction, but that the magnitude of sandwich formation was not enough. Several attempts were made to see if a change in the antibody, protein G, or the M13 phage concentrations could increase the amount of detector antibody immobilized, but no evident increase was observed to warrant further studies. The phage number was varied from 10 phage/ml to 10^{10} phage/ml, but the non-specific binding overrode the specific binding.

Another important factor in the development of a capillary-based immunoassay is the uniform density of the immobilized protein throughout the capillary surface. Each capillary was cut into 10 equal pieces, 10 cm each, and each piece was read for activity. Tables 9 to 16 show the distribution of the activity in different lengths of the capillary. It could be inferred that the intra assay CV% ranges from 3% to 9% for most of cases except two (Table 13), in which an outlier brings the CV% to 27% and 50%. This result depicts a generally uniform distribution of the protein being immobilized in most of the capillaries.

Thus, it could be concluded that the antibody was successfully immobilized onto the silica surface. The protein so immobilized was shown to have much greater density when immobilized covalently than when it was adsorbed. However, adsorption contributed ≈30% of the total amount of antibody being immobilized. When immobilized covalently, the antibody surface density/area was found to be 15.8 $\mu g/cm^2$. Protein G was used to

76
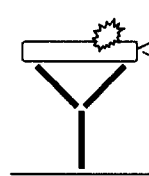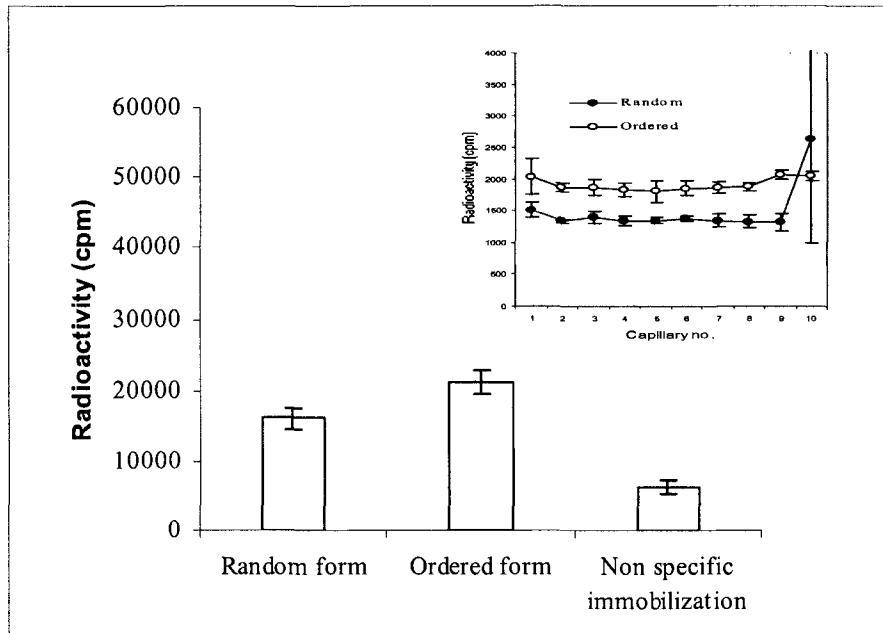
Figure 21: Binding of [^{125}I]-M13 phage to immobilized antibody

Inset shows the uniformity of the coating on the silica surface for the entire length of the capillary. Student paired t test: probability (p) was conducted by using Simple Interactive Statistical Analysis. (Ordered vs. random p=0.009; ordered vs. non specific p=0.008 and random vs. non specific p= 0.013).
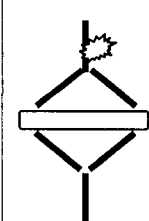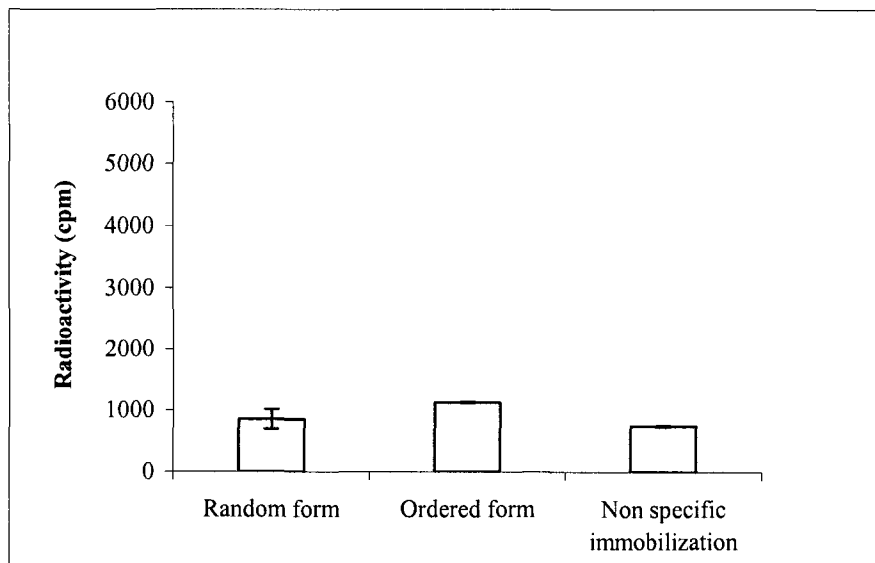
Figure 22: Binding of unlabeled antigen, M13 phage to the immobilized antibody and sandwich formation

Student paired t test: probability (p) was conducted by using Simple Interactive Statistical Analysis. (ordered vs. random p=0.09; ordered vs. non specific p=0.001 and random vs. non specific p=0.37).

77

capture antibody molecules because it increases the relative immobilization of the antibody and also offers very little binding through adsorption. $[^{125}I]$-M13 phage was captured by an antibody bound to the silica surface covalently. The immobilized antigen was quite appreciable, but when a sandwich was formed with the labeled antibody, a significant signal for the sandwich was not evident, perhaps due to the low specific activity of the $[^{125}I]$-M13. The amount of activity observed was marginally higher but not significantly different from the activity observed in the control (p= 0.001 for ordered orientation and p= 0.37 for random orientation), making this approach of direct immobilization of antibodies a less promising option with radiolabled-antibodies due to their low specific activity. It is likely that a fluorescent-labeled MAb of high specific activity could provide a better signal than that of radioactive MAbs. An alternative successful approach was recently reported (Chiem and Harrison, 1997; Lee et al., 1999) using antibody immobilized bead dams rather than the direct coupling of antibodies on capillary surfaces. In this approach, the group designed a prototype automated microchip platform, which was used to demonstrate an on-chip sandwich heterogeneous immunoassay based on the same principles as those used in a conventional immunosorbent assay.

78

Table 7: Binding of [^{125}I]-M13 phage to the covalently immobilized antibody

	Random form[1] (cpm)	Ordered form[2] (cpm)	Non specific Immobilization[3] (cpm)
Capillary 1	16384	20410	7261
Capillary 2	17577	22976	5296
Capillary 3	14571	20146	5988
Mean (cpm)	16177 ± 1513	21177± 1563	6181± 996
Within Run CV%	9.3%	7.3%	16.1%

Mean ± SD values for [^{125}I]-M13 phage immobilized were calculated from three different capillaries performed on the same day. Non-specific binding contributed 30-40% of the total activity being observed. Ordered form accounted for a 30% increase in the amount of the M13 phage being immobilized.

Student paired t test: probability (p) was conducted by using Simple Interactive Statistical Analysis. (ordered vs. random p=0.009; ordered vs. non specific p=0.008 and random vs. non specific p=0.013)

NOTE:
1. The antibody was covalently immobilized on the capillary (120 cm long). The capillary wall was blocked with 1% BSA, followed by incubation with [^{125}I]-M13 phage. The amount of immobilized antigen was determined by using a gamma counter
2. In a separate experiment the unlabeled antibody was immobilized by using protein G as the capture protein, which itself was covalently immobilized. The antibody was immobilized by following the same procedure explained in Step 1.
3. In a control experiment, BSA was adsorbed onto the fused silica wall, and the labeled M13 phage was passed through the capillary. In addition, the activity for the control samples was 376± 7 (for the capillary received from the manufacturer), 390 ± 12 (for the capillary with NaOH wash) and 327± 7 (for the scintillation vials themselves). The activity for the control samples was the average of 3 capillaries measured at the same time.

Table 8: Binding of unlabeled antigen, M13 phage to the immobilized antibody and sandwich formation

	Random form[1] (cpm)	Ordered form[2] (cpm)	Non specific Immobilization[3] (cpm)
Capillary 1	901	1126	739
Capillary 2	677	1130	755
Capillary 3	987	1138	
Mean (cpm)	855 ± 160	1131 ± 6	747 ± 11.3
Within Run CV%	18%	0.5%	1.5%

Mean $\pm$ SD values for [^{125}I]-anti-M13 MAb were calculated from three different capillaries performed on the same day.

Student paired t test: probability (p) was conducted by using Simple Interactive Statistical Analysis. (ordered vs. random p=0.09; ordered vs. non specific p=0.001 and random vs. non specific p=0.37)

NOTE

1. The antibody was covalently immobilized on the capillary (120 cm long). The capillary wall was blocked with 1% BSA, followed by incubation with unlabeled M13 phage. This immobilized M13 was detected by passing [^{125}I]anti-M13 MAb solution through the capillary. The amount of immobilized antibody was determined by using a gamma counter.

2. In a separate experiment, the unlabeled antibody was immobilized by using protein G as the capture protein which itself was covalently immobilized, and the procedure described in Point 1.

3. In a controlled experiment, PBS was passed instead of the M13 phage. In addition, the activity for the control samples was 376 ± 7 (for the capillary received from the manufacturer), 390 ± 12 (for the capillary with NaOH wash) and 327 ± 7 (for the scintillation vials themselves). The activity for the control samples was the average of 3 capillaries measured at the same time.

Table 9: Covalent immobilization of antibody:

Uniformity of the immobilization. The complete length of capillary was read (Table 6) and the capillary was cut into 10 equal parts each 10 cm in length. The capillary pieces were transferred to the liquid scintillation vials and read for activity by using a gamma counter.

Capillary fragment No.	Count for each 10 cm length			Within Run	
	Capillary I	Capillary II	Capillary III	Mean	SD
1	1883	1738	2148	1923	208
2	1897	1451	1443	1597	260
3	1777	1477	1478	1577	173
4	1838	1713	1518	1690	161
5	1741	1700	1620	1687	62
6	1775	1664	1734	1724	56
7	1659	1746	1692	1699	44
8	1586	1681	1654	1640	49
9	1560	1758	1827	1715	139
10	1254	1871	1639	1588	312
Mean	1697± 194	1680± 127	1675± 203	1684± 100	
CV%	11%	8%	12%	6%	

Table 10: Immobilization of antibody by passive adsorption:

Uniformity of the immobilization. The complete length of capillary was read (Table 6) and the capillary was cut into 10 equal parts each 10 cm in length. The capillary pieces were transferred to the liquid scintillation vials and read for activity by using a gamma counter.

Capillary fragment No.	Count for each 10 cm length			Within Run	
	Capillary I	Capillary II	Capillary III	Mean	SD
1	1158	1078	1065	1100	50
2	1022	1028	1138	1063	65
3	1134	1116	1185	1145	36
4	1087	1035	1141	1088	53
5	1105	1066	1175	1115	55
6	1118	1074	1173	1122	50
7	1149	1064	1175	1129	58
8	1087	1081	1162	1110	45
9	1050	1092	1021	1054	36
10	962	985	1077	1008	61
Mean	1087± 61	1062± 37	1131± 57	1093± 41	
CV%	6%	3%	5%	4%	

81

Table 11: Covalent immobilization of protein G:

Uniformity of the immobilization. The complete length of the capillary was read (Table 6) and the capillary was cut into 10 equal parts each 10 cm in length. The capillary pieces were transferred to the liquid scintillation vials and read for activity by using a gamma counter.

Capillary fragment No.	Count for each 10 cm length			Within Run	
	Capillary I	Capillary II	Capillary III	Mean	SD
1	358	374	340	357	17
2	334	375	388	366	28
3	359	395	386	380	19
4	364	349	359	357	8
5	360	364	388	371	15
6	338	352	373	354	18
7	346	364	368	359	12
8	341	380	368	363	20
9	361	-	368	365	5
10	378	-	439	409	43
Mean	354± 14	369±15	378±26	368±16	
CV%	4%	4%	7%	4%	

Table 12: Immobilization of protein G by passive adsorption:

Uniformity of the immobilization. The complete length of capillary was read (Table 7) and the capillary was cut into 10 equal parts each 10 cm in length. The capillary pieces were transferred to the liquid scintillation vials and read for activity by using a gamma counter.

Capillary fragment No.	Count for each 10 cm length			Within Run	
	Capillary I	Capillary II	Capillary III	Mean	SD
1	320	309	287	305	17
2	298	280	270	283	14
3	283	271	270	275	7
4	268	322	261	284	33
5	267	272	289	276	12
6	302	283	307	297	13
7	275	296	275	282	12
8	291	316	288	298	15
9	276	286	294	285	9
10	267	291	306	288	20
Mean	285±18	293±18	285±15	287±10	
CV%	6%	6%	5%	3%	

82

Table 13: Capture of [^{125}I]-M13 phage by random coating of MAb:

The [^{125}I]-M13 phage was captured by the unlabeled anti-M13 Mab, which was immobilized on silica coated with silane and GMBS crosslinker.

Capillary fragment No.	Count for each 10 cm length			Within Run	
	Capillary I	Capillary II	Capillary III	Mean	SD
1	1624	1406	1503	1511	109
2	1337	1294	1360	1330	34
3	1493	1340	1335	1389	90
4	1407	1266	1329	1334	71
5	1383	1354	1306	1348	39
6	1372	1405	1336	1371	35
7	1426	1374	1245	1348	93
8	1436	1254	1282	1324	98
9	1476	1246	1224	1315	140
10	1470		3791	2631	1641
Mean	1442±81	1327±63	1571±784	1490±405	
CV%	6%	5%	50%	27%	

Table 14: Capture of [^{125}I]-M13 phage by ordered coating of Mab:

The [^{125}I]-M13 phage was captured by the unlabeled anti-M13 MAb. The anti-M13 MAb was captured by Protein G immobilized covalently on the silica.

Capillary fragment No.	Count for each 10 cm length			Within Run	
	Capillary I	Capillary II	Capillary III	Mean	SD
1	1832	2238		2035	287
2	1830	1952	1813	1865	76
3	1957	1916	1720	1864	127
4	1943	1750	1791	1828	102
5	2005	1718	1696	1806	172
6	1969	1854	1731	1851	119
7	1936	1889	1761	1862	91
8	1910	1807	1914	1877	61
9	2114	1982	2111	2069	75
10	1994		2091	2043	69
Mean	1949±83	1901±8	1848±9	1910±5	
CV%	4%	8%	9%	5%	

83

Table 15: Sandwich formation: random Mab coating:

A sandwich was formed wherein unlabeled anti-M13 MAb was immobilized covalently. Unlabled M13 phage was passed through the capillary at 10^7 phage/ml concentration. The bound M13 phage was detected by the [^{125}I]-anti-M13 MAb.

Capillary fragment No.	Count for each 10 cm length			Within Run	
	Capillary I	Capillary II	Capillary III	Mean	SD
1	516	480	483	493	20
2	448	412	373	411	38
3	410	420	375	402	24
4	391	446	392	410	31
5	385	402	401	396	10
6	389	387	364	380	14
7	401	367	385	384	17
8	370	380	410	387	21
9	347	395	419	387	37
10	354	356	397	369	24
Mean	401±50	405±37	400±34	402±35	
CV%	12	9	8	9	

Table 16: Sandwich formation: ordered Mab coating:

A sandwich was formed wherein unlabeled protein G was immobilized covalently, it captured the anti-M13 MAb. Unlabled M13 phage was passed through the capillary at 10^7 phage/ml concentration. The bound M13 phage was detected by the [^{125}I]-anti-M13 MAb.

| Capillary fragment No.	Count for each 10 cm length			Within Run	
	Capillary I	Capillary II	Capillary III	Mean	SD
1	376	660	361	466	168
2	378	497	396	424	64
3	411	507	378	432	67
4	438	543	355	445	94
5	380	455	397	411	39
6	381	505	368	418	76
7	389	528	558	492	90
8	423	556	424	468	77
9	432	539	390	454	77
10	471	520	467	486	30
Mean	408±32	531±54	409±62	449±28	
CV%	8	10	15	6	

84

CHAPTER 4: Assessment of virus and antibody complex formation using capillary electrophoresis

4.1 Introduction

Protein-protein interactions are seen in various biological processes. From DNA replication to protein translation to the biological functions, many protein-protein interactions are involved. These interactions have been studied by several analytical methods on the basis that the complex has a distinct electrophoretic size and that the complex's other properties differ from those of the component molecules. Electrophoresis has been used to separate biomolecules and also to analyze biomolecular interactions, leading to the use of techniques collectively called "affinity electrophoresis". Among all the techniques, affinity electrophoresis in capillaries or affinity capillary electrophoresis (ACE) (Schmalzing et al., 2000, Chu et al., 1992) has demonstrated its value in the detection of complex formations, identification of an active component for binding in a multicomponent mixture, identification of structural requirements for recognition, determination of the equilibrium constants, the stoichiometry for binding reactions and the concentration measurements based on immunochemical recognition. ACE offers a short analysis time, requires a minute amount of sample, usually involves no radioactive component, and, most important, happens in a solution phase.

Affinity capillary electrophoresis (ACE) combines ligand-receptor interaction in the solution with the separation potential of capillary electrophoresis. For high-affinity systems, the components can be pre-incubated at different ratios, followed by CE analysis. When two molecules, A and B, having different electrophoretic mobility (μA and μB), form a complex AB, it can have a different mobility (μAB) from that of either of the component molecules due to the difference in q and/or m, i.e., $\mu AB \approx (\mu A + \mu B)/(mA + mB)^a$, where q is the number of charges on the particle migrating at a steady velocity, m is the molecular mass of the particle, μ is the electrophoretic mobility

85

and a is the coefficient ranging from 1/3 to 1 depending on the type and shape of the particle.

$$A \quad + \quad B \quad \leftrightarrow \quad AB$$
$$\mu A \qquad \mu B \qquad \mu AB$$
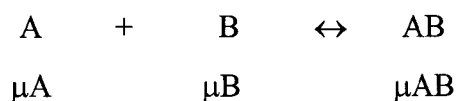
The mobility of the complex is usually intermediate between that of the components. Scatchard analysis of the electrophoretic mobility change of the protein as a function of the concentration of a charged ligand allows for the determination of its binding constant. ACE has been applied to study mainly the protein-protein interactions with small molecules. Until recently, the study of macromolecular interactions was limited to the compounds with a molecular weight of 200,000 (Lin et al., 1997; Qian and Tomer, 1998; Schmerr and Jenny, 1998) or lower. A recent report (Okun et al., 2000) studied the interaction of more complex molecules, human rhinovirus (HRV). The group successfully characterized the complex formation between rhinovirus and its respective antibody molecules, successfully demonstrating the use of ACE in distinguishing between different viral serotypes. The group demonstrated that subtle differences at the viral surface were sufficient to change its electrophoretic resolution. The group successfully established the stoichiometry for rhinovirus (molecular weight of $\approx 8 \times 10^6$ Da). We have attempted to demonstrate the complex formation between a much greater molecular weight virus particle and its respective antibody molecules.

The M13 phage is about 900 nm long and 6 to 10 nm thick, with a molecular weight of 12×10^6 Da. Its coat consists of 2700-3000 identical subunits of major coat protein and 5-8 subunits of minor coat protein. The minor coat protein is located exclusively at the ends of the filamentous phage (Figure 1). The electron microscopy results in Section 2.3.3 have demonstrated that the anti-M13 monoclonal antibody decorated the surface of the phage particle, thus complexing with the major coat protein.

At present, the assessment of the complex formation between a virus and an antibody requires the use of sucrose density gradient sedimentation or size-exclusion

86

chromatography to separate an excess of the antibody from the complex. Both of these methods need substantial time and the material or radiolabelled components for analysis. The purpose of this study was to demonstrate the formation of the complex between the M13 phage (molecular weight 12 X 10^6 Da) and the anti-M13 MAb. This approach was initiated because the formation of sandwich complexes in capillaries by the covalent or non-covalent methods described in Chapter 3 did not yield promising results with the radioiodinated approach.

4.2   Materials and methods

4.2.1 Apparatus

The CE system used was the Beckman Pace System 5010 (Beckman Coulter USA). The capillary used was the uncoated fused silica capillary, 50 μm inside diameter and 150 μm outside diameter, and a total length of 47 cm, was purchased from Capillary Polymicrotechnology, USA. The capillary was packed in the standard cassette regulated by a thermostat at a constant temperature. The data were collected by using the Beckman CE software (Beckman coulter, USA).

4.2.2 Reagents

A wild-type M13 phage was grown in bulk, as described in Chapter 2. The M13 phage used was purified by using the CsCl$_2$ gradient method (Liu, 1999). The number of M13 phage particles was determined by using a plaque-forming assay, as described in Chapter 2. P93, a murine hybridoma secreting anti-M13 monoclonal antibody (isotype IgG2a), was developed in our laboratory. The antibody was purified by Sepharose protein G affinity chromatography, as described in Section 2.2.5.2. The concentration of antibody was determined spectrophotometrically by using the extinction coefficient of 1.4 for 1mg/ml. The buffer solution was made in double-distilled water and was filtered through a 0.4 μm filter. Tricine buffer containing 0.01% tween 20 was the electrophoresis buffer (50 mM Tricine and 26 mM NaCl in double-distilled water). The pH was adjusted to 8 by

87

using NaOH. Tricine was purchased from Sigma Chemical Co., Canada. Sodium chloride was obtained from BDH Inc., Canada. The antibody and antigen solution were in 10 mM PBS pH 7.2.

4.3 Procedures

Before the capillary separation was carried out, the capillary was washed with 10 mM NaOH solution for 2 min, followed by a rinse with double-distilled water for 5 min. The capillary was equilibrated by using a tricine buffer pH 8 containing 0.01% tween-20 (as per established laboratory practice). The analytes were detected by means of an online UV detector at 200 nm.

4.3.1 CE profile of antibody

The antibodies were separated by capillary electrophoresis. A 36 μl aliquot of stock solution of anti-M13 monoclonal antibody (0.34 mg/ml, 0.31 μM of antibody) was added to 200 μl of PBS pH 7.2. The antibody (20 μl) was injected by pressure injection for 5 sec. PBS was used as the solution buffer, and tricine (tricine buffer containing 0.01% tween-20) was the electrophoresis buffer. The CE separation was carried out at 18 kV and 25 mA of constant current. The capillary cassette was regulated at 20° C temperature. Each separation run was for 10 min. The data were collected and analyzed by using the Beckman CE software. The detector signal was recorded by means of an online UV detector at 200 nm.

4.3.2 CE profile of M13 phage

M13 phages were separated by the same capillary electrophoresis. A 200 μl aliquot of M13 phage solution (10^{12} phage/ml) was diluted to 236 μl volume in PBS (equivalent to 1.27 nM M13 phage). The CE separation time was 10 min. The separation was conducted at 20 kV, 25 mA of constant current and 20° C temperature. Between each run, the capillary was washed with 10 mM NaOH for 2 min, with double-distilled water for 5

88

min, followed by the use of a tricine buffer containing 0.01% tween-20 for 10 min. This procedure was important as the M13 phage showed a lot of non-specific binding to the capillary wall.

4.3.3 Resolution of M13 phage-anti-M13 antibody complex formation

A mixture of antibody and M13 phage was incubated and separated on CE. A 72 μl aliquot of the purified antibody (0.34 mg/ml) was mixed with 100 μl of phage particles (10^{12} phage/ml) in a microvials, giving an antibody-to-antigen ratio of 963. The solution was incubated for 1 h at RT. The CE separation time was 10 min. All the separation conditions were same as those described in Section 4.3.2.

4.3.4 Interaction between M13 phage and antibody: effect of increasing concentration of antibody on constant number of M13 phage

The antibody was combined with a constant number of M13 phage particles at different antibody/antigen molar ratios, viz., 4000, 2000, 1000, 500 and 250. The molar concentration of the antibody was based on a molecular weight of 150,000. For the M13 phage, 100 phage particles were equivalent to 2.3 fg of the coat protein. The antibody stock solution was equivalent to 10 μM (1.5 mg/ml) and the M13 phage stock solution was equivalent to 19.2 nM (10^{13} phage/ml). 100 μM of o-pthallic acid were used as the internal standard. The antibody solution was dialyzed against the tricine buffer before use. All the solutions were made in a 50 mM tricine buffer.

Table 77: Antigen antibody complex formation as a function of the amount of antibody added

M13 phage concentration	Anti-M13 Mab	Ab/Ag molar ratio
1.92 nM*	7.62 μM	4000[1]
	3.84 μM	2000[2]
	1.92 μM	1000[3]
	0.96 μM	500[4]
	0.48μM	250[5]

* The molar concentration of M13 phage in each sample was 1.92 nM.

89

1. Antibody/antigen molar ratio of 4000: 5 µl of M13 stock (19.2 nM) were mixed with 38.4 µl of antibody stock (10 µM) with 6.6 µl of o-pthallic acid. The final volume was made to 50 µl with tricine buffer.

2. Antibody/antigen molar ratio of 2000: To 5 µl of M13 stock, 19.2 µl of antibody and 6.6 µl of o-phthalic acid were added. The final volume was made to 50 µl with tricine buffer.

3. Antibody/antigen molar ratio of 1000: 5 µl of M13 phage stock were mixed with 9.6 µl of antibody stock and 6.6 µl of o-phthalic acid. 23.8 µl of tricine buffer were added to make a final volume of 50 µl.

4. Antibody/antigen molar ratio of 500: 5 µl of antigen solution were added to 4.8 µl of the antibody stock plus 6.6 µl of 100 µM o-phthalic acid solution. The final volume was made with tricine buffer to 50 µl.

5. Antibody/antigen molar ratio of 250: 5 µl of M13 stock were added to 2.4 µl of antibody stock along with 6.6 µl of o-phthalic acid. The volume was made to 50 µl with tricine buffer.

Each antibody-virus mixture was incubated for 1 h at RT before CE separation was conducted. The separation time was 20 min. The antibody and M13 phage equilibrium mixture was injected by pressure injection for 5 sec. The CE separation was carried out on an untreated fused silica capillary, 47-cm-long (50 µm internal diameter) at 18 kV and 25 mA of constant current. The capillary cassette was regulated at 20° C temperature. The electrophoresis buffer was 50 mM Tricine containing 0.01% tween-20.

4.4 Results and discussion

4.4.1 Determination of antibody, antigen and antigen-antibody complex formation

The antibody, antigen and the complex formed between the antibody and antigen were analyzed by using capillary electrophoresis. In the first run, PBS was the solution buffer,

90

and tricine (tricine buffer containing 0.01% tween-20) was the electrophoresis buffer. Experiments were run to determine the electrophoretic mobility of the individual components (antibody and M13 phage) compared with the electrophoretic mobility of the complex between the virus and antibody. The electrophoretic profile of each component (antibody and M13 phage) was reproducible under a given set of conditions. The analytes were detected at 200 nm. Figure 23 shows that when PBS itself was separated on the capillary, a sharp fall and rise in the absorbance occurred at nearly 2 min separation time. This rise and fall could be attributed to the change in the refractive index from the solution buffer to the electrophoresis buffer. A broad peak was observed for the M13 phage on capillary electrophoresis separation. When anti-M13 monoclonal antibody was run on the capillary, a short sharp peak emerged at nearly 3 min separation time. The antigen and antibody equilibrium mixture were separated on the capillary. It could be clearly inferred that the electrophoretic mobility of the antibody-antigen complex was greatly reduced compared to that of M13 phage alone. The separation time of the virus-antibody complex almost overlapped the antibody separation time. The antibody-antigen complex emerged as a sharp peak, and it could be concluded that a complex formation occurred between the M13 phage and the anti-M13 monoclonal antibody.

4.4.2 Virus-antibody complex formation as a function of antibody concentration

For the characterization of the antibody-antigen complex formation, the components must be resolved clearly or the migration behavior of one of them must be altered upon complex formation. As well, the complex must be stable during the time required to reach the detector. To assess if the antigen-antibody complex is formed, an increasing amount of anti-M13 monoclonal antibody was added to a constant amount of M13 phage. The complex so formed was assumed to have a high affinity, as was demonstrated by electron microscopy. Figure 24 illustrates the resolution of the internal standard followed by the small peaks, which represent the antigen-antibody complex at different antibody/antigen molar ratios. Figure 25 presents the magnified view of the antigen-antibody complex peaks (highlighted by circles). It could be inferred that at a low antibody-to-virus molar ratio, the peaks corresponding to the complex were broad, suggesting the presence of a

91

heterogeneous population of virus aggregates with a varying number of antibodies per virion. At a higher molar ratio between the antibody and antigen, the peak became sharper, indicating the potential saturation of the 2700 equivalent epitopes with the divalent antibody.

The protein-protein interaction between the virus and antibody is influenced by many different factors compared to the interaction in a low-molecular-weight ligand receptor system. The change in mobility behavior of the virus-antibody complex is influenced by various factors such as changes in surface charge, conformation, molecular mass and hydrodynamic properties (Okun et al., 2000). The complex formation between the virus and the antigen is also influenced by the stability of the complex or the on-and-off kinetics of the binding reaction. The virus-antibody system tested here has shown a higher level of binding or generally slower kinetics, thus, an equilibrium mixture analysis could be performed. On the other hand, if the same virus-antibody complex had a rapid kinetics, a mobility-change analysis could be performed wherein, the complexes could be analyzed by the zone electrophoresis of one component in the presence of the other component present in the electrophoresis buffer. Multiple association and dissociation reactions in the course of electrophoresis provide the evidence of the complexation in the form of a mobility change of the molecule. The ultraviolet absorption monitor in CE has a sensitivity of 0.1 to 1 ng for proteins. Therefore, the concentration of the protein samples must be more than 0.1 mg to 1 mg/ml.

We demonstrated that capillary electrophoresis could be used to resolve the virus-antibody complex from the free M13 as previously demonstrated by Okun et al. (2000). This method could be adapted and modified in the future to screen the virus-complex formation and also to screen potential antibodies or capsid binders. The combination of CE, fluorescence labeling and LIF detection could provide an efficient way to quantify the amount of unlabelled molecules in the form of a fluorescent complex. The CE-based immunoassays are typical examples of this kind of application.

92
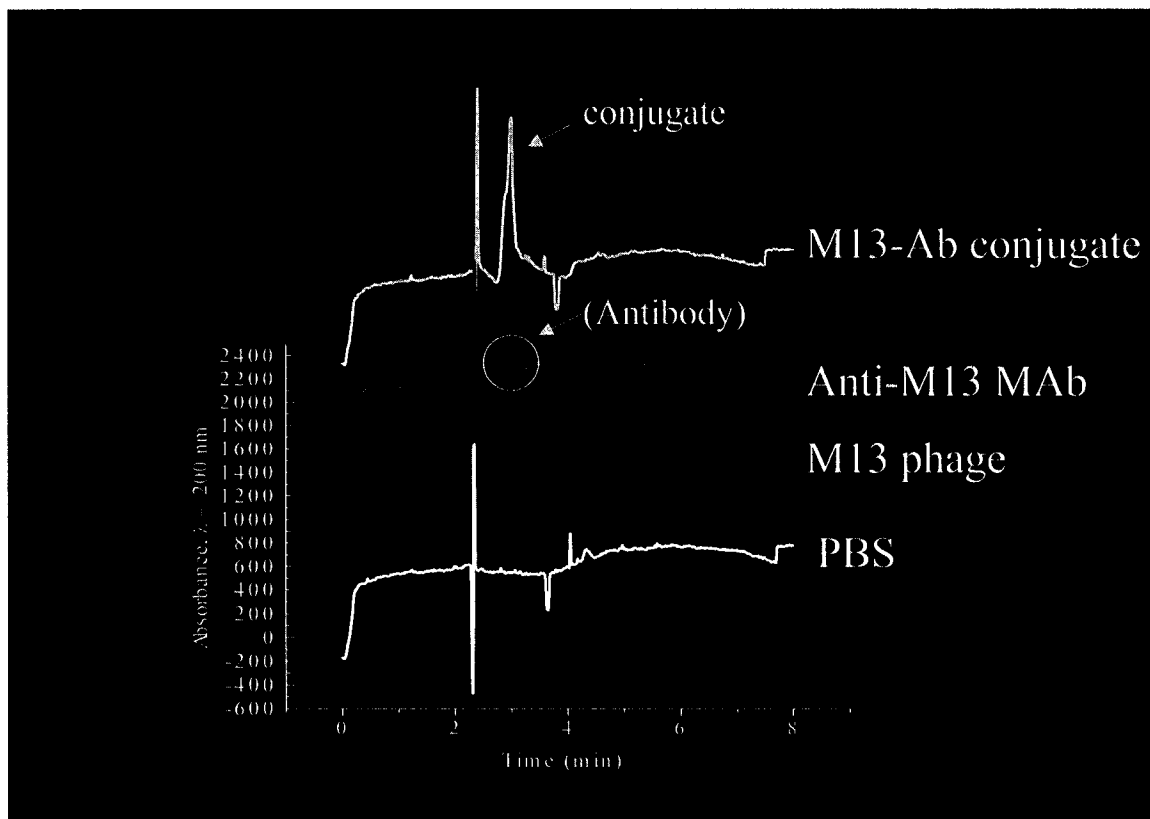
Figure 23: CE profile of antigen-antibody complex formation

The antibody (0.31 μM), the M13 phage (1.27 nM) and the M13 phage-antibody equilibrium mixture were injected by pressure injection for 5 sec. The CE separation was carried out at 18 kV and 25 mA of constant current. The capillary cassette was regulated at 20° C temperature. Each separation run was for 10 min.

Electrophoresis buffer: 50 mM tricine buffer pH 8 containing 0.01% tween 20.
Untreated fused silica capillary: 47 cm in length: 50 μm internal diameter.

93

Figure 24: Formation of M13-anti-M13 MAb complex as a function of the amount of the antibody added as analyzed by CE

The antibody was mixed with a constant number of M13 phage particles (1.92 nM) giving different antibody/antigen molar ratios, viz., 2000, 1000 and 250. The antibody-antigen equilibrium mixture was incubated in a final volume of 50 µl for 60 min at RT, followed by CE analysis. The 100 µM o-pthallic acid was used as the internal standard (IS). Electrophoresis buffer: 50 mM tricine buffer pH 8 containing 0.01% tween 20.

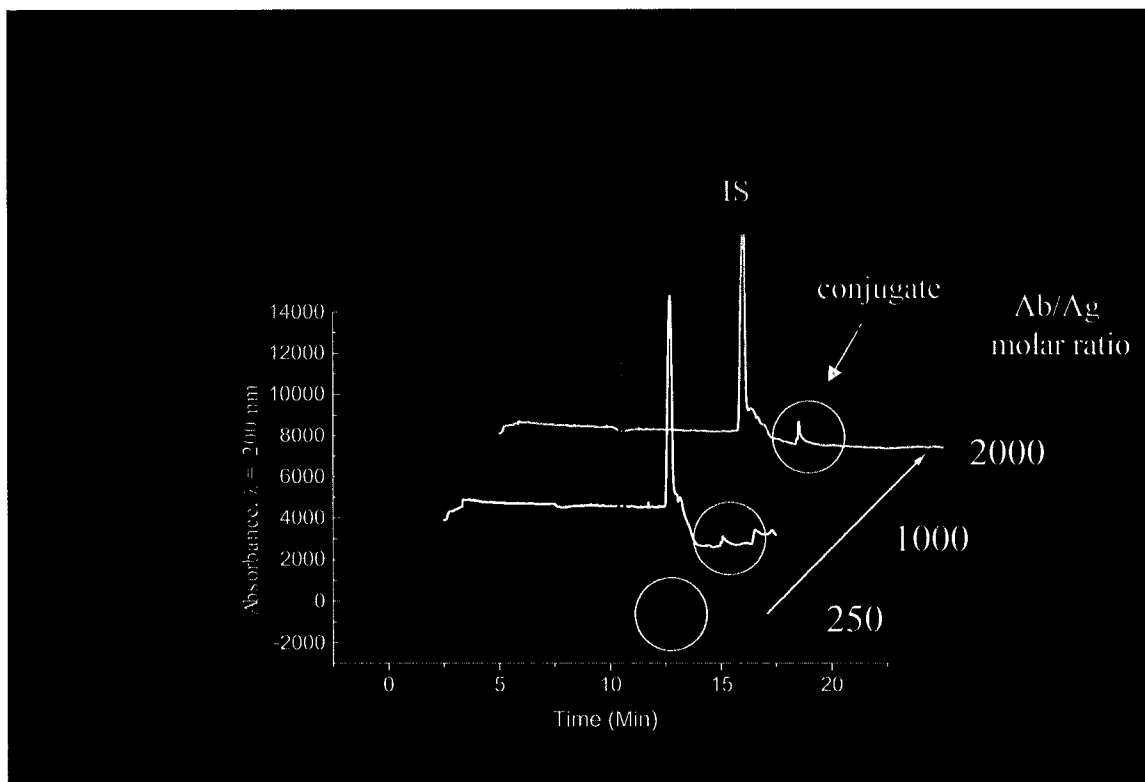*Conditions*: untreated fused silica capillary: 47 cm in length: 50 µm internal diameter. Voltage: 25 kV at constant current conducted at room temperature.

94
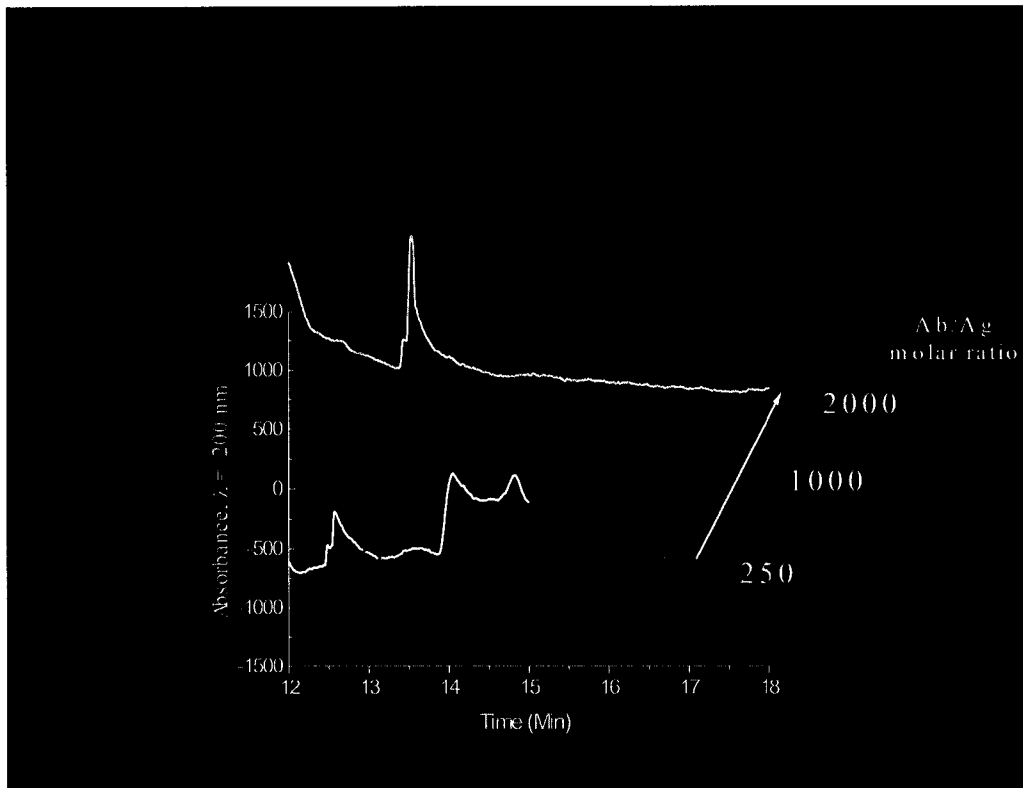
Figure 25: Figure 25: Formation of M13-anti-M13 MAb complex as a function of the amount of the antibody (expansion of region of interest)

The conjugate peaks represent the focused conjugate peaks from Figure 25. It could be inferred that at low antibody-to-virus molar ratio, the peaks corresponding to the complex were broad, suggesting the presence of a heterogeneous population of virus aggregates with a varying number of antibodies per virion. At a higher molar ratio between the antibody and antigen, the peaks became sharper, indicating the potential saturation of the 2700 equivalent epitopes with the divalent antibody.

95

CHAPTER 5: Conclusions, discussion and future studies

This thesis reports on the experimental studies of the development of ultrasensitive immunoassays in a microtiter format and the attempts to translate it into a capillary format. In addition, the immobilization of proteins on a fused silica capillary by using heterobifunctional crosslinkers and assessment of the virus-antibody complex formation by using capillary electrophoresis were also studied in order to achieve this objective.

An enzyme-amplified immunoassay for the detection of the M13 phage by using monoclonal antibodies has been developed. Alkaline Phosphatase was used as the amplifying enzyme label. The catalytic properties of the enzyme trigger resulted in an enzyme-amplification cascade that resulted in an increase in signal. The M13 phage was chosen as a model virus wherein the gene VIII protein formed a tubular array of ~2,700 identical subunits surrounding the viral genome. Anti-M13 MAb was purified on a Sepharose protein G column. An ultrasensitive homosandwich ELISA for detecting viruses was developed by using this monoclonal antibody coupled with a cyclic amplified ELISA procedure. The lower limit of the detection of the assay (mean ± 2 SD) was ~100 phage particles, which is approximately 2.3 fg of the phage protein. This result represents a 1000-fold increase in sensitivity compared to that of the conventional sandwich ELISA. This type of monoclonal antibody probe and ELISA format could be extended to determine the viral load of other medically important viruses such as HIV and HCV and to monitor the effectiveness of the anti-viral therapeutics.

In order to further increase the sensitivity, CE methods of analysis were pursued. Monoclonal antibodies were covalently immobilized on a fused silica capillary (50 µm internal diameter) by using thiol-terminal silanes and heterobifunctional crosslinkers. The [^{125}I]-labeled/unlabeled proteins were immobilized on fused silica both by adsorption and covalent linking. It was clearly seen that the amount of protein immobilized on the silica surface was significantly more when immobilized covalently, but at the same time, 30-35% of the protein immobilized was due to passive adsorption. The antibody was

96

immobilized at 15.8 ± 0.4 $\mu g/cm^2$. It was also concluded that the protein G-bound monoclonal antibody (protein G captured the Fc portion of antibody) bound a greater amount of the M13 phage in comparison to the antibody adsorbed or covalently immobilized. This result could be due to the formation of an ordered array of antibody molecules with their antigen-combining sites maximized for virus capture. It was also concluded that protein G molecules did not bind non-specifically to the silica surface while for the M13 phage non-specific binding contributed 30-40% of the total activity observed. A sandwich was formed wherein antigen was captured by the covalently linked monoclonal antibody, and the captured antigen was reported by labeled antibody. The sandwich was demonstrable, but the magnitude of the difference in activity was not high compared to that of the background, perhaps due to the low specific activity of the [^{125}I]-MAb. It is likely that this could be improved by employing a fluorescent labeled M13 MAb so that potentially, every molecule could be labeled.

The complex formation between the M13 phage and the antibody (anti-M13 MAb) was also investigated by using capillary electrophoresis. The method is based on the preincubation of the virus with the antibody, followed by capillary electrophoretic analysis. At a low antibody-to-virus molar ratio, the peaks corresponding to the complexes were broad, suggesting the presence of a heterogeneous population of virus aggregates with varying number of antibodies bound per virion. At a higher molar ratio between the antibody and the virus, the peak became narrow again, indicating the potential saturation of the 2700 equivalent epitopes with the divalent antibody. We demonstrated that the virus-antibody complex could be detected by using capillary electrophoresis as was previously demonstrated by okun et al. (2000). The group demonstrated a complex formation of human rhinovirus with nonaggregating neutralizing monoclonal antibodies by affinity capillary electrophoresis.

5.1   Future studies

1.   Further improving the sensitivity of the ultrasensitive immunoassay by using fluorophores instead of iodinated antibodies.

97

2. Further optimizing the protein immobilization on a fused silica surface and the use of a fluorescent antibody compared to the $[^{125}I]$-MAb.

3. Using a combination of CE, fluorescence and LIF to quantitate the phage particles.

4. Further studying protein-protein interaction to determine the stoichiometry and binding constants for virus-antibody complex formation by using capillary electrophoresis.

5. Developing a microchip-based immunoassay by using affinity capillary electrophoresis or the bead-based sandwich immunoassays.

6. Developing bivalent bispecific MAb to combine avidity, high specific activity and clean backgrounds to further improve sensitivity towards the ultimate limit of detection of one virus particle.

98

References

Ahluwalia A, De Rossi D, Ristori C, Schirone A, Serra G., 1992. A comparative study of protein immobilization techniques for optical immunosensors. Biosens Bioelectron 7(3), 207-14.

Aldhous MC, Raab GM, Mok JY, Doherty KV, Bird AG, Froebel KS., 1996. CD4 and CD8 lymphocytes in diagnosis and disease progression of pediatric HIV infection. Pediatr AIDS HIV Infect. 7(1), 20-30.

Amos RA., 1995. Biomaterial surface modification using photochemical coupling technology. In: Encyclopedic Handbook of Biomaterials and Bioengineering. New York, Mercel Dekker 895-926.

Anderson GP, Jacoby MA, Ligler FS, King KD., 1997. Effectiveness of protein A for antibody immobilization for a fiber optic biosensor. Biosens Bioelectron 12(4), 329-36.

Anderson N, Doane FW., 1972. Agar diffusion method for negative staining of microbial suspensions in salt solutions. Appl Microbiol. 24(3), 495-6.

Arentoft AM, Frokiaer H, Michaelsen S, Sorensen H, Sorensen S., 1993. High-performance capillary electrophoresis for the determination of trypsin and chymotrypsin inhibitors and their association with trypsin, chymotrypsin and monoclonal antibodies. J Chromatogr A. 652(1), 189-98.

Avrameas A, Broun G, Thomson D., 1984. Immobilization of active protein by cross-linking to inactive protein. U.S. Patent 4,464,468.

Bagasra O, Pomerantz RJ., 1994. In situ polymerase chain reaction and HIV-1. Clin Lab Med. 14(2), 351-65.

Beck E, Zink B., 1981. Nucleotide sequence and genome organisation of filamentous bacteriophages fl and fd. Gene 16(1-3), 35-58.

Benne CA, Harmsen M, De Jong JC, Kraaijeveld CA., 1994. Neutralization enzyme immunoassay for influenza virus. J Clin Microbiol. 32(4), 987-90.

Bhatia SK, Shriver-Lake LC, Prior KJ, Georger JH, Calvert JM, Bredehorst R, Ligler FS., 1989. Use of thiol-terminal silanes and heterobifunctional crosslinkers for immobilization of antibodies on silica surfaces. Anal Biochem. 178(2), 408-13.

Bobrow MN, Harris TD, Shaughnessy KJ, Litt GJ., 1989. Catalyzed reporter deposition, a novel method of signal amplification. Application to immunoassays. J Immunol Methods. 125(1-2), 279-85.

Bobrow MN, Shaughnessy KJ, Litt GJ., 1991. Catalyzed reporter deposition, a novel method of signal amplification. II. Application to membrane immunoassays. J Immunol Methods. 137(1), 103-12.

Bradford MM., 1976. A rapid and sensitive method for the quantitation of microgram quantities of protein utilizing the principle of protein-dye binding. Anal Biochem.72, 248-54.

Burgi W, Briner M, Franken N, Kessler AC., 1988. One-step sandwich enzyme immunoassay for insulin using monoclonal antibodies. Clin Biochem. 21(5), 311-4.

Casillas AM, Nyamathi AM, Sosa A, Wilder CL, Sands H., 2003. A current review of Ebola virus: pathogenesis, clinical presentation, and diagnostic assessment. Biol Res Nurs. 4(4), 268-75.

Chen DY, Dovichi NJ., 1994.Yoctomole detection limit by laser-induced fluorescence in capillary electrophoresis. J Chromatogr B Biomed Appl. 657(2), 265-9.

Chen FT, Evangelista RA., 1994. Feasibility studies for simultaneous immunochemical multianalyte drug assay by capillary electrophoresis with laser-induced fluorescence. Clin Chem. 40(9), 1819-22.

Chetcuti AF, Wong DK, Stuart MC., 1999. An indirect perfluorosulfonated ionomer-coated electrochemical immunosensor for the detection of the protein human chorionic gonadotrophin. Anal Chem. 71(18), 4088-94.

Chiem N, Harrison DJ., 1997. Microchip-based capillary electrophoresis for immunoassays: analysis of monoclonal antibodies and theophylline. Anal Chem. 69(3), 373-8.

Chow VT, Tambyah PA, Yeo WM, Phoon MC, Howe J., 2000. Diagnosis of nipah virus encephalitis by electron microscopy of cerebrospinal fluid. J Clin Virol. 19(3), 143-7.

Chu YH, Avila LZ, Biebuyck HA, Whitesides GM., 1992. Use of affinity capillary electrophoresis to measure binding constants of ligands to proteins. J Med Chem. 35(15), 2915-7.

Clark PM, Price CP., 1986. Enzyme-amplified immunoassays: a new ultrasensitive assay of thyrotropin evaluated. Clin Chem. 32(1 Pt 1), 88-92.

Cook DB, Self CH., 1993. Determination of one thousandth of an attomole (1 zeptomole) of alkaline phosphatase: application in an immunoassay of proinsulin. Clin Chem. 39(6), 965-71.

Crick FH, Watson JD., 1956. Structure of small viruses. Nature 177(4506), 473-5.

Crowther JR, Reckziegel PO, Prado JA., 1995. Quantification of whole virus particles (146S) of foot-and-mouth disease virus in the presence of virus subunits (12S), using monoclonal antibodies in a sandwich ELISA. Vaccine 13(12), 1064-75.

De Rossi A, Ades AE, Mammano F, Del Mistro A, Amadori A, Giaquinto C, Chieco-Bianchi L., 1991. Antigen detection, virus culture, polymerase chain reaction, and in vitro antibody production in the diagnosis of vertically transmitted HIV-1 infection. AIDS 5(1), 15-20.

Dhahir FJ, Cook DB, Self CH., 1992. Amplified enzyme-linked immunoassay of human proinsulin in serum (detection limit: 0.1 pmol/L). Clin Chem. 38(2), 227-32.

Diamandis EP,.1991. Multiple labeling and time-resolvable fluorophores. Clin Chem. 37, 1486-91.

Diamandis EP., 1988. Immunoassays with time-resolved fluorescence spectroscopy: principles and applications. Clin Biochem. 21(3), 139-50.

Diane SL., 1996. Viral isolation of traditional cell cultures. In: Clinical Virology, Saunders, USA, p. 53.

Doche C, Thome M, Dimet I, Bienvenu J., 1996. Evaluation of the fully automated Cobas Core enzyme immunoassay for the quantitation of antibodies against hepatitis B virus surface antigen. Eur J Clin Chem Clin Biochem. 34(4), 365-8.

Dubuco M., 1981. Enzymoimmunoassay of the main core protein (p28) of mouse mammary tumour virus (MMTV). Europ J Cancer. 17(1), 81-7.

Engvall E., 1980. Enzyme immunoassay ELISA and EMIT. Methods Enzymol. 70(A), 419-39.

Feinstone SM, Kapikian AZ, Purceli RH., 1973. Hepatitis A: detection by immune electron microscopy of a virus like antigen associated with acute illness. Science 182(116), 1026-8.

Ferre F., 1994. Polymerase chain reaction and HIV. Clin Lab Med. 14(2), 313-33.

Flewett TH, Bryden AS, Davies H., 1973. Letter: Virus particles in gastroenteritis. Lancet 2(7844), 1497.

Fox CH., 1996. HIV viral load assay. Science 271(5252), 1043.

Garson JA., 1994. The polymerase chain reaction and hepatitis C virus diagnosis. FEMS Microbiol. Rev.14(3), 229-39.

Gerentes L, Kessler N, Aymard M., 1998. A sensitive and specific ELISA immunocapture assay for rapid quantitation of influenza A/H3N2 neuraminidase protein. J Virol Methods. 73(2), 185-95.

Gerna G, Sarasini A, Di Matteo A, Parea M, Torsellini M, Battaglia M., 1989. Rapid detection of human rotavirus strains in stools by single-sandwich enzyme-linked immunosorbent assay systems using monoclonal antibodies. J Virol Methods. 24(1-2), 43-56.

Gould EA, Buckley A, Cammack N., 1985. Use of the biotin-streptavidin interaction to improve flavivirus detection by immunofluorescence and ELISA tests. J Virol Methods. 11(1), 41-8.

Gronowitz JS, Kallander CF., 1983. A sensitive assay for detection of deoxythymidine kinase and its application to herpesvirus diagnosis. Curr Top Microbiol Immunol. 104, 235-45.

Halamek J, Makower A, Skladal P, Scheller FW., 2002. Highly sensitive detection of cocaine using a piezoelectric immunosensor. Biosens Bioelectron. 17(11-12), 1045-50.

Hamaguchi Y, Kato K, Fukui H, Shirakawa I, Okawa S., 1976. Enzyme-linked sandwich immunoassay of macromolecular antigens using the rabbit antibody-coupled glass rod as a solid phase. Eur J Biochem. 71(2), 459-67.

Hames BD., 1998. Gel Electrophoresis of Proteins: A practical approach, 3rd Edition. University Press. New York.

Hashida S, Ishikawa E., 1990. Detection of one milliattomole of ferritin by novel and ultrasensitive enzyme immunoassay. J Biochem (Tokyo). 108(6), 960-4.

Hemmila I., 1985. Fluoroimmunoassays and immunofluorometric assays. Clin Chem. 31(3), 359-70.

Ho DW, Field PR, Cunningham AL., 1989. Rapid diagnosis of acute Epstein-Barr virus infection by an indirect enzyme-linked immunosorbent assay for specific immunoglobulin M (IgM) antibody without rheumatoid factor and specific IgG interference. J Clin Microbiol. 27(5), 952-8.

Hoffman AS, Kiaci D, Safranj A et al., 1991. Binding of proteins and platelets to gas discharge-deposited polymers. Clin Mat. 8, 3-8.

Horne RW, Wildy P., 1961. Symmetry in virus architecture. Virology 15, 348-73.

Hosogaya S, Kume S., 1995. Enzyme amplification in enzyme immunoassay. Nippon Rinsho 53(9), 2203-7

Hsiung GD, Fong CK, August MJ., 1979. The use of electron microscopy for diagnosis of virus infections: an overview. Prog Med Virol. 25, 133-59.

Hyypia T., 1989. Identification of human picornaviruses by nucleic acid probes. Mol Cell Probes. 3(4), 329-43.

Ishikawa E, Hashida S, Kohno T, Hirota K., 1990. Ultrasensitive enzyme immunoassay. Clin Chim Acta. 194(1), 51-72.

Jansons J, Harnett GB, Bucens MR., 1985. Electron microscopy after direct ultracentrifugation. Pathology. 17(1), 29-30.

Jill KV, Lise WD., 1996. Covalent immobilization of biomolecules to preactivated surfaces. IVD Technology Mar/Apr, 26-31.

Johannsson A, Ellis DH, Bates DL, Plumb AM, Stanley CJ., 1986. Enzyme amplification for immunoassays. Detection limit of one hundredth of an attomole. J Immunol Methods. 87(1), 7-11.

Johannsson A, Stanley CJ, Self CH., 1985. A fast highly sensitive colorimetric enzyme immunoassay system demonstrating benefits of enzyme amplification in clinical chemistry. Clin Chim Acta. 148(2), 119-24.

Jonsson U, Malmqvist M, Ronnberg I., 1985. Immobilization of immunoglobulins on silica surfaces. Kinetics of immobilization and influence of ionic strength. Biochem J. 227(2), 373-8.

Kajiwara H, Hirano H, Oono K., 1991. Binding shift assay of parvalbumin, calmodulin and carbonic anhydrase by high-performance capillary electrophoresis. J Biochem Biophys Methods. 22(4), 263-8.

Kaneko S, Miller RH, Di Bisceglie AM, Feinstone SM, Hoofnagle JH, Purcell RH., 1990. Detection of hepatitis B virus DNA in serum by polymerase chain reaction. Application for clinical diagnosis. Gastroenterology 99(3), 799-804.

Kapikian AZ, Wyatt RG, Dolin R, Thornhill TS, Kalica AR, Chanock RM., 1972. Visualization by immune electron microscopy of a 27-nm particle associated with acute infectious nonbacterial gastroenteritis. J Virol. 10(5), 1075-81.

Karyakin AA, Presnova GV, Rubtsova MY, Egorov AM., 2000. Oriented immobilization of antibodies onto the gold surfaces via their native thiol groups. Anal Chem. 72(16), 3805-11.

Kelkar SD, Bhide VS, Ranshing SS, Bedekar SS., 2004. Rapid ELISA for the diagnosis of rotavirus. Indian J Med Res. 119, 60-65.

Koutny LB, Schmalzing D, Taylor TA, Fuchs M., 1996. Microchip electrophoretic immunoassay for serum cortisol. Anal Chem. 68(1), 18-22.

Kricka LJ., 1993. Ultrasensitive immunoassay techniques. Clin Biochem. 26(5), 325-31.

Krugman S, Hoofnagle JH, Gerety RJ, Kaplan PM, Gerin JL., 1974. Viral hepatitis, type B, DNA polymerase activity and antibody to hepatitis B core antigen. N Engl J Med. 290(24), 1331-5.

Landry ML, Mayo DR, Hsiung GD., 1982. The need for a rapid and accurate viral diagnosis. Pharmacol Ther. 18(1):107-32.

Laviada MD, Babin M, Dominguez J, Sanchez-Vizcaino JM., 1992. Detection of African horsesickness virus in infected spleens by a sandwich ELISA using two monoclonal antibodies specific for VP7. J Virol Methods. 38(2), 229-42.

Lee EW, Jemere AB, Attiya S. et al., 1999. Automated microchip platform for immunoassay analysis. J Cap Elec and Microchip Tech. 006, 1-2.

Leland DS., 1996. Clinical Virology. W.B. Saunders Company p.167.

Lin S, Hsiao IY, Hsu SM., 1997. Determination of the dissociation constant of phosvitin-anti-phosphoserine interaction by affinity capillary electrophoresis. Anal Biochem. 254(1), 9-17.

Ling CM, Overby LR., 1972. Prevalence of hepatitis B virus antigen as revealed by direct radioimmune assay with 125 I-antibody. J Immunol. 109(4), 834-41.

Liu DJ, Day LA., 1994. Pf1 virus structure: helical coat protein and DNA with paraxial phosphates. Science 265(5172), 671-4.

Liu F, Guttikonda S, Suresh MR., 2003. Bispecific monoclonal antibodies against a viral and an enzyme: utilities in ultrasensitive virus ELISA and phage display technology. J Immunol Methods. 274(1-2), 115-27.

Liu, F., 1999. Development of bispecific monoclonal antibodies and their application in ultrasensitive virus ELISA. Phage display technology and viral purification. MSc. Thesis University of Alberta, Edmonton, Canada.

Lopez J, Webster RE., 1983. Morphogenesis of filamentous bacteriophage f1: orientation of extrusion and production of polyphage. Virology 127(1), 177-93.

Lynch C, Seth R, Bates DL, Self CH., 1988. Calcitonin determination by a fast and highly sensitive enzyme amplified immunoassay. J Immunoassay. 9(2), 179-92.

Metcalf TG, Xi JA, Estes MK, Melnick JL., 1988. Nucleic acid probes and molecular hybridization for detection of viruses in environmental samples. Prog Med Virol. 35, 186-214.

Meurman O., 1983. Detection of antiviral IgM antibodies and its problems--a review. Curr Top Microbiol Immunol. 104, 101-31.

Mize PD, Hoke RA, Linn CP, Reardon JE, Schulte TH., 1989. Dual-enzyme cascade--an amplified method for the detection of alkaline phosphatase. Anal Biochem. 79(2), 229-35.

Mortensson-Egnund K, Kjeldsberg E., 1986. Improved ELISA for the detection of adenovirus antigen in faeces extracts by the biotin/streptavidin interaction. J Virol Methods. 14(1), 57-63.

Moss DW, Self CH, Whitaker KB, Bailyes E, Siddle K, Johannsson A, Stanley CJ, Cooper EH., 1985. An enzyme-amplified monoclonal immunoenzymometric assay for prostatic acid phosphatase. Clin Chim Acta. 152(1-2), 85-94.

Mullis KB., 1990. The unusual origin of the polymerase chain reaction. Sci Am. 262(4), 56-61, 64-5.

Munro HS., 1988. The surface photooxidation of polymers. Plym Mater Sci Eng. 58, 344-48.

Nerurkar LS, Namba M, Brashears G, Jacob AJ, Lee YJ, Sever JL., 1984. Rapid detection of herpes simplex virus in clinical specimens by use of a capture biotin-streptavidin enzyme-linked immunosorbent assay. J Clin Microbiol. 20(1), 109-14.

Nesheim S, Lee F, Kalish ML, Ou CY, Sawyer M, Clark S, Meadows L, Grimes V, Simonds RJ, Nahmias A., 1997. Diagnosis of perinatal human immunodeficiency virus infection by polymerase chain reaction and p24 antigen detection after immune complex dissociation in an urban community hospital. J Infect Dis. 175(6), 1333-6.

Nielsen RG, Rickard EC, Santa PF, Sharknas DA, Sittampalam GS., 1991. Separation of antibody-antigen complexes by capillary zone electrophoresis, isoelectric focusing and high-performance size-exclusion chromatography. J Chromatogr. 539(1), 177-85.

Obel N, Andersen HK, Jensen IP, Mordhorst CH., 1995. Evaluation of Abbott TestPack RSV and an in-house RSV ELISA for detection of respiratory syncytial virus in respiratory tract aspirates. APMIS. 103(6), 416-8.

Obringer AR, Rote NS, Walter A., 1995. Antiphospholipid antibody binding to bilayer-coated glass microspheres. J Immunol Methods. 185(1), 81-93.

Obzansky DM, Rabin BR, Simons DM, Tseng SY, Severino DM, Eggelte H, Fisher M, Harbron S, Stout RW, Di Paolo MJ., 1991. Sensitive, colorimetric enzyme amplification cascade for determination of alkaline phosphatase and application of the method to an immunoassay of thyrotropin. Clin Chem. 37(9), 1513-8.

Oellerich M., 1984. Enzyme-immunoassay: a review. J Clin Chem Clin Biochem. 22(12), 895-904.

Okun VM, Ronacher B, Blaas D, Kenndler E., 2000. Affinity capillary electrophoresis for the assessment of complex formation between viruses and monoclonal antibodies. Anal Chem. 72(19), 4634-9.

Parry RP, Love C, Robinson GA., 1990. Detection of rubella antibody using an optical immunosensor. J Virol Methods. 27(1), 39-48.

Pearce EM, Kwei TK, Chien YY., 1987. Ultraviolet radiation induced oxidation of polymer mixtures. Polym Prepr. 28, 305-6.

Peterman JH, Tarcha PJ, Chu VP, Butler JE., 1988. The immunochemistry of sandwich-ELISAs. IV. The antigen capture capacity of antibody covalently attached to bromoacetyl surface-functionalized polystyrene. J Immunol Methods. 111(2), 271-5.

Pillay D., 2002. HIV viral load: the myth of the undetectable? Rev Med Virol. 12(6), 391-6.

Plant AL, Locascio-Brown L, Haller W, Durst RA., 1991. Immobilization of binding proteins on nonporous supports. Comparison of protein loading, activity, and stability. Appl Biochem Biotechnol. 30(1), 83-98.

Plebani A, Ugazio AG, Avanzini AM, Monafo V, Burgio GR., 1986. An enzyme-linked immunosorbent assay for cow's milk protein-specific IgE using biotinylated antigen. Avoidance of interference by specific IgG. J Immunol Methods. 90(2), 241-6.

Polson A., 1993. Chicken IgY-Fc antibody elicited in a rabbit as first coat on frosted glass beads in immunoassays. Immunol Invest. 22(5), 353-63.

Pritchett T, Evangelista RA, Chen FT., 1995. Capillary electrophoresis-based immunoassays. Biotechnology (NY) 13(13), 1449-50.

Qian XH, Tomer KB., 1998. Affinity capillary electrophoresis investigation of an epitope on human immunodeficiency virus recognized by a monoclonal antibody. Electrophoresis 19(3), 415-9.

Reif OW, Freitag R., 1995. Studies of complexes between proteases, substrates and the protease inhibitor alpha 2-macroglobulin using capillary electrophoresis with laser-induced fluorescence detection. J Chromatogr A. 716(1-2), 363-9.

Richman D, Schmidt N, Plotkin S, Yolken R, Cherensky M, McIntosh K, Mattheis M., 1984. Summary of a workshop on new and useful methods in rapid viral diagnosis. J Infect Dis. 150(6), 941-51.

Roberts A, Kemp C., 2001. Ebola and Marburg hemorrhagic fevers. J Am Acad Nurse Pract. 13(7), 291-2.

Rubin RL, Hardtke MA, Carr RI., 1980. The effect of high antigen density on solid-phase radioimmunoassays for antibody regardless of immunoglobulin class. J Immunol Methods. 33(3), 277-92.

Saha GB, Whitten J, Go RT., 1989. Conditions of radioiodination with iodogen as oxidizing agent. Int J Rad Appl Instrum B. 16(4), 431-3.

Schlauder GG, Mushahwar IK., 1994. Detection of hepatitis C and E virus by the polymerase chain reaction. J Virol Methods. 47(3), 243-53.

Schmalzing D, Buonocore S, Piggee C., 2000. Capillary electrophoresis-based immunoassays. Electrophoresis 21(18), 3919-30.

Schmerr MJ, Jenny A., 1998. A diagnostic test for scrapie-infected sheep using a capillary electrophoresis immunoassay with fluorescent-labeled peptides. Electrophoresis 19(3), 409-14.

Schramm W, Yang T, Midgley AR., 1987. Surface modification with protein A for uniform binding of monoclonal antibodies. Clin Chem. 33(8), 1338-42.

Self CH., 1982, European patent application no. 82301170.5 (EP60123), abstracted in Chemical Abstracts 97, 212066D.

Self CH., 1985. Enzyme amplification - a general method applied to provide an immunoassisted assay for placental alkaline phosphate. J Immunol Methods. 76, 389-93.

Shenoy NR, Bailey JM, Shively JE., 1992. Carboxylic acid-modified polyethylene: a novel support for the covalent immobilization of polypeptides for C-terminal sequencing. Protein Sci. 1(1), 58-67.

Shimura K, Karger BL., 1994. Affinity probe capillary electrophoresis: analysis of recombinant human growth hormone with a fluorescent labeled antibody fragment. Anal Chem. 66(1), 9-15.

Shriver-Lake LC, Donner B, Edelstein R, Breslin K, Bhatia SK, Ligler FS., 1997. Antibody immobilization using heterobifunctional crosslinkers. Biosens Bioelectron. 12(11), 1101-6.

Sigrist H, Gao H, Wegmuller B., 1992. Light-dependent, covalent immobilization of biomolecules on 'inert' surfaces. Biotechnology (NY) 10(9), 1026-8.

Smith KO, Melnick JL., 1962. A method for staining virus particles and identifying their nucleic acid type in the electron microscope. Virology 17, 480-90.

Sogo JM, Schneider IR, Koller T., 1974. Size determination by electron microscopy of the RNA of tobacco ringspot satellite virus. Virology 57(2), 459-66.

Stabell EC, Olivo PD., 1992. Isolation of a cell line for rapid and sensitive histochemical assay for the detection of herpes simplex virus. J Virol Methods. 38, 195-204.

Stanley CJ, Johannsson A, Self CH., 1985. Enzyme amplification can enhance both the speed and the sensitivity of immunoassays. J Immunol Methods. 83(1), 89-95.

Tijssen P., 1985. Practice and theory of enzyme immunoassays. Elsevier, Amsterdam.

Turkova J., 1999. Oriented immobilization of biologically active proteins as a tool for revealing protein interactions and function. J Chromatogr B Biomed Sci Appl. 722 (1-2), 11-31.

Turpen TH., 1999. Tobacco mosaic virus and the virescence of biotechnology. Philos Trans R Soc Lond B Biol Sci. 354(1383), 665-73.

Van der Merwe, 1984. Carrier bound immunosorbent. U.S. Patent 4,478,946.

Vandamme AM., 1994. Polymerase chain reaction (PCR) as a diagnostic tool in HIV infection. Verh K Acad Geneeskd Belg. 56(3), 231-65.

Vander Schalie J, Bradway DS, Besser TE, Evermann JF., 1994. Evaluation of a kinetic enzyme-linked immunosorbent assay for detection of caprine arthritis-encephalitis virus-specific antibodies. J Vet Diagn Invest. 6(1), 30-3.

Wilchek M, Bayer EA., 1988. The avidin-biotin complex in bioanalytical applications. Anal Biochem. 171(1), 1-32.

Winger LA, Dessi JL, Self CH., 1996. Enhanced specificity for small molecules in a convenient format which removes a limitation of competitive immunoassay. J Immunol Methods. 199(2), 185-91.

Wolff AM., 1988. The use of carbon-coated formvar films as bacterial adhesion substrates for scanning electron microscopy. J Electron Microsc Tech. 10(3), 315-6.

Wood WG, Gadow A., 1983. Immobilisation of antibodies and antigens on macro solid phases--a comparison between adsorptive and covalent binding. A critical study of macro solid phases for use in immunoassay systems. Part I. J Clin Chem Clin Biochem. 21(12), 789-97.

Wu DL, Walters RR., 1988. Protein immobilization on silica supports. A ligand density study. J Chromatogr. 458, 169-74.

Xu K, Zhang Y, Wang Y, Mbawuike I., 2002. Assay for simultaneous detection of HIV p24 antigen and anti-HIV antibody. Zhonghua Shi Yan He Lin Chuang Bing Du Xue Za Zhi. 16(4), 377-9.

Zaaijer HL, v Exel-Oehlers P, Kraaijeveld T, Altena E, Lelie PN., 1992. Early detection of antibodies to HIV-1 by third-generation assays. Lancet 340(8822), 770-2.

Zhao Z, Malik A, Lee ML., 1993. Solute adsorption on polymer-coated fused-silica capillary electrophoresis columns using selected protein and peptide standards. Anal Chem. 65(20), 2747-52.